NASA / TP-1999-209107

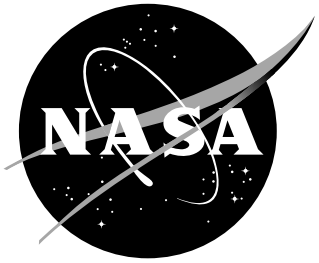

Progressive Failure Analysis Methodology for Laminated Composite Structures

David W. Sleight
Langley Research Center, Hampton, Virginia

March 1999

The NASA STI Program Office ... in Profile

Since its founding, NASA has been dedicated to the advancement of aeronautics and space science. The NASA Scientific and Technical Information (STI) Program Office plays a key part in helping NASA maintain this important role.

The NASA STI Program Office is operated by Langley Research Center, the lead center for NASA's scientific and technical information. The NASA STI Program Office provides access to the NASA STI Database, the largest collection of aeronautical and space science STI in the world. The Program Office is also NASA's institutional mechanism for disseminating the results of its research and development activities. These results are published by NASA in the NASA STI Report Series, which includes the following report types:

- TECHNICAL PUBLICATION. Reports of completed research or a major significant phase of research that present the results of NASA programs and include extensive data or theoretical analysis. Includes compilations of significant scientific and technical data and information deemed to be of continuing reference value. NASA counterpart of peer-reviewed formal professional papers, but having less stringent limitations on manuscript length and extent of graphic presentations.

- TECHNICAL MEMORANDUM. Scientific and technical findings that are preliminary or of specialized interest, e.g., quick release reports, working papers, and bibliographies that contain minimal annotation. Does not contain extensive analysis.

- CONTRACTOR REPORT. Scientific and technical findings by NASA-sponsored contractors and grantees.

- CONFERENCE PUBLICATION. Collected papers from scientific and technical conferences, symposia, seminars, or other meetings sponsored or co-sponsored by NASA.

- SPECIAL PUBLICATION. Scientific, technical, or historical information from NASA programs, projects, and missions, often concerned with subjects having substantial public interest.

- TECHNICAL TRANSLATION. English-language translations of foreign scientific and technical material pertinent to NASA's mission.

Specialized services that complement the STI Program Office's diverse offerings include creating custom thesauri, building customized databases, organizing and publishing research results ... even providing videos.

For more information about the NASA STI Program Office, see the following:

- Access the NASA STI Program Home Page at *http://www.sti.nasa.gov*

- E-mail your question via the Internet to help@sti.nasa.gov

- Fax your question to the NASA STI Help Desk at (301) 621-0134

- Phone the NASA STI Help Desk at (301) 621-0390

- Write to:
  NASA STI Help Desk
  NASA Center for AeroSpace Information
  7121 Standard Drive
  Hanover, MD 21076-1320

NASA / TP-1999-209107

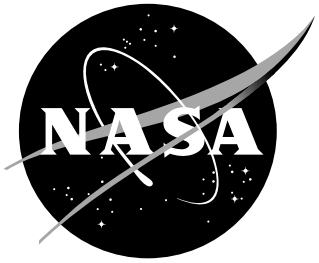

Progressive Failure Analysis Methodology for Laminated Composite Structures

David W. Sleight
Langley Research Center, Hampton, Virginia

National Aeronautics and
Space Administration

Langley Research Center
Hampton, Virginia 23681-2199

March 1999

Acknowledgments

The author would like to thank his research advisor Dr. Norman F. Knight, Jr., whose support, guidance, understanding, and knowledge have made this work possible. A special thanks is also expressed to Dr. John Wang for serving on my thesis committee and being a mentor for my professional development. The author would also like to thank Ms. Tina Lotts for the countless times she has helped me with COMET.

Available from:

NASA Center for AeroSpace Information (CASI)
7121 Standard Drive
Hanover, MD 21076-1320
(301) 621-0390

National Technical Information Service (NTIS)
5285 Port Royal Road
Springfield, VA 22161-2171
(703) 605-6000

TABLE OF CONTENTS

TABLE OF CONTENTS, continued.

LIST OF TABLES

LIST OF FIGURES

ABSTRACT

A progressive failure analysis method has been developed for predicting the failure of laminated composite structures under geometrically nonlinear deformations. The progressive failure analysis uses C^1 shell elements based on classical lamination theory to calculate the in-plane stresses. Several failure criteria, including the maximum strain criterion, Hashin's criterion, and Christensen's criterion, are used to predict the failure mechanisms and several options are available to degrade the material properties after failures. The progressive failure analysis method is implemented in the COMET finite element analysis code and can predict the damage and response of laminated composite structures from initial loading to final failure. The different failure criteria and material degradation methods are compared and assessed by performing analyses of several laminated composite structures. Results from the progressive failure method indicate good correlation with the existing test data except in structural applications where interlaminar stresses are important which may cause failure mechanisms such as debonding or delaminations.

INTRODUCTION

Composite materials have been increasingly used in aerospace and automotive applications over the last three decades and have seen a dramatic increase in usage in non-aerospace products in the few years. The use of composite materials is very attractive because of their outstanding strength, stiffness, and light-weight properties. An additional advantage of using composites is the ability to tailor the stiffness and strength to specific design loads. However, a reliable methodology for fully predicting the performance of composite structures beyond initial localized failure has yet to be developed. Since most composite materials exhibit brittle failure, with little or no margin of safety through ductility as offered by many metals, the propagation of the brittle failure mechanism in composite structures must be understood and reliable prediction analysis methods need to be available. For example, laminated composite structures can develop local failures or exhibit local damage such as matrix cracks, fiber breakage, fiber-matrix debonds, and delaminations under normal operating conditions which may contribute to their failure. The ability to predict the initiation and growth of such damage is essential for predicting the performance of composite structures and developing reliable, safe designs which exploit the advantages offered by composite materials. Hence, the need for a reliable methodology for predicting failure initiation and propagation in composite laminated structures is of great importance.

Overview of Progressive Failure

In recent years, the progression of damage in composite laminates has been a focus of extensive research. Ochoa and Reddy [1] present an excellent overview of the basic steps for performing a progressive failure analysis. A typical methodology for a progressive failure analysis is illustrated in Figure 1. At each load step, a nonlinear analysis is performed until a converged solution is obtained assuming no changes in the material model. Then using this equilibrium state, the stresses within each lamina are determined from the nonlinear analysis solution. These stresses are then compared with material allowables and used to determine failure according to certain failure criteria. If lamina failure is detected, as indicated by a failure criterion, the lamina properties are changed according to a particular

degradation model. Since the initial nonlinear solution no longer corresponds to an equilibrium state, equilibrium of the structure needs to be re-established utilizing the modified lamina properties for the failed lamina while maintaining the current load level. This iterative process of obtaining nonlinear equilibrium solutions each time a local material model is changed is continued until no additional lamina failures are detected. The load step is then incremented until catastrophic failure of the structure is detected as determined by the progressive failure methodology.

Therefore, typical progressive failure analysis methods involve five key features. First, a nonlinear analysis capability is used to establish equilibrium. Second, an accurate stress recovery procedure is needed in order to establish the local lamina stress state. Third, failure criteria are needed in order to detect local lamina failure and determine the mode of failure. Fourth, material degradation or damage models are needed in order to propagate the failure and establish new estimates for the local material properties. Finally, a procedure to re-establish equilibrium after modifying local lamina properties is needed. This research will focus on the last four features since nonlinear analysis procedures are already well established.

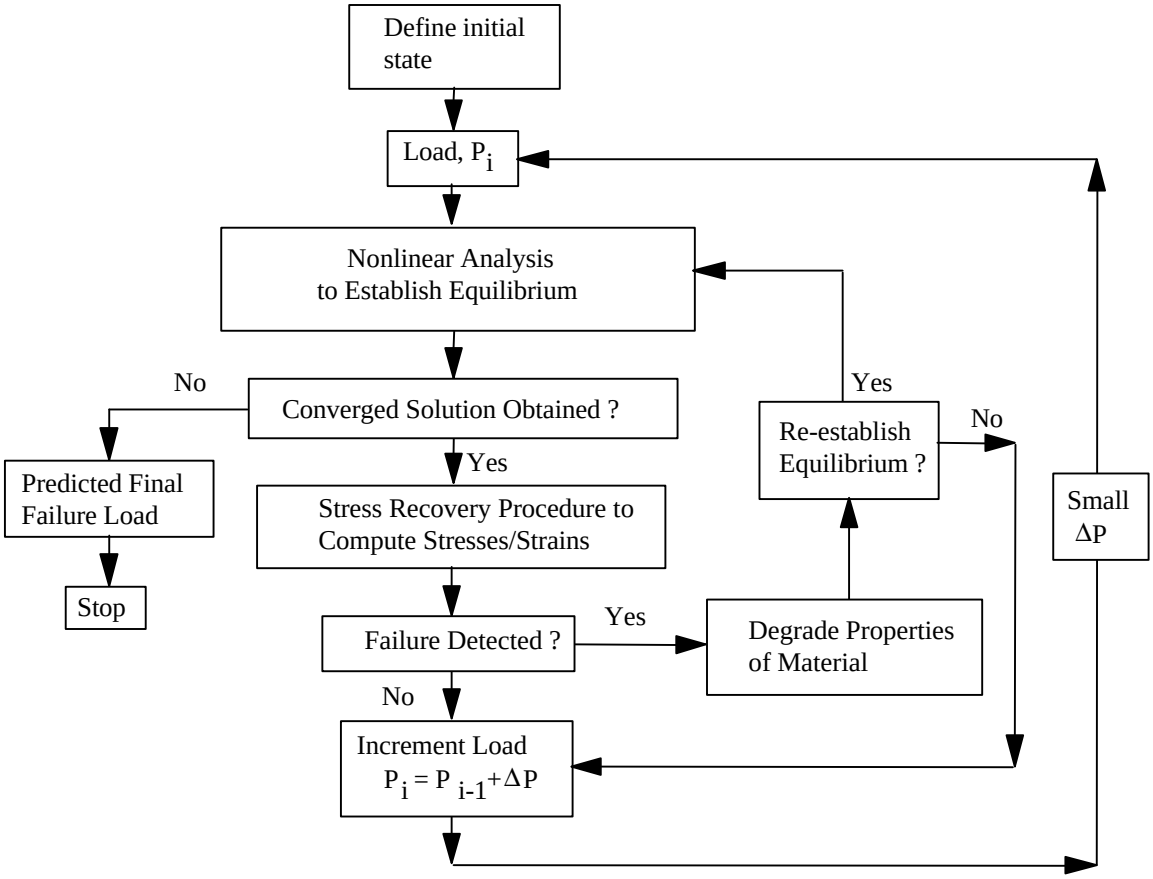

Figure 1. Typical progressive failure analysis methodology.

Nonlinear Analysis

A nonlinear analysis is performed to account for the geometrically nonlinear behavior in the progressive failure analysis. The assembled finite element equations are given by

$$[K_T(\{D\})]\{D\} = \{P\} \tag{1}$$

in which $\{D\}$ is the displacement vector, $\{P\}$ is the applied load vector, and $[K_T]$ is the assembled tangent stiffness matrix. Composite laminates typically behave in a linear elastic manner until local structural failures develop. After local failures within the laminate, the global structural stiffness changes. Hence, the tangent stiffness matrix $[K_T]$ depends on the material properties as well as the unknown displacement solution $\{D\}$. In this progressive failure analysis, a nonlinear analysis is performed until a converged solution is obtained for a constant set of material properties. The nonlinear analysis involves solving the linearized finite element equations for the k^{th} iteration

$$\begin{aligned} [K_T]^{(k)}\{\Delta D\} &= \{R\}^{(k)} \\ \{D\}^{(k+1)} &= \{D\}^{(k)} + \{\Delta D\} \end{aligned} \tag{2}$$

where the tangent stiffness matrix $[K_T]^{(k)}$ and force imbalance vector $\{R\}^{(k)}$ are functions of the displacements $\{D\}^{(k)}$. Solving the equilibrium equations is an iterative process where the k^{th} step requires computing the displacement increment $\{\Delta D\}$ for the $k+1$ load step using the k^{th} tangent stiffness matrix. Then the k^{th} displacement vector $\{D\}$ is updated using $\{\Delta D\}$. Having a new displacement solution, the force imbalance vector $\{R\}$ and possibly the tangent stiffness matrix $[K_T]$ are updated, and the process is continued for the next iteration. The solution process is continued until convergence is achieved by reducing the force imbalance $\{R\}$, and consequently $\{\Delta D\}$ to within some tolerance.

Using this nonlinear solution corresponding to a given load step, the lamina stresses are determined and used with a failure criterion to determine whether any failures have occurred during this load increment. If no failures are detected, then the applied load is increased, and the analysis continues. When a failure in the lamina occurs, a change in the stiffness matrix due to a localized failure is calculated based on the material degradation model. This adjustment accounts for the material nonlinearity associated with a progressive failure analysis embedded within a nonlinear finite element analysis. If the load step size is too large, static equilibrium needs to be re-established by repeating the nonlinear analysis at the current load step using the new material properties in the tangent stiffness matrix. This process is repeated until no additional failures are detected. Alternatively, small load step sizes can be used thereby minimizing the effect of not re-establishing equilibrium at the same load level. This incremental iterative process is performed until a lack of convergence in the nonlinear solution occurs.

The most popular iterative schemes for the solution of nonlinear finite element equations are forms of the Newton-Raphson procedure which is widely used because it generally converges quite rapidly. However, one of the drawbacks of the Newton-Raphson procedure is the large amount of computational resources needed to evaluate, assemble, and decompose the tangent stiffness matrix at each iteration. To reduce the computational effort, a modified Newton-Raphson procedure is commonly used. The modified Newton-Raphson procedure differs from the Newton-Raphson method in that the tangent stiffness matrix is not updated on each iteration but periodically during the analysis, such as at the beginning of each new load step.

Strain/Stress Recovery

Once the nodal values of generalized displacements have been obtained by performing the nonlinear analysis at a particular load step, the element strains are evaluated by differentiating the displacements. These element strains can be computed at any point in the finite element such as the center of the element or at the Gauss points. These recovered strains are midplane strains and changes in curvature obtained by using the strain-displacement relations for the laminate. With these values, the strains through the laminate thickness can be determined and then the stresses can be determined based on the constitutive relations.

Since the displacements calculated from the finite element analysis are in global coordinates, and the failure criteria used in the laminate analysis require stresses and strains in the material (lamina) coordinates, the strains and stresses must be transformed from global coordinates to material coordinates for each layer of the laminate. Once the strains are transformed to the material coordinates, the lamina constitutive equations are used to compute the in-plane stresses (σ_{xx}, $\sigma_{yy,}$ σ_{xy}). The transverse stresses (σ_{xz}, $\sigma_{yz,}$ σ_{zz}) can be computed either by the lamina constitutive equations for shear deformable C^0 elements or by integration of the 3-D equilibrium equations [1],

$$\frac{\partial \sigma_{xx}}{\partial x} + \frac{\partial \sigma_{xy}}{\partial y} + \frac{\partial \sigma_{xz}}{\partial z} = 0$$

$$\frac{\partial \sigma_{xy}}{\partial x} + \frac{\partial \sigma_{yy}}{\partial y} + \frac{\partial \sigma_{yz}}{\partial z} = 0 \qquad (3)$$

$$\frac{\partial \sigma_{xz}}{\partial x} + \frac{\partial \sigma_{yz}}{\partial y} + \frac{\partial \sigma_{zz}}{\partial z} = 0$$

where the body forces are neglected. The accuracy of the computed strains and stresses can be improved by smoothing algorithms [2].

Failure Analysis

The catastrophic failure of a composite structure rarely occurs at the load corresponding to the initial or first-ply failure. Instead, the structure ultimately fails due to the propagation or accumulation of local failures (or damage) as the load is increased. Initial failure of a layer within the laminate of a composite structure can be predicted by applying an appropriate failure criterion or first-ply failure theory. The subsequent failure prediction requires an understanding of failure modes and failure propagation.

Laminated composites may fail by fiber breakage, matrix cracking, or by delamination of layers [1]. The mode of failure depends upon the loading, stacking sequence, and specimen geometry. The first three of these failure modes depend on the constituent's strength properties, whereas delamination may be due to manufacturing anomalies during lay-up or curing or out-of-plane effects. In addition, failure mechanisms such as skin-stiffener separation can be included if needed. However, this progressive failure methodology only includes predictions for fiber breakage and matrix cracking.

Various failure criteria have been proposed in the literature [3-18]. Most failure criteria are based on the stress state in a lamina. Ideally, a three-dimensional model is desirable for obtaining accurate stresses

and strains. However, due to the extensive amount of computational time required for a three-dimensional analysis, two-dimensional failure analyses are usually performed using plate and shell finite element models. Failure criteria are intended to predict macroscopic failures in the composite laminate and are based on the tensile, compressive, and shear strengths of the individual lamina. If an allowable stress limit or failure criterion within a layer is not exceeded, the material properties in the layer are not changed and then the other layers within the laminate are checked. When a material allowable value or failure criterion is exceeded in a given layer, the engineering material constants corresponding to that the particular mode of failure are reduced depending on the material degradation model.

Failure criteria for composite materials are often classified into two groups: namely, non-interactive failure criteria and interactive failure criteria. Several papers can be found which list the most commonly used composite failure theories [3,4,5].

Non-Interactive Failure Criteria A non-interactive failure criterion is defined as one having no interactions between the stress or strain components. These criteria, sometimes called independent failure criteria, compare the individual stress or strain components with the corresponding material allowable strength values. The maximum stress and maximum strain criteria belong to this category. Both failure criteria indicate the type of failure mode. The failure surfaces for these criteria are rectangular in stress and strain space, respectively [6].

Interactive Failure Criteria Interactive failure criteria involve interactions between stress and strain components. Interactive failure criteria are mathematical in their formulation. Interactive failure criteria fall into three categories: (1) polynomial theories, (2) direct-mode determining theories, and (3) strain energy theories. The polynomial theories use a polynomial based upon the material strengths to describe a failure surface [1]. The direct-mode determining theories are usually polynomial equations based on the material strengths and use separate equations to describe each mode of failure. Finally, the strain energy theories are based on local strain energy levels determined during a nonlinear analysis.

Most of the interactive failure criteria are polynomials based on curve-fitting data from composite material tests. The most general polynomial failure criterion for composite materials is the tensor polynomial criterion proposed by Tsai and Wu [7]. The criterion may be expressed in tensor notation as

$$F_i\sigma_i + F_{ij}\sigma_i\sigma_j + F_{ijk}\sigma_i\sigma_j\sigma_k \geq 1 \qquad i, j, k = 1,\ldots,6 \tag{4}$$

where F_i, F_{ij}, and F_{ijk} are components of the lamina strength tensors in the principal material axes. The usual contracted stress notation is used except that $\sigma_4 = \tau_{23}$, $\sigma_5 = \tau_{13}$ and $\sigma_6 = \tau_{12}$. However, the third-order tensor F_{ijk} is usually ignored from a practical standpoint due to the large number of material constants required [7]. Then, the general polynomial criterion reduces to a general quadratic criterion given by

$$F_i\sigma_i + F_{ij}\sigma_i\sigma_j \geq 1 \qquad i, j = 1,\ldots,6 \tag{5}$$

or in explicit form,

$$\begin{aligned} &F_1\sigma_1 + F_2\sigma_2 + F_3\sigma_3 + 2F_{12}\sigma_1\sigma_2 + 2F_{13}\sigma_1\sigma_3 + 2F_{23}\sigma_2\sigma_3 + F_{11}{\sigma_1}^2 \\ &+ F_{22}{\sigma_2}^2 + F_{33}{\sigma_3}^2 + F_{44}{\sigma_4}^2 + F_{55}{\sigma_5}^2 + F_{66}{\sigma_6}^2 \geq 1. \end{aligned} \tag{6}$$

The F_4, F_5 and F_6 terms associated with σ_4 and σ_6, respectively, are assumed to be zero since it is assumed that the shear strengths are the same for positive and negative shear stress. Various quadratic criteria differ in the way that the tensor stress components are determined. Other popular quadratic failure criteria include those by Tsai-Hill [8,9], Azzi and Tsai [10], Hoffman [11], and Chamis [12]. These quadratic failure criteria can be represented in terms of the general Tsai-Wu quadratic criterion and are summarized in Table 1 where X, Y, and Z are lamina strengths in the *x, y,* and *z* directions, respectively, and R, S, and T are the shear strengths in the *yz, xz,* and *xy* planes, respectively. The subscripts *T* and *C* in X, Y, and Z refer to the normal strengths in tension and compression. The failure surfaces for these quadratic criteria are elliptical in shape. One of the disadvantages of these quadratic failure criteria is that they predict the initiation of failure but say nothing about the failure mode or how the composite fails.

Table 1. Quadratic Polynomial Failure Criteria

	Quadratic Polynomial Failure Criteria				
	Tsai-Wu	Tsai-Hill*	Azzi-Tsai*	Hoffman	Chamis*†
F_1	$\frac{1}{X_T}-\frac{1}{X_C}$	0	0	$\frac{1}{X_T}-\frac{1}{X_C}$	0
F_2	$\frac{1}{Y_T}-\frac{1}{Y_C}$	0	0	$\frac{1}{Y_T}-\frac{1}{Y_C}$	0
F_3	$\frac{1}{Z_T}-\frac{1}{Z_C}$	0	0	$\frac{1}{Z_T}-\frac{1}{Z_C}$	0
F_{12}	$-1/2\sqrt{X_T X_C Y_T Y_C}$	$-\frac{1}{2}\left(\frac{1}{X^2}+\frac{1}{Y^2}-\frac{1}{Z^2}\right)$	$-\frac{1}{X^2}$	$-\frac{1}{2}\left(\frac{1}{X_T X_C}+\frac{1}{Y_T Y_C}-\frac{1}{Z_T Z_C}\right)$	$-\frac{K_{12}}{XY}$
F_{13}	$-1/2\sqrt{X_T X_C Z_T Z_C}$	$-\frac{1}{2}\left(\frac{1}{Z^2}+\frac{1}{X^2}-\frac{1}{Y^2}\right)$	0	$-\frac{1}{2}\left(\frac{1}{X_T X_C}+\frac{1}{Z_T Z_C}-\frac{1}{Y_T Y_C}\right)$	$-\frac{K_{13}}{XZ}$
F_{23}	$-1/2\sqrt{Y_T Y_C Z_T Z_C}$	$-\frac{1}{2}\left(\frac{1}{Y^2}+\frac{1}{Z^2}-\frac{1}{X^2}\right)$	0	$-\frac{1}{2}\left(\frac{1}{Z_T Z_C}+\frac{1}{Y_T Y_C}-\frac{1}{X_T X_C}\right)$	$-\frac{K_{23}}{YZ}$
F_{11}	$\frac{1}{X_T X_C}$	$\frac{1}{X^2}$	$\frac{1}{X^2}$	$\frac{1}{X_T X_C}$	$\frac{1}{X^2}$
F_{22}	$\frac{1}{Y_T Y_C}$	$\frac{1}{Y^2}$	$\frac{1}{Y^2}$	$\frac{1}{Y_T Y_C}$	$\frac{1}{Y^2}$
F_{33}	$\frac{1}{Z_T Z_C}$	$\frac{1}{Z^2}$	0	$\frac{1}{Z_T Z_C}$	$\frac{1}{Z^2}$
F_{44}	$\frac{1}{R^2}$	$\frac{1}{R^2}$	0	$\frac{1}{R^2}$	$\frac{1}{R^2}$
F_{55}	$\frac{1}{S^2}$	$\frac{1}{S^2}$	0	$\frac{1}{S^2}$	$\frac{1}{S^2}$
F_{66}	$\frac{1}{T^2}$	$\frac{1}{T^2}$	$\frac{1}{T^2}$	$\frac{1}{T^2}$	$\frac{1}{T^2}$

* X, Y, and Z are either X_C, Y_C, and Z_C or X_T, Y_T, and Z_T depending upon the sign of σ_1, σ_2 and σ_3 respectively.

† K_{12}, K_{13}, and K_{23} are the strength coefficients depending upon material.

Direct-mode determining failure criteria are very useful in progressive failure analysis because they also describe the failure mode of the composite laminate. Hashin [13,14] stated that the Tsai-Wu theory had an intrinsic problem since it could not distinguish among the various different failure modes of the composite material. He instead proposed a quadratic failure criterion in piecewise form based on material strengths, where each smooth branch represents a failure mode. In unidirectional composites, there are two primary failure modes: a fiber mode and a matrix mode subdivided into either tension or compression failure. In the fiber mode, the lamina fails due to fiber breakage in tension or fiber buckling in compression. In the matrix mode, failure is due to matrix cracking.

Lee [15] also proposed a direct-mode determining failure criterion. His criterion was a polynomial equation for each mode of failure based upon the three-dimensional stress calculations. The modes of failure determined included fiber failures, matrix failures, and delaminations. Christensen [16] introduced a quasi-three-dimensional laminate theory which accounted for the out-of-plane stress terms. He then developed a strain-based failure criterion which distinguished between fiber failure and fiber-matrix interaction failure.

A nonlinear total strain energy failure criterion was developed by Sandhu [17]. This criterion is based on the concept that the lamina fails when the sum of the ratios of energy levels (due to longitudinal, transverse, and shear loading) to the corresponding maximum energies equals unity. A similar failure criterion by Abu-Farsakh and Abdel-Jawad [18] was introduced based on an energy concept. However, the failure modes could not be identified for either criterion which poses difficulties for material degradation modeling and failure propagation.

Material Degradation

If failure is detected in a particular lamina of the composite material, the properties of that lamina must be adjusted according to a material property degradation model. A number of post-failure material property degradation models have been proposed for progressive failure analyses [3]. Most of these material degradation models belong to one of three general categories: instantaneous unloading, gradual unloading, or constant stress at ply failure [19]. Figure 2 illustrates these three categories. For the instantaneous loading case, the material property associated with that mode of failure is degraded instantly to zero. For the gradual unloading case, the material property associated with that mode of failure is degraded gradually (perhaps exponentially) until it reaches zero. For the constant stress case, the material properties associated with that mode of failure are degraded such that the material cannot sustain additional load. The behavior of the lamina as it fails, as well as which elastic constants are degraded, depends on the failure mode of the composite laminate.

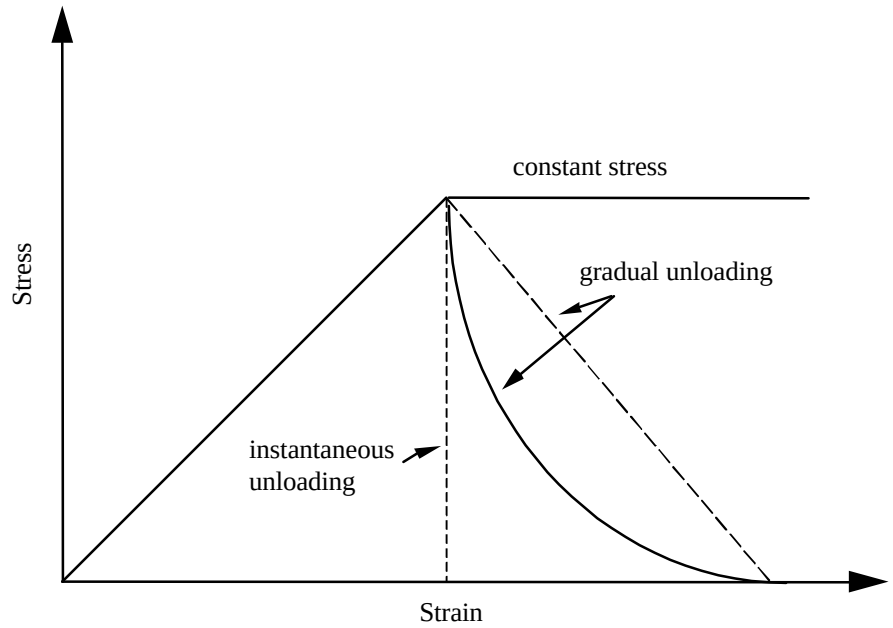

Figure 2. Post-failure degradation behavior in composite laminates.

The Hahn-Tsai method [20] assumes that a failed lamina will support its load (load at initial lamina failure) until total failure of the laminate occurs. This is an example of the constant stress category of material degradation methods. In the gradual unloading model, the material elastic properties are gradually reduced depending upon the extent of damage within a lamina until the lamina has completely unloaded or failed. The unloading can be either linear or exponential in behavior. Petit and Waddoups' work [21] was the first effort in material degradation by gradual unloading. Sandhu [17] also used a degradation model by gradual unloading based on nonlinear stress-strain relations. Other gradual unloading models are the exponential degradation model by Nahas [3] and the Weibull distribution used by Chang [22]. Reddy and Reddy [23] used a constant degradation method in which the degraded properties are assumed to be a constant multiple of the original properties of the undamaged material. They divided the constant degradation methods into two types: independent and interactive. In the independent method, it is assumed that each stress only contributes toward the degradation of the corresponding stiffness property. In the interactive method, coupling is assumed between the normal and shear stiffness lamina properties.

One of the most common methods used for degradation of material properties is the ply-discount theory [19] which belongs to the instantaneous unloading category. In this method, one or more of the elastic material properties of a lamina are set to equal zero or a small fraction of the original value once failure is detected. As in the gradual unloading category, the degradation can be either independent or interactive corresponding to the mode of failure. This method is described later in the paper.

Re-establishment of Equilibrium

Once a lamina fails and the stiffness properties have been degraded, it is often necessary to re-calculate the element stiffness matrices and update the tangent stiffness matrix of the model. This new tangent stiffness matrix accounts for the local changes in material stiffness as well as any large deformation effects associated with geometric nonlinearities. The nonlinear analysis procedure described earlier is then used to re-establish equilibrium at the same load level for the composite structure with localized failures. To establish equilibrium, additional iterations may be required until a new converged solution is reached. Once obtained, checks for subsequent lamina failures are necessary. If the load steps are restricted to be small, such a procedure may not be needed.

Literature Review on Progressive Failure

This section summarizes some of the research done in progressive failure analyses over the past two decades. The summary discusses the type of analysis (linear or nonlinear) used in performing the progressive failure analyses, failure criterion chosen, and prediction of progressive failure analyses compared to experimental results.

Reddy and Pandey [6] developed a finite element procedure based on first-order, shear-deformation theory for first-ply failure analysis of laminated composite plates subjected to in-plane and/or transverse loads. A tensor polynomial failure criterion with failure predictions by the maximum stress, maximum strain, Tsai-Hill, Tsai-Wu, and Hoffman failure criteria was used to predict lamina failures at the element Gauss points. For laminates subjected to in-plane loading, all the failure criteria satisfactorily predicted first-ply failure. However, for laminates subjected to transverse loads, the failure locations and failure loads predicted by either the Tsai-Hill or maximum strain criteria were different than those predicted using the other criteria.

Pandey and Reddy [24] extended their earlier work on first-ply failure of two-dimensional laminated composites to include a progressive failure analysis capability. However, only a linear finite element analysis was performed. Again, the same failure criteria as in the previous study were used for the prediction of failure within the composite laminate. The elastic constants of a failed lamina were reduced according to the dominant failure indices determined from the individual contributions of each stress component. The individual contributions α_i of each stress component to the failure index are first determined and then the corresponding elastic properties are multiplied by a factor $R(1-\alpha_i)$ where R is a pre-selected reduction parameter ranging from 0 to 1. After the stiffness properties are reduced, the stress analysis is repeated until no additional ply failures are predicted. This progressive failure analysis method was applied to a laminated plate with a hole subjected to uniaxial tension and to a rectangular plate subjected to a uniform transverse pressure. Comparisons with experimental results were not provided in this reference.

Reddy and Reddy [25] calculated and compared the first-ply failure loads obtained by using both linear and nonlinear finite element analyses on composite plates. The finite element model was based on first-order shear deformation theory. The maximum stress, maximum strain, Tsai-Hill, Tsai-Wu, and Hoffman failure criteria were used for failure prediction of composite plates subject to in-plane (tensile) loading and transverse loading. The failure loads and locations predicted by the different failure criteria differed significantly from one other. The differences between the linear and nonlinear failure loads was found much larger for the cases involving transverse loading than for the cases involving in-plane (tensile) loading.

Reddy and Reddy [23] then developed a three-dimensional (3-D) progressive failure algorithm for composite laminates under axial tension. The finite element analysis used Reddy's Layerwise Laminated Plate Theory (LWLT) and predicted both in-plane and interlaminar stresses at the reduced integration Gauss points. In the analysis, the Tsai-Wu failure criterion along with other various failure criteria were compared to experimental results. The other failure criteria used included maximum stress, maximum strain, Tsai-Hill, and Hoffman criteria. Two different types of stiffness reduction methods, an independent type and an interactive type, were considered to study the influence on the failure loads and strains of stiffness reduction at the Gauss points where failed plies were detected. In the independent method, it was assumed that each stress only contributes toward the degradation of the corresponding stiffness property. In the interactive method, coupling was assumed between the normal and shear stiffness properties. A parametric study was performed to investigate the effect of out-of-plane material properties, 3-D stiffness reduction methods, and boundary conditions on the failure loads and strains of a composite laminate under axial tension. Results showed the progressive failure algorithm accurately predicted the failure loads and strains. Also, results showed that the maximum stress and maximum strain failure criteria tend to overpredict the failure loads while the Hoffman and Tsai-Wu failure criteria tend to underpredict the failure loads for all laminates. Also, it was noted that the Tsai-Hill failure criteria did not consistently follow the experimental trends.

In an earlier paper, Ochoa and Engblom [26] presented a progressive failure analysis for composite laminates in uniaxial tension using a higher-order plate theory with shear deformable elements. Hashin's failure criterion [13] was used to identify fiber and matrix failures while Lee's criterion [15] was used to identify delaminations. Stiffness reduction of failed lamina was carried out at the Gauss points for the entire laminate. Equilibrium was then re-established and failure detection was again checked at the same load increment before advancing to the next load increment. Analyses were performed on a plate subjected to uniaxial tension and to four-point bending. However, comparisons with experimental results were not provided.

Engelstad, Reddy, and Knight [27] investigated the postbuckling response and failure prediction of flat composite unstiffened panels loaded in axial compression using 9-node shear deformable elements. The finite element formulation accounted for transverse shear deformation and was based on virtual displacements using the total Lagrangian description. The Newton-Raphson method was used to solve the nonlinear analysis. For failure prediction, the maximum stress and Tsai-Wu failure criteria were implemented and compared with limited experimental results. The stresses for the in-plane and transverse stress components were calculated at the element Gauss points in the plane of the element and at the middle of each lamina in the thickness direction using the constitutive relations. If failure occurred, a reduction in the material properties was applied to the material properties at the Gauss point corresponding to the dominant failure mode. For example, if a lamina failed due to fiber failure, the modulus E_{11} was reduced to zero or if a lamina failure due to matrix failure, the modulus E_{22} was reduced to zero. Equilibrium was re-established after the material properties were degraded. Good correlation between the experimentally obtained and analytically predicted postbuckling responses was obtained for deflections and surface strains. The Tsai-Wu method more closely estimated the apparent failure observed than the maximum stress method due to the interaction of the stress components in the failure criterion.

Hwang and Sun [28] performed a failure analysis of laminated composites by using an iterative three-dimensional finite element method. A modified form of the Tsai-Wu failure criterion was used to predict fiber breakage and matrix cracking while quadratic interactive formulas by Lee [15] and Chang [29] were used to identify delaminations. The progressive failure problem was solved using the modified Newton-Raphson method for the nonlinear analysis. A post-failure reduced stiffness approach was used where

the lamina properties are degraded depending on the failure mode. For fiber failure, only the corresponding constitutive terms in the stiffness matrix were set to zero. For matrix failure, only the corresponding transverse and shear properties of the stiffness matrix were removed. If damage included both fiber and matrix modes, then the entire stiffness matrix of the failed element was removed. Elements with delaminations were re-modeled with a new free surface at the lamina interface. After the stiffness properties were degraded, equilibrium was re-established iteratively by the nonlinear analysis. The three-dimensional analytical results agree favorably with the experimental results for notched and unnotched specimens loaded in tension. However, the analytical predictions underestimated the experimental results for angle-plied laminates with holes.

Huang, Bouh, and Verchery [30] implemented a progressive failure analysis of composite laminates using triangular elements which include transverse shear effects. A new method was introduced for the calculation of the shear correction factors using a parabolic function. Several failure criteria were used to determine first-ply failure and distinguish the failure modes into fiber breakage or buckling, matrix cracking, and delaminations.

Chang and Chang [31] developed a progressive failure damage model for laminated composites containing stress concentrations. The progressive failure method used a nonlinear finite element analysis using the modified Newton-Raphson iteration scheme to calculate the state of stress in a composite plate. A modified form of the Yamada-Sun [32] failure criterion, which accounted for shear deformation and incorporated Sandhu's strain energy failure criterion [17], predicted fiber breakage and fiber-matrix shearing failures. A modified form of Hashin's failure criterion using Sandhu's strain energy failure criterion to account for nonlinear shear deformation was used for the matrix failure modes. For fiber failure or fiber-matrix shearing, the degree of property degradation was dependent upon the size of the damage predicted by the failure criterion. The property degradation model was based on a micromechanics approach for fiber-bundle failure. For fiber failure, both the transverse modulus E_{22} and Poisson's ratio ν_{12} were set to zero, and the longitudinal E_{11} and shear moduli G_{12} were reduced according to the exponential Weibull distribution. For matrix cracking in a lamina, the transverse modulus and the Poisson's ratio were reduced to zero, whereas the longitudinal and shear moduli remained unchanged. After the properties were degraded, the stresses and strains in the composite laminate were redistributed by performing the Newton-Raphson iteration again with the updated properties until no additional failures were found. Chang and Chang applied this progressive failure method to bolted composite joints [33], and Chang and Lessard to a laminated composite plate containing a hole [34]. Comparisons were made to experimental results in these studies and reasonable correlation to the data was reported.

Tolson and Zabaras [35] developed a two-dimensional finite element analysis for determining failures in composite plates. In their finite element formulations, they developed a seven degree-of-freedom plate element based on a higher-order shear-deformation plate theory. The in-plane stresses were calculated from the constitutive equations, but the transverse stresses were calculated from the three-dimensional equilibrium equations. The method gave accurate interlaminar shear stresses very similar to the three-dimensional elasticity solution. The stress calculations were performed at the Gaussian integration points. The stresses were then inserted into the appropriate failure criterion to determine if failure had occurred within a lamina. The maximum stress, Lee, Hashin, Hoffman, and Tsai-Wu failure criteria were used. Since the Hoffman and Tsai-Wu failure criteria do not determine the mode of failure, the relative contributions of the shear stress terms, transverse direction terms, and fiber direction terms were used to determine the failure mode. Once the failure mode was determined, the stiffness was reduced at the Gauss points. For fiber failure at all four Gauss points, the σ_1, σ_5, and σ_6 stress terms were set to zero by degrading the corresponding stiffness matrix terms. If less than four Gauss points failed, then the appropriate stiffness components were proportionally reduced by the fraction of the failed area in the

element. Similarly, the σ_2, σ_4, and σ_6 stresses were reduced to zero for matrix failure at all four Gauss points and proportional values were prescribed if failure occurred at less than the four Gauss points. Delamination was also predicted by examining the interlaminar stresses according to a polynomial failure equation. If delaminations occurred, then the stiffness matrix in both lamina adjacent to the delamination would be reduced such that the σ_3, σ_4, and σ_5 stresses would vanish. Obviously, when all the terms in the element stiffness matrix have been reduced to zero, the element makes no further contribution to the plate stiffness and is considered to have undergone total failure. Once the stiffness properties were reduced, equilibrium iterations were performed until no further failures were predicted. Next, the load was incremented and the failure process was repeated until total failure of the structure was predicted. The results obtained from the progressive failure method were compared to experimental results from composite laminates loaded in uniaxial tension and under a transverse pressure. The Lee criterion gave the best results for the cases tested.

One of the first finite-element-based failure analyses of composite was performed by Lee [15]. Lee performed a three-dimensional finite element analysis and used his own direct-mode determining failure criterion to predict the failures. He determined the stresses at the center of each element and the stresses at the center of the interface of each element to identify the failure. According to the modes of failure, the stiffness matrix of the element with failures was modified. Equilibrium was then re-established to give a new stress distribution and subsequent failure zones. The process was repeated until the ultimate strength of the laminate was obtained. The procedure was applied to a plate with a central hole subject to uniaxial and biaxial loadings. Comparisons with experimental results were not reported.

Coats [36,37,38] developed a nonlinear progressive failure analysis for laminated composites that used a constitutive model describing the kinematics of matrix cracks via volume averaged internal state variables. The evolution of the internal states variables was governed by an experimentally based damage evolutionary relationship. The methodology was used to predict the initiation and growth of matrix cracks and fiber fracture. Most of the residual strength predictions were within 10% of the experimental failure loads.

Objectives and Scope

The overall objective of this research is to develop a progressive failure analysis methodology for laminated composite structures. From the literature review, few studies have been performed on predicting the failure of composite panels based on nonlinear analyses and comparing with experimental data. Nonlinear analyses should be used in predicting the failure of composite structures to account for the geometric nonlinearity deformations. The progressive failure methodology in this research is implemented into a general purpose finite element analysis code called COMET (Computational Mechanics Testbed) [39,40]. The progressive methodology was implemented into COMET by Pifko [41,42] using the constitutive material models developed by Moas [43]. The methodology is then validated by comparing analytical predictions using nonlinear progressive failure analyses with experimental data. The progressive failure methodology is also applied to a built-up composite structure, a component of a subsonic composite aircraft. This effort incorporates some of the failure criteria and material degradation models discussed in the literature review into a single computational structural mechanics framework. Specific goals of this research include:

1. Establish state-of-the-art perspective on computational models for progressive failure analysis.

2. Develop and implement a progressive failure analysis methodology which accommodates various formulations for detecting failure and degrading material properties.

3. Compare and assess different formulation methods for detecting failure and degrading material properties.

4. Perform progressive failure analysis and compare with existing test data.

The scope of the present work is limited to C^1 shell elements and neglects the effects of transverse shear deformations. The lamina properties are assumed to behave in a linear elastic manner and any nonlinear behavior of the in-plane shear stiffness is ignored. The results from these simulations are compared with existing experimental and analytical results. No new experimental results are presented. This work was in partial fulfillment for a graduate degree at Old Dominion University in 1996 [44].

PROGRESSIVE FAILURE METHODOLOGY

To implement and perform the progressive failure methodology described earlier, a structural analysis software system is needed. The framework to accomplish this task is a structural analysis software system called COMET (Computational Mechanics Testbed) [39,40]. The Appendix presents a brief description of COMET, its element processor, its constitutive processor, the implementation process for the failure and damage models incorporated in the progressive failure methodology, and the nonlinear analysis solution procedure.

The progressive failure analysis methodology uses C^1 shell elements based on classical lamination theory to calculate the in-plane stresses which ignores transverse shear stresses. The nonlinear Green-Lagrange strain-displacement relations are used in the element formulation, and large rotations are treated through the element-independent corotational formulation in COMET. The progressive failure methodology implemented in COMET accommodates the maximum strain criterion [6], Christensen's criterion [16], and Hashin's criterion [13,14]. When a failure is detected, the progressive failure model classifies the mode of failure as fiber failure, matrix failure, or shear failure. Two material degradation models are implemented including instantaneous reduction and gradual reduction of the material properties for use with the ply-discount theory.

Failure Detection

Once the strains and stresses are known throughout the composite laminate, a failure theory is used to detect failures for each lamina at a given load level. The failure theory should be able to predict the failure load and also the mode of failure such as fiber failure and/or matrix failure. Three failure criteria are considered in this implementation for a progressive failure analysis.

Maximum Strain Criterion

In the maximum strain criterion, failure is assumed to occur if any of the following conditions are satisfied:

$$\begin{aligned} \varepsilon_1 \geq X_{\varepsilon_T} \quad \text{or} \quad |\varepsilon_1| \geq X_{\varepsilon_C} \quad & \text{fiber failure} \\ \varepsilon_2 \geq Y_{\varepsilon_T} \quad \text{or} \quad |\varepsilon_2| \geq Y_{\varepsilon_C} \quad & \text{matrix failure} \\ |\gamma_{12}| \geq T_{\varepsilon} \quad & \text{shear failure} \end{aligned} \tag{7}$$

where X_{ε_T}, X_{ε_C}, Y_{ε_T}, Y_{ε_C}, and T_{ε} are the material allowable strains denoted as

$$\begin{aligned} X_{\varepsilon_T} &= \text{critical tensile strain in fiber direction} \\ X_{\varepsilon_C} &= \text{critical compressive strain in fiber direction} \\ Y_{\varepsilon_T} &= \text{critical tensile strain in matrix direction} \\ Y_{\varepsilon_C} &= \text{critical compressive strain in matrix direction} \\ T_{\varepsilon} &= \text{critical shear strain} \end{aligned}$$

The absolute value sign on γ_{12} indicates that the sign of the shear strain is assumed to not affect the failure criterion. As discussed in Section 1, the maximum strain criterion is a non-interactive failure theory in strain space. Since the maximum strain criterion provides different conditions for failure, the mode of failure can be identified as either fiber failure, matrix failure, or shear failure.

Hashin's Criterion

Hashin and Rotem [14] have proposed a stress-based failure criterion that has the ability to predict the modes of failure. In this report this failure criterion will be denoted as Hashin's Criterion. As stated earlier, observation of failure in unidirectional fibrous composites indicates that there are two primary failure modes: a fiber mode in which the composite fails due to fiber breakage in tension or fiber buckling in compression; and a matrix mode in which matrix cracking occurs. Since different failure mechanisms occur in tension and compression, Hashin further subdivided each failure mode into a tension and compression mode. The failure modes are summarized for the case of plane stress as follows:

Tensile Fiber Mode, $\sigma_1 > 0$

$$\left(\frac{\sigma_1}{X_T}\right)^2 + \left(\frac{\tau_{12}}{T}\right)^2 \geq 1 \tag{8}$$

Compressive Fiber Mode, $\sigma_1 < 0$

$$\left(\frac{\sigma_1}{X_C}\right)^2 \geq 1 \tag{9}$$

Tensile Matrix Mode, $\sigma_2 > 0$

$$\left(\frac{\sigma_2}{Y_T}\right)^2 + \left(\frac{\tau_{12}}{T}\right)^2 \geq 1 \tag{10}$$

Compressive Matrix Mode, $\sigma_2 < 0$

$$\frac{\sigma_2}{Y_C}\left[\left(\frac{Y_C}{2T}\right)^2 - 1\right] + \left(\frac{\sigma_2}{2T}\right)^2 + \left(\frac{\tau_{12}}{T}\right)^2 \geq 1 \tag{11}$$

Christensen's Criterion

Christensen [16] introduced a quasi-three-dimensional lamination theory which accounted for the out-of-plane stress terms. In related work, Christensen then proposed a strain-based failure criterion which distinguished the modes of failure into either fiber failure or fiber/matrix interaction failure. The corresponding equations for failure are as follows:

Fiber Failure

$$X_{\varepsilon_C} \le \varepsilon_1 \le X_{\varepsilon_T} \tag{12}$$

Fiber/Matrix Failure

$$\beta \varepsilon_{kk} + e_{ij} e_{ij} \ge k^2 \tag{13}$$

where β and k are determined from experimental failure data and e_{ij} is the deviatoric strain tensor given by

$$e_{ij} = \varepsilon_{ij} - \frac{1}{3} \delta_{ij} \varepsilon_{kk} \tag{14}$$

In Christensen's analyses, the two parameters β and k in Equation (13) are evaluated to fit failure data for tensile and compressive failure with no shear stress.

Damage Modeling

A common method for degrading the material properties in laminates with fiber or matrix failure is the ply-discount method [18]. This method belongs to the instantaneous unloading category described in the first section. With this method, one or more of the material properties (or constitutive components) of a location with failures are set equal to zero or reduced to a fraction of the original values. It is assumed that the material degradation is restricted to the ply that fails.

In the present implementation of the material degradation model, the material properties which are degraded depend upon the failure criterion chosen. The maximum strain failure criterion has three options for material degradation. The first two are for unidirectional composites, and the third one is for a fabric composite. These options allow failure in one direction to be independent of other failures, or have the failures in one direction to cause failure in other directions. In Option 1, when fiber failure is detected, the moduli E_{11} and the Poisson's ratio ν_{12} are degraded. Similarly for matrix failure, the moduli E_{22} and the Poisson's ratio ν_{12} are degraded. The Poisson's ratio ν_{12} is reduced to zero if a failure occurs in both of these options to allow the constitutive matrix for the lamina to remain symmetric. Finally for shear failure, only the shear modulus G_{12} is degraded. Options 2 and 3 are similar to Option 1 but also include an induced coupling based on heuristic arguments. For example, fiber failure often induces shear failure. Table 2 shows the material degradation model for the maximum strain criterion for each of the three degradation options. The other two failure criteria implemented, Hashin's criterion and Christensen's criterion, both include induced shear failure for fiber and matrix failure. Table 3 summarizes the material degradation for these two failure criteria.

Table 2. Options for Material Degradation for Maximum Strain Criterion

	Option 1		Option 2		Option 3	
Primary Failure Direction	Induced Additional Failure	Degraded Properties	Induced Additional Failure	Degraded Properties	Induced Additional Failure	Degraded Properties
Fiber Failure	None	E_{11}, υ_{12}	Shear	$E_{11}, G_{12}, \upsilon_{12}$	Shear	$E_{11}, G_{12}, \upsilon_{12}$
Matrix Failure	None	E_{22}, υ_{12}	Shear	$E_{22}, G_{12}, \upsilon_{12}$	Shear	$E_{22}, G_{12}, \upsilon_{12}$
Shear Failure	None	G_{12}	Matrix	$E_{22}, G_{12}, \upsilon_{12}$	Fiber	$E_{11}, G_{12}, \upsilon_{12}$

Table 3. Material Degradation for Hashin's and Christensen's Failure Criteria

	Hashin's Criterion		Christensen's Criterion	
Primary Failure Direction	Induced Additional Failure	Degraded Properties	Induced Additional Failure	Degraded Properties
Fiber Failure	Shear	$E_{11}, G_{12}, \upsilon_{12}$	Shear	$E_{11}, G_{12}, \upsilon_{12}$
Matrix Failure	Shear	$E_{22}, G_{12}, \upsilon_{12}$	Shear	$E_{22}, G_{12}, \upsilon_{12}$

In the damage modeling implemented in this study, the material properties can be slowly degraded over subsequent nonlinear load steps or can be instantaneous reduced to zero if a failure occurs. The properties are assumed to be a constant multiple of the original material properties of the undamaged material if no previous failures have occurred. If failures have occurred, then the degraded properties are assumed to be a constant multiple of the updated material properties which have been previously degraded. The material properties which are degraded depend upon the failure mode type as already discussed. The material properties are degraded according to

$$\begin{aligned} E_{11\,\text{new}} &= \alpha\, E_{11\,\text{previous}} \\ E_{22\,\text{new}} &= \alpha\, E_{22\,\text{previous}} \\ G_{12\,\text{new}} &= \alpha\, G_{12\,\text{previous}} \quad \text{where } \alpha = 10^{-n}\ (0 \le n \le 20,\ n = \text{integer}) \\ \upsilon_{12\,\text{new}} &= \alpha\, \upsilon_{12\,\text{previous}} \\ \upsilon_{21\,\text{new}} &= 0 \end{aligned} \tag{15}$$

Therefore, if $n = 0$ then the properties are not degraded if failures occur. If $n = -1$, then the material properties are degraded to 10% of the previous material properties each time a failure occurs. The constitutive matrix for the degraded lamina remains symmetric. In the present implementation, the material properties are automatically reduced to zero if $n = 20$ in which $\alpha = 10^{-20}$. Studies are performed to determine the effect of this delayed material degradation implementation.

Nonlinear Analysis Solution Continuation

After the element material properties have been degraded for a failed ply, the historical database for the element material properties is updated for the current load step in the nonlinear analysis. The tangent stiffness matrix in the nonlinear analysis is then recalculated for the new element material properties and the Newton-Raphson solution procedure continues. In general, static equilibrium must also be re-established after the material properties have been degraded by repeating the nonlinear analysis at the current load step. However, by incrementing the nonlinear analysis by small load increment sizes, changes in the force imbalance vector should be very small and the step of re-establishing equilibrium may be omitted.

NUMERICAL RESULTS

The progressive failure methodology described in the previous sections was successfully implemented in COMET. Several laminated composite structures are now considered to evaluate the performance of the progressive failure model, and simulation results are compared to their experimental results. The first problem is a composite laminate under rail-shear loading. The second problem is a composite laminate with a central circular hole under tension loading. The third problem is a laminated composite panel subject to an axial compressive load. The fourth problem is a laminated composite panel with an offset circular hole subject to an axial compressive load. The final problem is a laminated composite blade-stiffened panel with discontinuous stiffener loaded in axial compression. Numerical results obtained using the present progressive failure methodology are compared with other reported analytical and experimental results.

These problems are of interest because of the available experimental data and their applicability in aircraft structures. The first two problems are essential membrane problems with the nonlinear behavior due to material failure. The latter problems involve combined membrane and bending behavior and combined material degradation and geometric nonlinearities.

For the problems considered, determining the structural response involves several steps using COMET. For the problems with compressive loadings, the first step is to perform a linear static analysis. Using the linear static analysis, the primary equilibrium path is found which produces no out-of-plane deflection. The next step is a linear stability analysis to find the point at which the primary path will bifurcate to a secondary equilibrium path. Along the secondary path, the transverse deflections will increase. The third step is forming the initial geometric imperfection which serves as a trigger for the geometric nonlinearities. For the problems with tension or shear loadings, these first three steps are omitted. For all problems, the next step is to perform an elastic nonlinear analysis to understand how the structure behaves without any material failures. Finally, a progressive failure analysis which includes combined material degradation and geometric nonlinear analysis is performed.

In all problems considered, a prescribed displacement is applied to the structure to simulate the test conditions. The initial displacement of the nonlinear analysis is applied as an initial displacement factor times the applied displacement. Each successive displacement in the nonlinear analysis is incremented by a displacement increment times the applied displacement. The modified energy norm error convergence criterion with estimates of total strain energy is used in the nonlinear analysis solution unless otherwise stated. The specified energy norm error tolerance used for convergence in the nonlinear analysis is set to 10^{-3}. The COMET element used in all analyses is the ES5/ES410 which is a 4-node quadrilateral element with five Gauss quadrature points (see Appendix). Through the thickness integrations of the element use three integration points for each layer in the laminate. The total number of layer-integration points in an element is 5x3xNumber-of-layers.

Rail-Shear Panel

Rail-shear fixtures are frequently used to measure ply in-plane shear strength. The ply shear strength is defined as the ultimate shear strength which is the shear load at failure divided by the area over which the load was applied. Note that ply shear strength determined this way corresponds to the failure strength of the laminate rather than the ply shear strength corresponding to the first matrix cracking.

Chang and Chen [45] performed a series of rail-shear tests on $[0_n / 90_n]_s$ clustered laminates where the number of layers *n* was varied. Their results showed that as the laminate thickness increased (larger number of *n* clustered plies), the in-plane shear strength decreased.

Problem Statement

The rail-shear specimen used in this analysis is a cross-ply laminate performed by Chang and Chen [45] and reported in the analytical results by Shahid [46]. The specimen used is a 24-ply $[0_6 / 90_6]_s$ laminate fabricated from a T300/976 graphite-epoxy composite with a ply thickness of 0.0052 inches. The specimen is 6-inches long and 1-inch wide. In order to represent the boundary conditions of the specimen in a rail-shear fixture, one edge of the specimen is firmly fixed, while on the other parallel edge, deformations are only allowed parallel to the edge in the *y*-direction and restrained from motion in the *x*-direction. Upon loading, a displacement increment is applied along the latter edge. The material properties for the T300/976 material system are shown in Table 4.

Table 4. Material Properties for T300/976 Material System

Material Properties		Value [46,47]
Longitudinal Young's Modulus	E_{11}	20.2 msi
Transverse Young's Modulus	E_{22}	1.41 msi
Poisson's Ratio	ν_{12}	0.29
In-Plane Shear Modulus	G_{12}	0.81 msi
Longitudinal Tensile Strength	X_T	220.0 ksi
Longitudinal Compression Strength	T_C	231.0 ksi
Transverse Tensile Strength	Y_T	6.46 ksi
Transverse Compression Strength	Y_C	36.7 ksi
In-Plane Shear Strength	T	6.0 ksi

A finite element model of this specimen with 48 4-node elements along the length and 8 4-node elements along the width is shown in Figure 3. The accuracy of this spatial discretization is established by considering a finer finite element mesh of 72 4-node elements along the length and 12 4-node elements along the width.

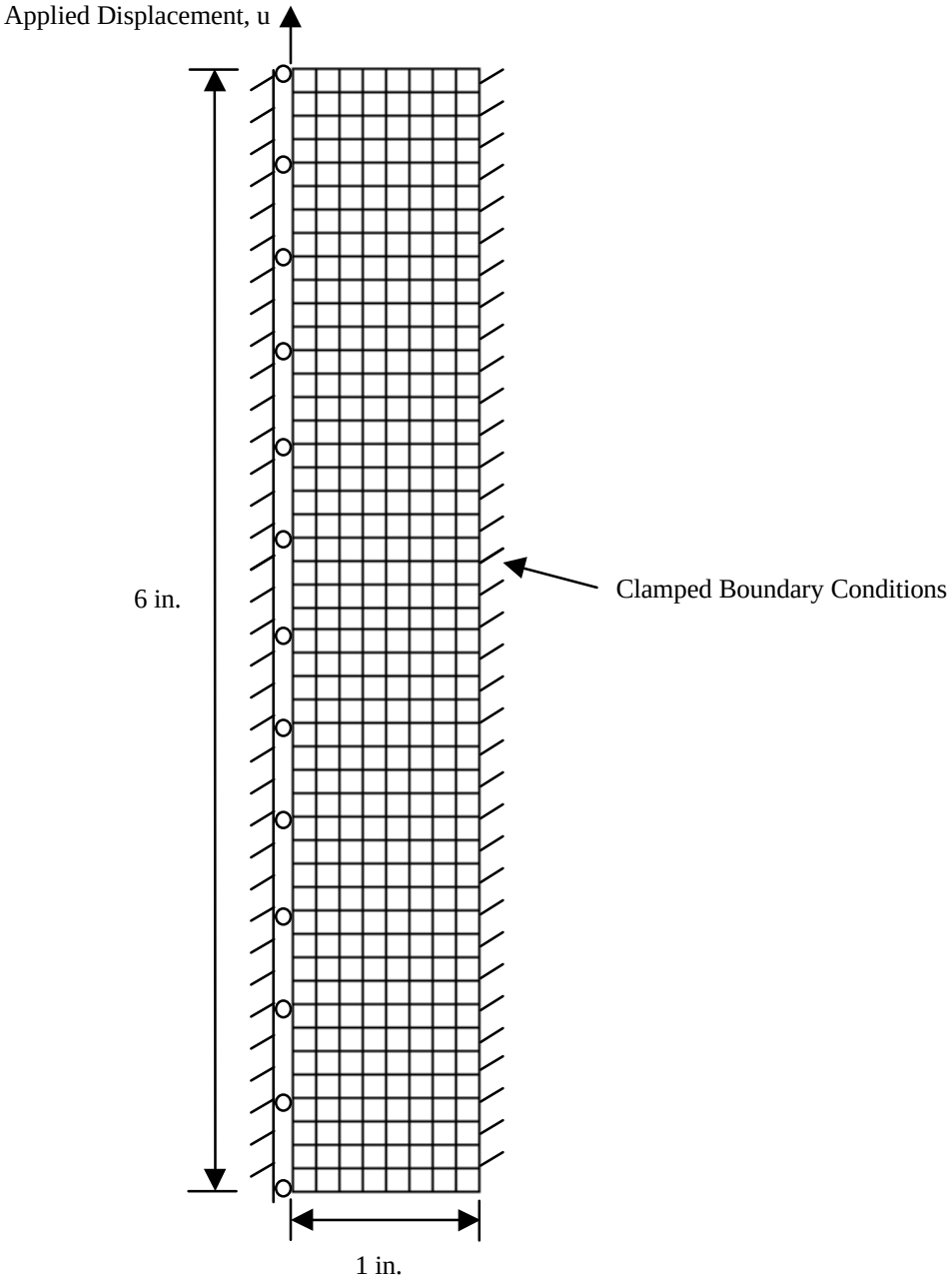

Figure 3. Geometry, loading, and boundary conditions of rail-shear specimen with 48 x 8 finite element mesh.

Structural Response

The structural response of the rail-shear specimen is studied. Progressive failure studies are performed on the model to evaluate the three failure criteria methods, finite element mesh refinement, rate of material degradation, and finally displacement increment of the progressive failure analysis. For all analyses, an initial displacement of 0.00050 inches is applied to the rail-shear specimen.

In the first progressive failure analysis study on the rail-shear specimen, the effect of mesh refinement on the model is analyzed. Hashin's criterion is chosen as the failure criterion. Two rail-shear models were analyzed: one with a mesh refinement of 48 x 8 elements and the other with a refinement of 72 x 12 elements. The displacement increment is 0.00050 inches and the degradation factor α is 10^{-20} (properties were set to zero). The progressive failure results are compared to the analytical ultimate failure load from Shahid [46] and the test data from Chang and Chen [45] in Table 5. The results indicate that the mesh refinement of 48 x 8 elements is sufficient predicting the final failure load. However, the mesh refinement did affect the prediction of the first ply failure load.

Table 5. Rail-Shear Problem: Effect of Mesh Size - Hashin's Criterion.

Mesh Size	First Ply Failure Load (lbs.)	Final Failure Load (lbs.)	Dominant Failure Mode Type
48 x 8 elements	2406	4016	Matrix Tension (Dominated by Shear Failure)
72 x 12 elements	2101	4008	Matrix Tension (Dominated by Shear Failure)
Shahid's Results [46]	Unavailable	4010	Shear
Test Data [45]	Unavailable	3850	Shear

Since equilibrium is not re-established after the material properties have been degraded in the current progressive failure analysis procedure, the load increment sizes must be small for accurate results. In the next progressive failure analysis study, the effect of the displacement increment size for the nonlinear analysis is studied. Two edge displacement increment sizes are studied: one with a displacement increment of 0.00025 inches and the other with a displacement increment of 0.00050 inches. Again, Hashin's criterion is chosen for the failure criterion and the model has a mesh refinement of 48 x 8 elements. The material degradation factor α is again chosen to be 10^{-20} (properties were set to zero). The results of this study are shown in Figure 4. Table 6 summarizes the progressive failure load predictions with the test data and Shahid's analytical results. The analysis using a displacement increment of 0.00050 inches had a converged solution for an applied edge displacement of 0.075 inches, but failed to get a converged solution at 0.080 inches. The analysis using a displacement increment of 0.00025 inches also had a converged solution for an applied edge displacement of 0.075 inches, and also had a converged solution at an additional load step at 0.0775 inches in the progressive failure analysis. The results indicate that the displacement increment sizes of 0.00050 inches and 0.00025 inches predict nearly the same failure load at a given applied edge displacement. Even though the analysis using the smaller displacement increment of 0.00025 inches predicted a higher final failure load, this final failure load was only 2.7% higher than the final failure load predicted by the larger displacement increment of 0.00050 inches. Therefore, a displacement increment size of 0.00050 inches is sufficient for accurate progressive failure prediction. The jump in the load-deflection curve at a displacement of 0.005 inches for the progressive failure analyses was due to a load redistribution after a large number of failures occurred.

The progressive failure results also differed slightly from Shahid's results. This can be attributed to Shahid modeling the nonlinear behavior of the shear modulus in his analysis which was not modeled in the COMET progressive failure analysis.

Table 6. Rail-Shear Problem: Effect of Displacement Increment Size, Hashin's Criterion

Displacement Increment Size	First Ply Failure Load (lbs.)	Final Failure Load (lbs.)	Dominant Failure Mode Type
0.00050	2406	4016	Matrix Tension (Dominated by Shear Failure)
0.00025	2406	4126	Matrix Tension (Dominated by Shear Failure)
Shahid's Results [46]	Unavailable	4010	Shear
Test Data [45]	Unavailable	3850	Shear

The next study to be analyzed is the effect of the material degradation factor α on the progressive failure analysis results. Three values of α are chosen to be studied: 10^{-1}, 10^{-2}, and 10^{-20}. For this study Christensen's criterion is chosen for the failure criterion, the mesh refinement is 48 x 8 elements, and the displacement increment is 0.00050 inches. Table 7 shows the progressive failure results of this study for the ultimate failure load with the test data and Shahid's analytical results. The results show that the material degradation factor α has little effect on the final failure prediction in this example.

Table 7. Rail-Shear Problem: Effect of Material Degradation Factor α, Christensen's Criterion

Material degradation factor, α	First Ply Failure Load (lbs.)	Final Failure Load (lbs.)	Dominant Failure Mode Type
10^{-1}	2105	3972	Fiber-Matrix interaction
10^{-2}	2105	3965	Fiber-Matrix interaction
10^{-20}	2105	3964	Fiber-Matrix interaction
Shahid's Results [46]	Unavailable	4010	Shear
Test Data [45]	Unavailable	3850	Shear

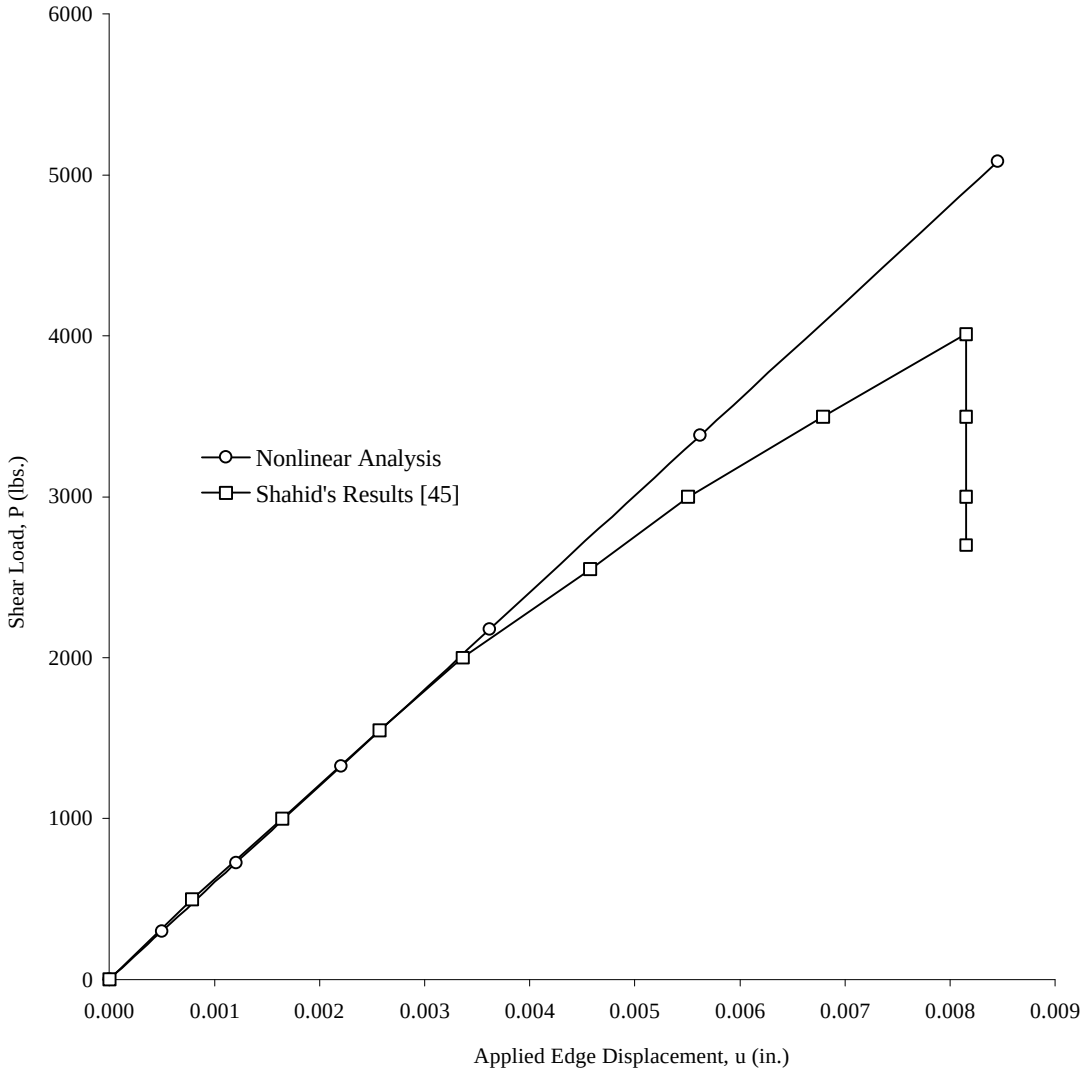

Figure 4. Rail-Shear problem: Effect of displacement increment size, Hashin's criterion.

In the next study, the options of the maximum strain criterion described earlier are investigated. For this study, the displacement increment is set at 0.0005 inches and α is set at 10^{-20}. Table 8 presents the results from this study. Option 1 of the maximum strain criterion, which allows no induced failures, comes closest to the test data.

Table 8. Rail-Shear Problem: Comparison of Maximum Strain Options

Option	First Ply Failure Load (lbs.)	Final Failure Load (lbs.)	Dominant Failure Mode Type
1	2707	4065	Shear
2	2707	4312	Shear
3	2707	4269	Shear
Shahid's Results [46]	Unavailable	4010	Shear
Test Data [45]	Unavailable	3850	Shear

A summary of the results for the three failure criteria is presented in Table 9. A load-deflection curve is included in Figure 5 which compares the three failure criteria with Shahid's analytical results. The load-displacement curve data with the test data was not available for comparison. All progressive failure results agree very well with Shahid's analytical results. Figure 6 shows the structural response of the panel at final failure using Christensen's criterion. The left figure indicates the percentage failure of an element which is quantified as the percentage of ply-integration points with failures within an element (total number of integration points with failures divided by the total number of integration points in an element). The right figure depicts the N_{xy} stress resultant distribution. Dark regions indicate high values. The progressive failure analyses of the other criteria show similar structural responses. The panel experiences 100% failure along the edges of the panel where the shear loading is applied. Consequently, the load carrying capability along the edges is zero.

Table 9. Rail-Shear Problem: Summary of Progressive Failure Results

Failure Criterion	First Ply Failure Load (lbs.)	Final Failure Load (lbs.)	Dominant Failure Mode Type
Hashin, $\alpha = 10^{-20}$	2406	4016	Matrix Tension
Christensen, $\alpha = 10^{-20}$	2105	3964	Fiber-Matrix interaction
Maximum Strain $\alpha = 10^{-20}$, Option 1	2707	4065	Shear
Shahid's Results [46]	Unavailable	4010	Shear
Test Data [45]	Unavailable	3850	Shear

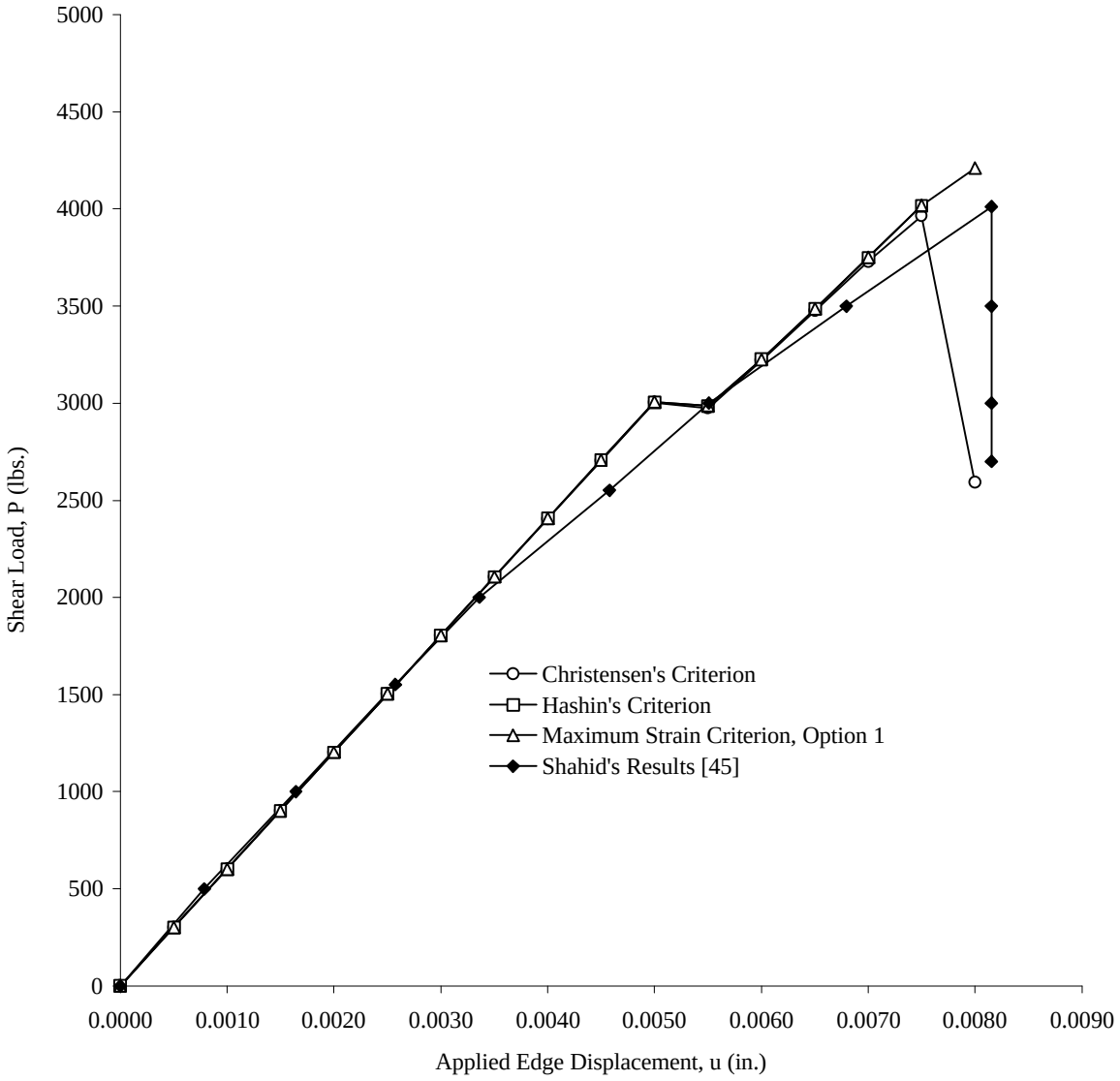

Figure 5. Rail-shear problem: Load-deflection results, $\alpha = 10^{-20}$.

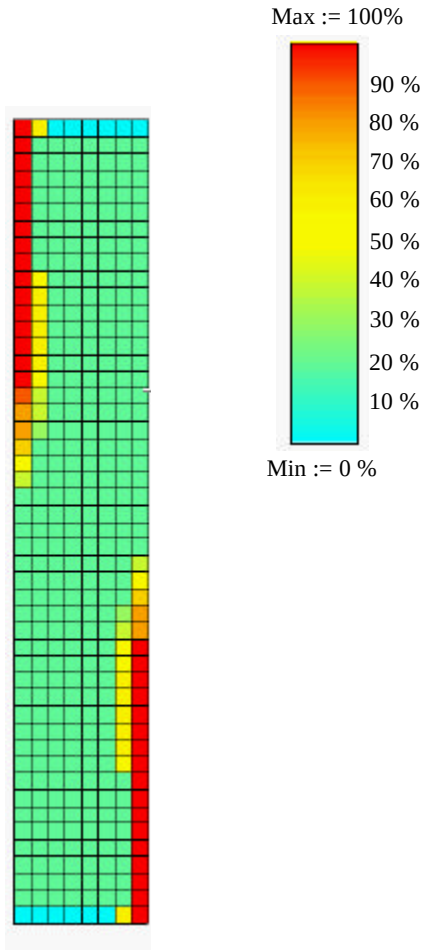

a) Percentage Failure

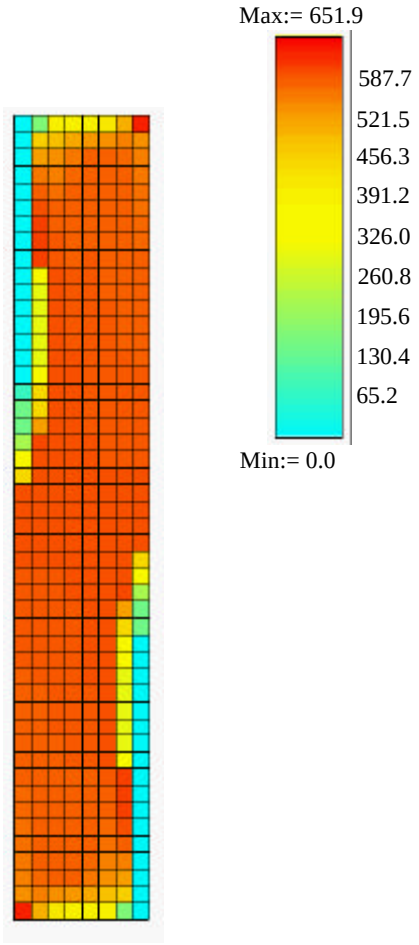

b) N_{xy} Stress Distribution, lb./in.

Figure 6. Rail-shear problem: Structural response at final failure, (3964 lbs.).
Christensen's Criterion, $\alpha = 10^{-20}$

Tension-Loaded Laminate with Hole

Problem Statement

In order to assess the accuracy of the progressive failure methodology, a 20-ply tensile specimen containing a centrally located circular hole is considered. The calculated results are compared to experimental results by Chang and Chang [31] and Tan [48]. The composite laminate is 8-inches long and 1-inch wide with a hole diameter of 0.25 inches. The thickness of each ply is 0.00515 inches, and the laminate stacking sequence is $[0/(\pm 45)_3/90_3]_s$. The specimen is fabricated from T300/1034-C graphite/epoxy. A finite element mesh for the laminate with the boundary conditions is shown in Figure 7. The sides of the laminate are free, and the loaded ends are clamped. The lamina properties for this laminate are given in Table 10.

Table 10. Material Properties for T300/1034 Material System

Material Properties		Value [31]
Longitudinal Young's Modulus	E_{11}	21.3 msi
Transverse Young's Modulus	E_{22}	1.65 msi
Poisson's Ratio	ν_{12}	0.30
In-Plane Shear Modulus	G_{12}	8.97 msi
Longitudinal Tensile Strength	X_T	251.0 ksi
Longitudinal Compression Strength	X_C	200.0 ksi
Transverse Tensile Strength	Y_T	9.65 ksi
Transverse Compression Strength	Y_C	38.9 ksi
In-Plane Shear Strength	T	19.4 ksi

Structural Response

The structural response of the laminate with an open circular hole is studied. An initial displacement of 0.0005 inches is applied to the laminate. The progressive failure analysis of the tensile specimen is analyzed using a displacement increment of 0.001 inch and a material degradation factor of $\alpha = 10^{-20}$. A study was performed on the effect of the finite element mesh of the laminate. The original finite element mesh with 768 elements is shown in Figure 7. Figure 8 shows a coarse mesh with 568 elements and a fine mesh with 1,264 elements of the laminate model. Christensen's criterion was used for the failure criteria in this study. The first mesh (Figure 7) had eight rings of elements around the hole. The coarse mesh had six rings of elements around the hole. The fine mesh had 12 rings of elements round the hole. Table 11 summarizes the results of this study. These results indicate the sensitivity of the local stress distribution near the hole in predicting final failure. The fine mesh predicted the lowest final failure load. However, since the difference was not very significant and because the fine mesh analysis needed more computational time, the mesh with 768 elements is used for all other analyses. Another study is performed to analyze the effect of the material degradation factor. However, varying the α parameter had little effect on the progressive failure results.

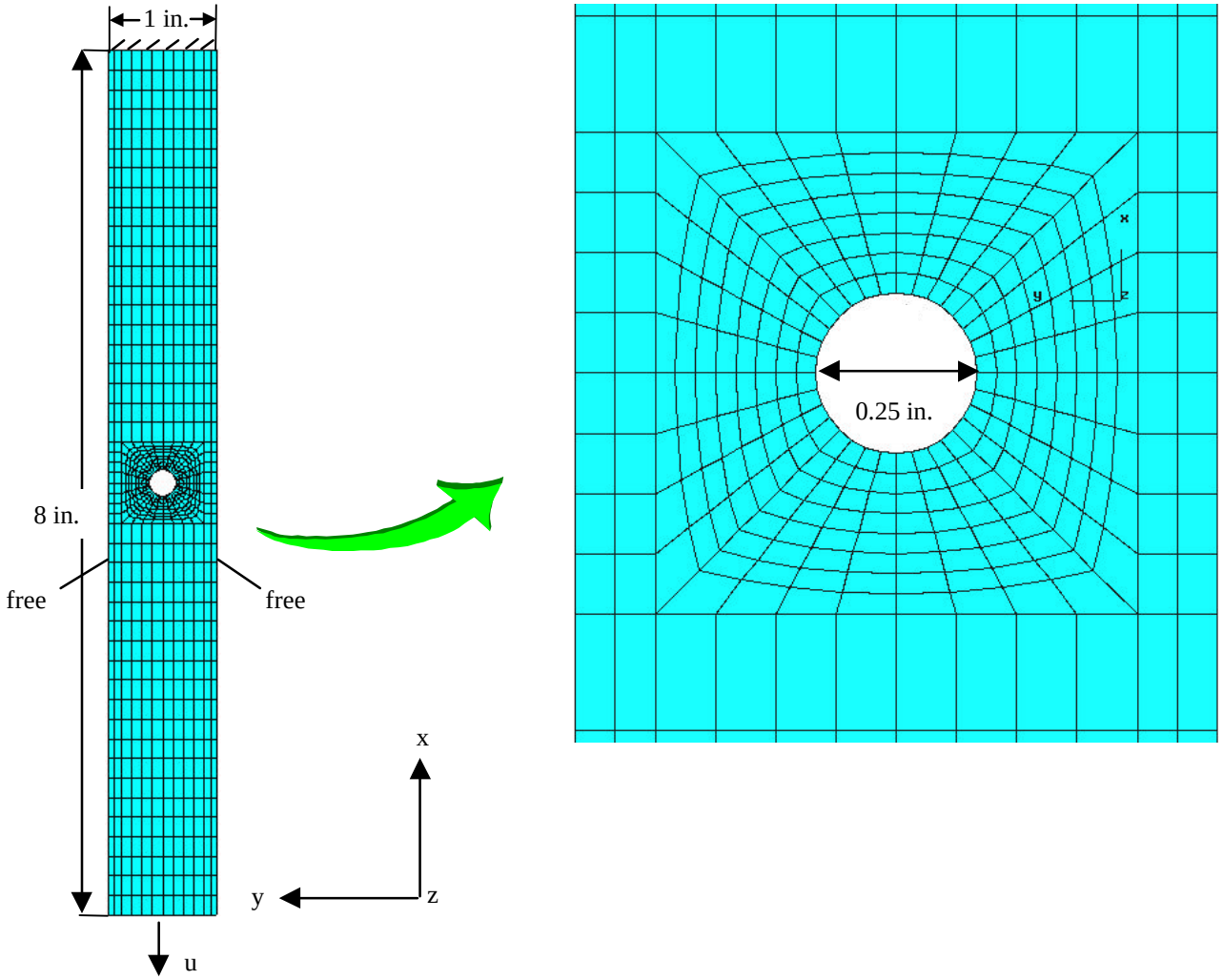

Figure 7. Geometry, loading, and boundary conditions of tension-loaded laminate with hole.

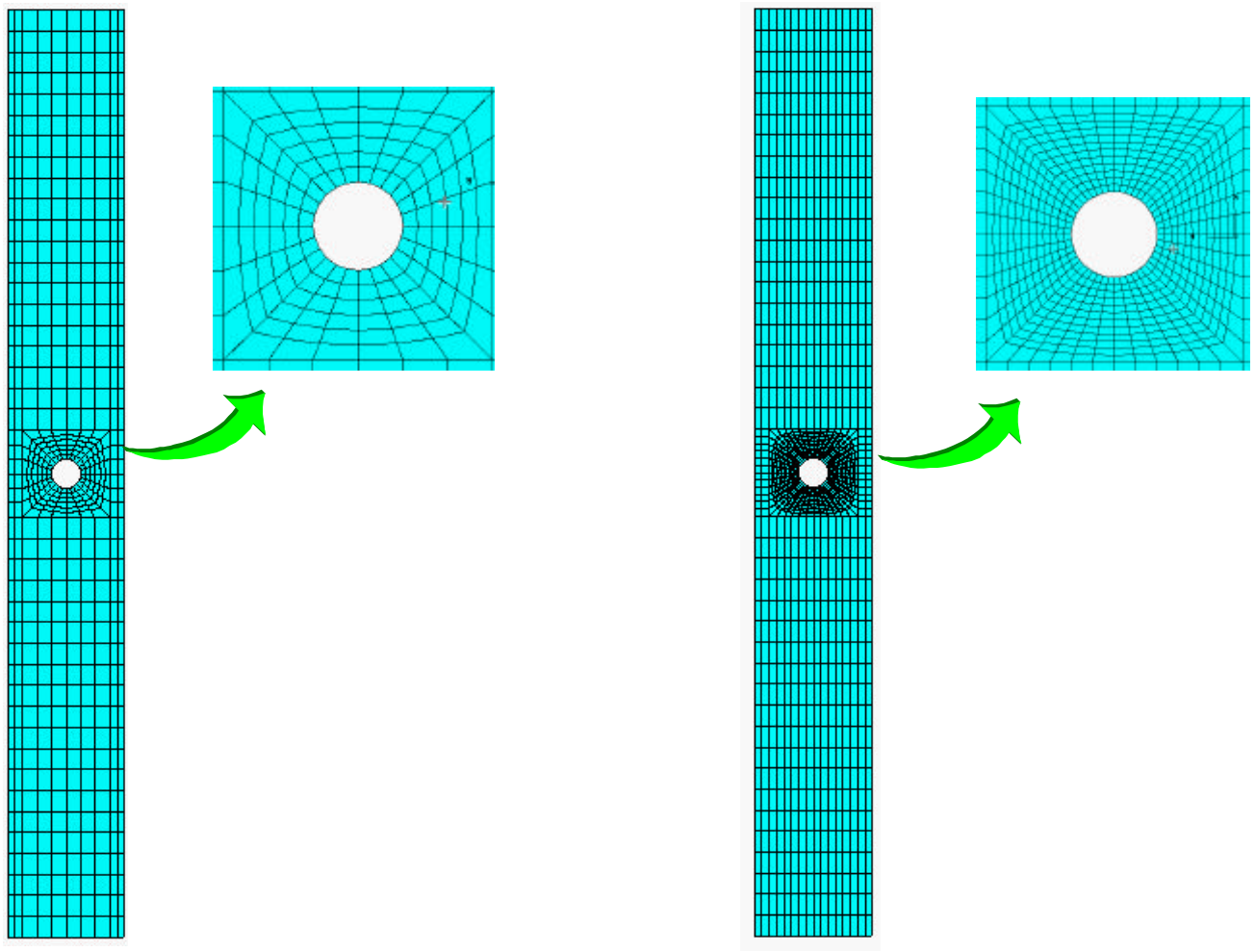

a) Coarse Mesh Model

b) Fine Mesh Model

Figure 8. Meshes for tension-loaded laminate with hole.

Next, a progressive failure analysis is performed using Hashin's criterion. The mesh with 768 elements is used in this analysis with the same parameters of displacement increment sizes and material degradation factor used in the previous study. A comparison of the progressive failure results for Hashin's criterion is shown in Table 12 with experimental results and the results using Christensen's criterion. The Maximum Strain criterion was not included in this study because it does not include any strain interaction between the failure modes. The progressive failure results agree reasonably well with the experimental results from Chang [31]. A load-displacement curve for these analyses is shown in Figure 9.

Figures 10 and 11 show comparisons of the structural response at final failure using Hashin's and Christensen's criteria. Each figure displays a close-up view of the region near the hole. The left figure indicates the percentage of failure within an element, and the right figure depicts the N_x stress resultant distribution. Dark regions indicate high values. The results indicate that for this problem there is little difference between the Hashin's criterion and Christensen's criterion in predicting the failure loads. The N_x stress resultant distribution for Christensen's criterion showed a larger high stress region around the edge of the hole than Hashin's criterion.

Table 11. Tension-Loaded Laminate with Hole: Effect of Finite Element Mesh, Christensen's Criterion

Number of Elements	First Ply Failure Load (lbs.)	Final Failure Load (lbs.)	Dominant Failure Mode Type
568	1520	3263	Fiber/Matrix Interaction
768	1520	3261	Fiber/Matrix Interaction
1,264	1446	3195	Fiber/Matrix Interaction

Table 12. Tension-Loaded Laminate with Hole: Comparison of Failure Results

Failure Criterion	First Ply Failure Load (lbs.)	Final Failure Load (lbs.)	Dominant Failure Mode Type
Hashin's Criterion	1520	3212	Matrix Tension
Christensen's Criterion	1520	3261	Fiber/Matrix Interaction
Experimental Results [31]	Unavailable	3523	Unavailable

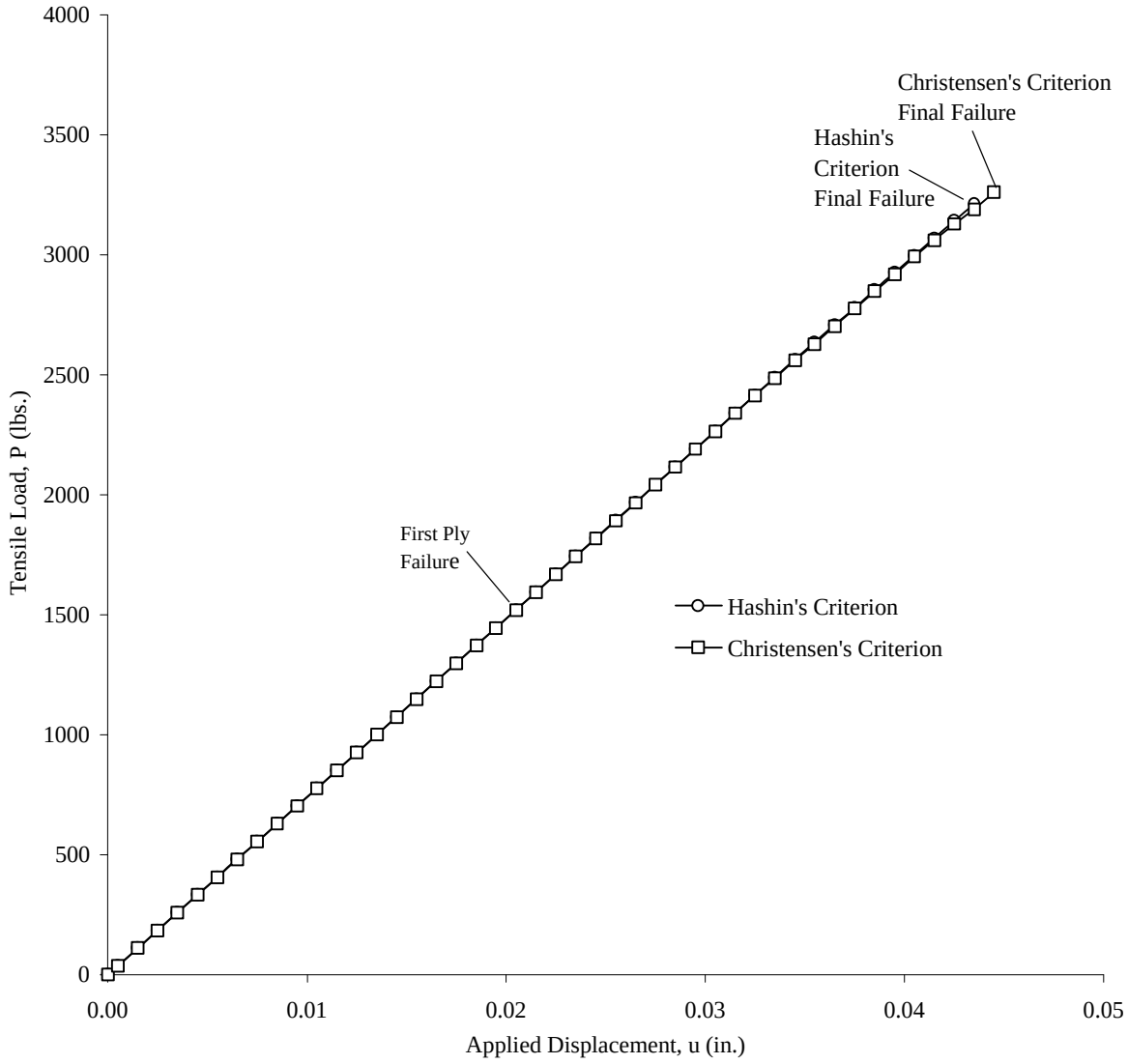

Figure 9. Tension-loaded laminate with hole: Load-deflection results, $\alpha = 10^{-20}$.

.

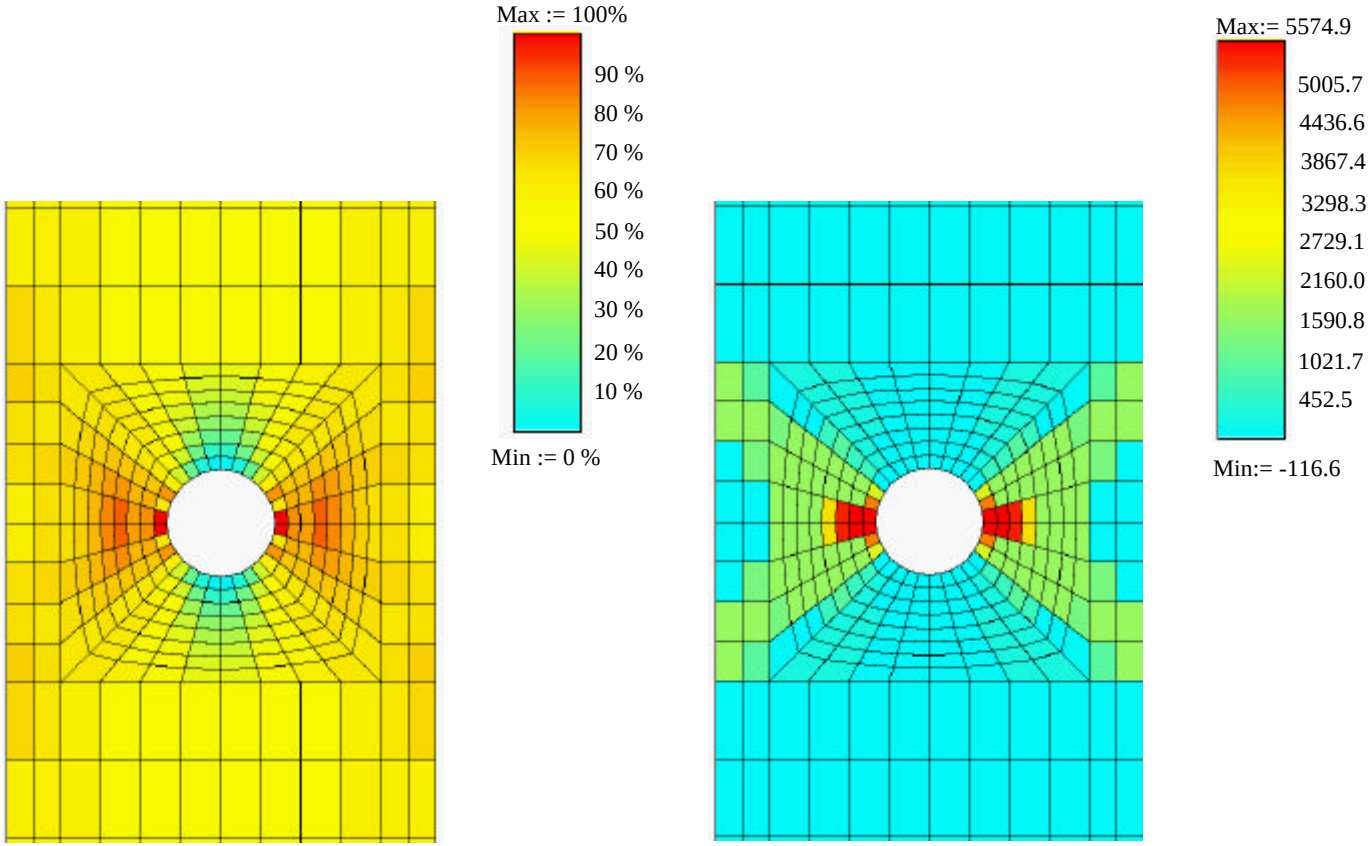

a) Percentage Failure

b) N_x Stress Distribution, lb./in.

Figure 10. Tension-loaded laminate with hole: Structural response at final failure (3212 lbs.). Hashin's criterion, $\alpha = 10^{-20}$

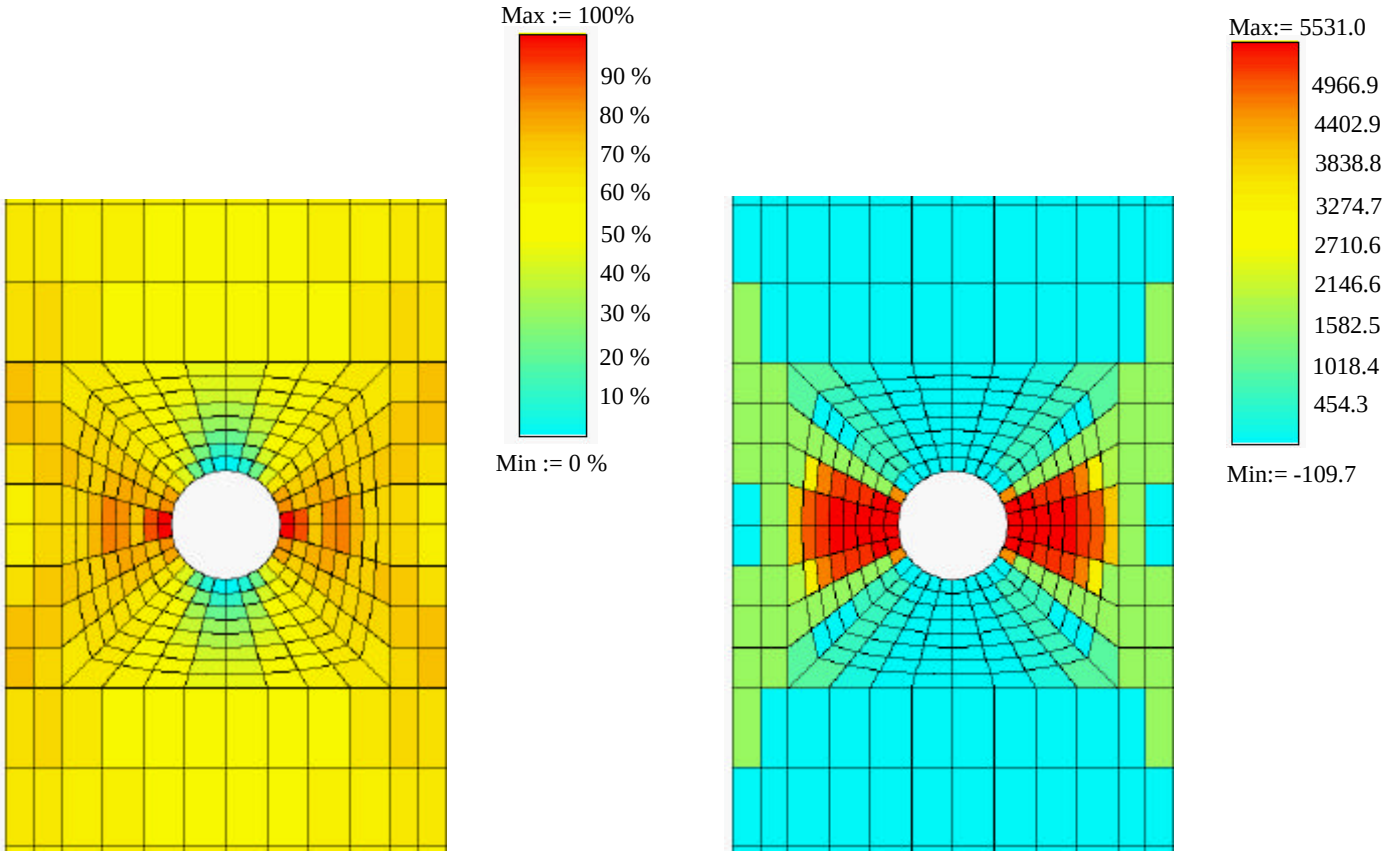

a) Percentage Failure

b) N_x Stress Distribution, lb./in.

Figure 11. Tension-loaded laminate with hole: Structural response at final failure (3261 lbs.). Christensen's criterion, $\alpha = 10^{-20}$

Compression-Loaded Composite Panel

Problem Statement

The next problem is a composite rectangular panel loaded in axial compression. The panel length is 20.0 inches and the width is 6.75 inches and is denoted Panel C4 in the experimental results reported by Starnes and Rouse [49]. The panel used is a 24-ply orthotropic lay-up. The thickness of each ply is 0.00535 inches and the laminate stacking sequence is $[\pm 45/0_2/\pm 45/0_2/\pm 45/0/90]_S$. The panel is fabricated from unidirectional Thornel 300 graphite-fiber tapes preimpregnated with 450K cure Narmco 5208 thermosetting epoxy resin. The lamina properties for this panel are given in Table 13.

Table 13. Material Properties for C4 Panel, T300/5208 Material System

Material Properties		Value [49,27]
Longitudinal Young's Modulus	E_{11}	19.0 Msi
Transverse Young's Modulus	E_{22}	1.89 Msi
Poisson's Ratio	ν_{12}	0.38
In-Plane Shear Modulus	G_{12}	0.93 Msi
Longitudinal Tensile Strength	X_T	200.0 Ksi
Longitudinal Compression Strength	X_C	165.0 Ksi
Transverse Tensile Strength	Y_T	11.74 Ksi
Transverse Compression Strength	Y_C	27.41 Ksi
In-Plane Shear Strength	T	10.0 Ksi

The finite element model of this panel has 40 4-node elements along the length and 14 4-node elements along the width as shown in Figure 12. The loaded ends of the panel are clamped by fixtures, and the unloaded ends are simply supported by knife-edge supports to prevent the panel from buckling as a wide column.

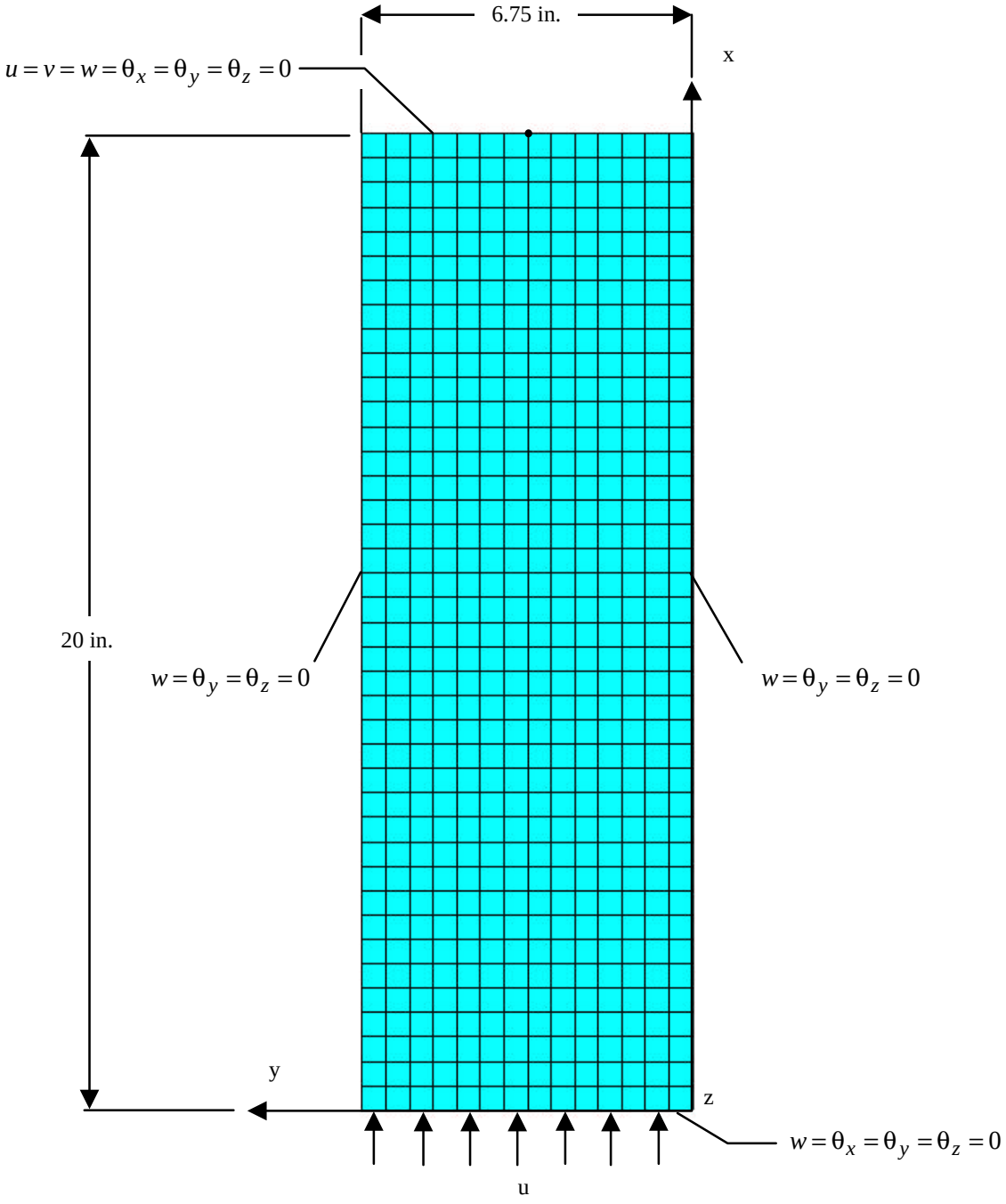

Figure 12. Geometry, loading, and boundary conditions for C4 panel.

Structural Response

The structural response of the C4 panel is studied. A fringe plot of the first buckling mode from the linear stability analysis is shown in comparison to the moiré-fringe plot from the Starnes and Rouse experiment [49] in Figure 13. The results indicate that the first buckling mode from the analysis and the experiment are in agreement with each other. The first buckling mode has two longitudinal half-waves with a buckling mode line at the panel midlength. An initial geometric imperfection is formed by using the first buckling mode shape normalized by its maximum component. This normalized mode shape is then scaled by 5% of the panel thickness and added to the nodal coordinates. The eccentricity is added to the initial geometry to allow efficient progress past the critical buckling point, but does not affect the results in the postbuckling range. The initial displacement applied to the panel is 0.001 inch. A comparison between the test results and the elastic nonlinear analysis (no damage) results is shown in Figure 14. The elastic nonlinear analysis response without damage correlates very well with the experimental result up to the final failure of the panel and then continues on until a maximum load level is reached.

Progressive failure analyses using Hashin's and Christensen's criteria were performed on the C4 panel using a material degradation factor of $\alpha = 10^{-20}$. Similar progressive failure results have also been performed by Engelstad et al. [27]. A displacement increment of 0.0025 inches is used for the first 10 steps in the progressive failure analysis. Then a smaller increment of 0.001 inch is chosen for the next 5 load (steps 11-15) so the analysis could pass the buckling load. In load steps 16-40, a displacement increment of 0.0025 inches is used for the analysis. Finally, a displacement increment of 0.001 inch is used near the failure of the panel (steps 41 to failure).

The progressive failure results for the C4 panel are presented in Figures 15 and 16 for Hashin's and Christensen's criteria. Figure 15 shows the comparison of experimental and analytical out-of-plane deflections near a point of maximum deflection as a function of the applied load. The analytical results correlate reasonably well to the experimental results up to the buckling load and then are lower than the experimental results in the postbuckling regime. Figure 16 shows a comparison of analytical and experimental end shortening results as a function of the applied load. The progressive failure results for load-end shortening also agree with the experimental results. At some point in the progressive failure analysis, a dramatic change in the slope of the end shortening curve indicates an inability for the panel to support any additional load. This location is designated as the analytical failure load, and the final experimental data point is called the test failure load. The final failure loads predicted by both criteria are very close to each other. Hashin's criterion was less than 3% from the test failure load and Christensen's criterion was 8% from the test failure load. However, the first ply failure (FPF) load of Christensen's criterion was much lower than Hashin's criterion. Both failure criteria predicted slightly higher failure loads than the results from the experiment. Starnes and Rouse reported that the test failure mode was due to transverse shear effects near the node line in the buckle pattern as shown in Figure 17. Since the current progressive failure analysis capability does not include a transverse shear failure mode, these analytical results cannot capture this failure mode. Despite this, the progressive failure analysis predictions still are in good agreement with the test results. Table 14 provides a summary of the failure loads (first ply failure and final failure) and the dominant failure mode type for both failure criteria and the test results. The dominant failure mode of Christensen's criterion is fiber/matrix interaction and the dominant mode of Hashin's criterion is failure in matrix tension. In the experiment, the panel failed along the nodal line due to transverse shear failure as a result of coupling of large out-of-plane deflections and high transverse shear strains near the panel's edges.

The structural response of the C4 panel at final failure is given in Figures 18 and 19 using Hashin's criterion. Figures 20 and 21 show the structural response at the final failure load using Christensen's criterion. Figures 18 and 20 display the percentage of failures within an element, the N_x stress distribution, and the out-of-plane deflection of selected steps in the progressive failure analysis while Figures 19 and 21 show the N_y and N_{xy} stress distribution. The results show that the damage is concentrated along the nodal line just as the test results showed. The final failure results obtained using Hashin's criterion in Figure 18 and Christensen's criterion in Figure 20 also reveal the possible failure event. The deflection pattern exhibits large deflections and high local gradients. The high in-plane membrane stress resultants and their gradients near the buckle nodal line contribute to the failure propagation and final failure.

Table 14. C4 Panel: Comparison of Failure Results, $\alpha = 10^{-20}$

Failure Criterion	First Ply Failure Load (lbs.)	Final Failure Load (lbs.)	Dominant Failure Mode Type
Christensen's Criterion	18615	22454	Fiber/Matrix Interaction
Hashin's Criterion	21778	23526	Matrix Tension
Test Results [49]	Unavailable	21910	Transverse Shear

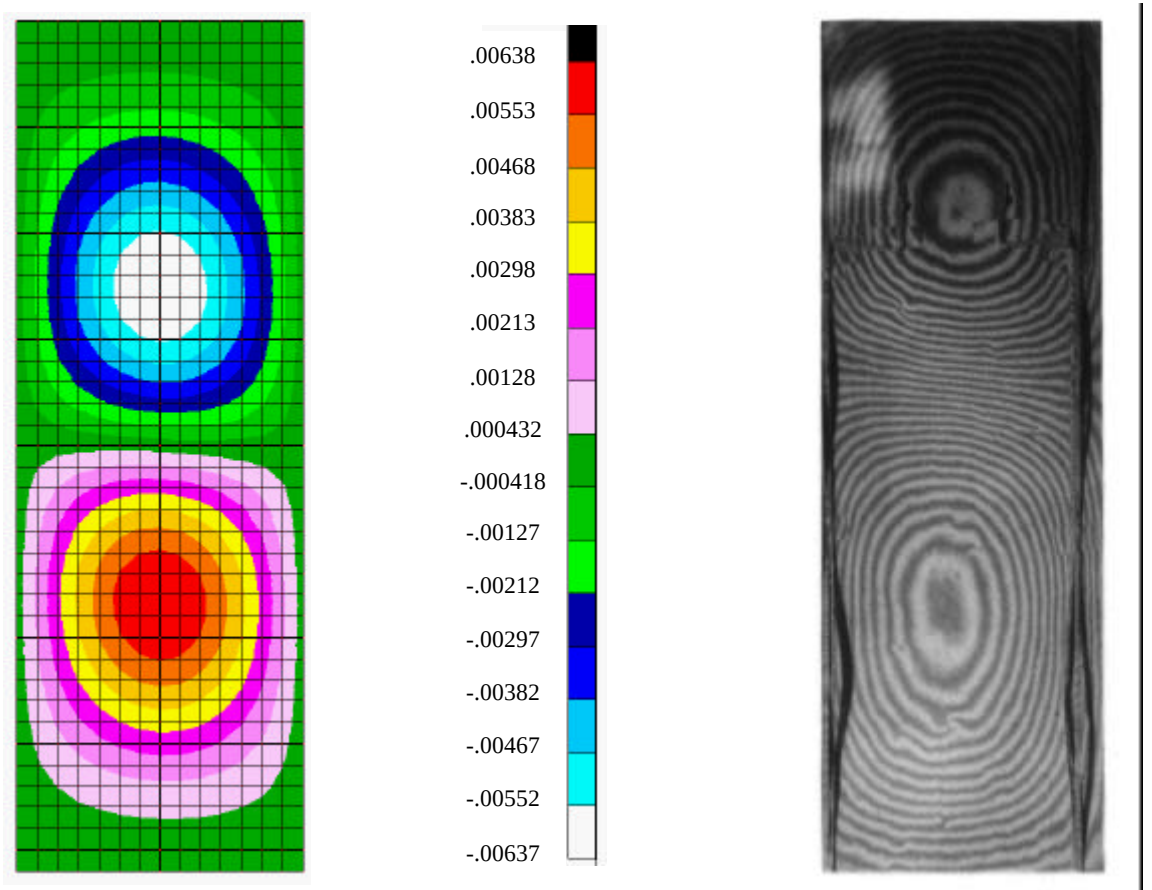

a) Fringe Plot of FEM Results, in.

b) Photograph of Moiré-Fringe Pattern [49]

Figure 13. C4 panel: Comparison of experimental and analytical linear buckling mode 1.

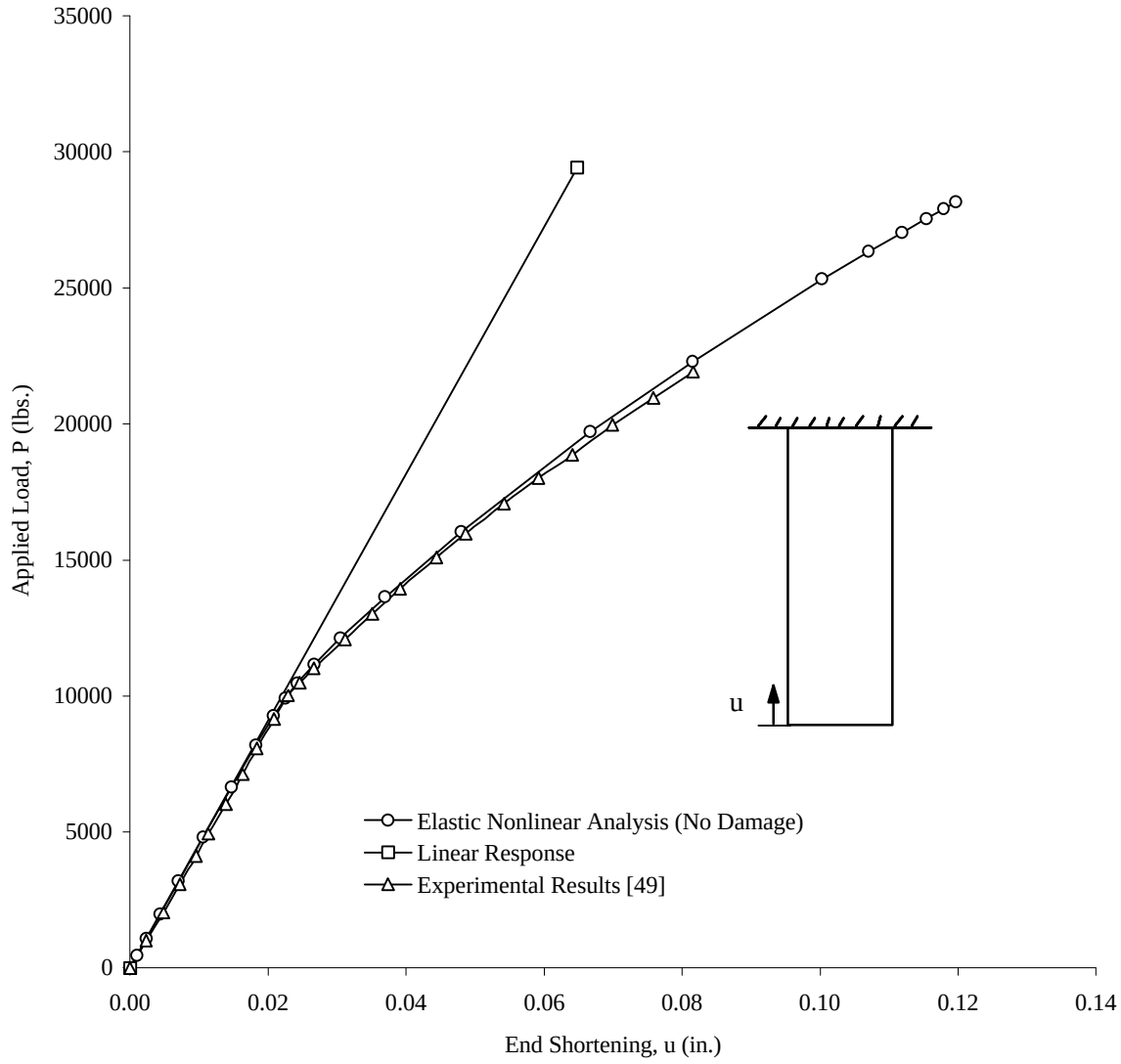

Figure 14. C4 panel: End-shortening results.

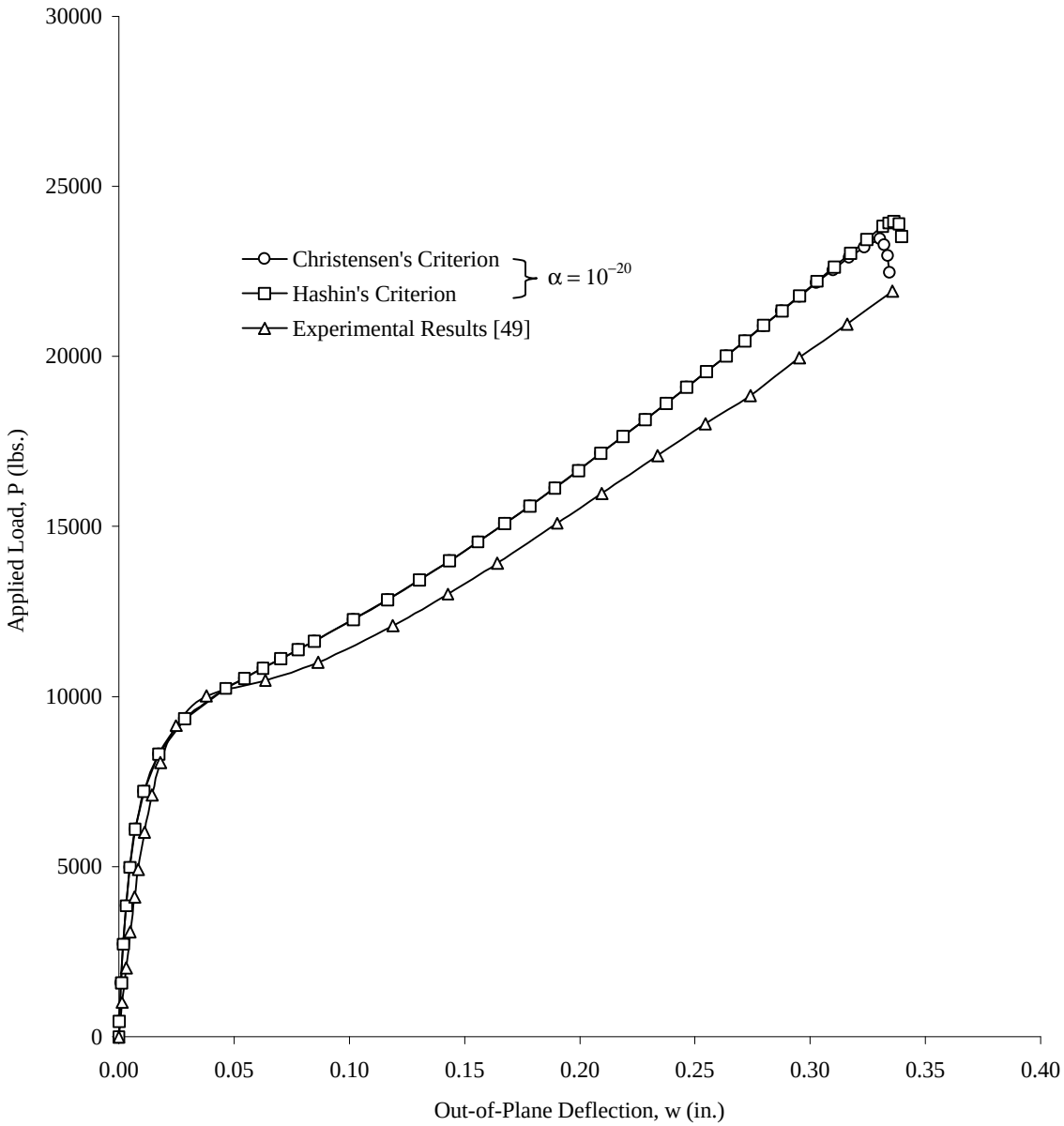

Figure 15. C4 panel: Out-of-plane deflection comparison.

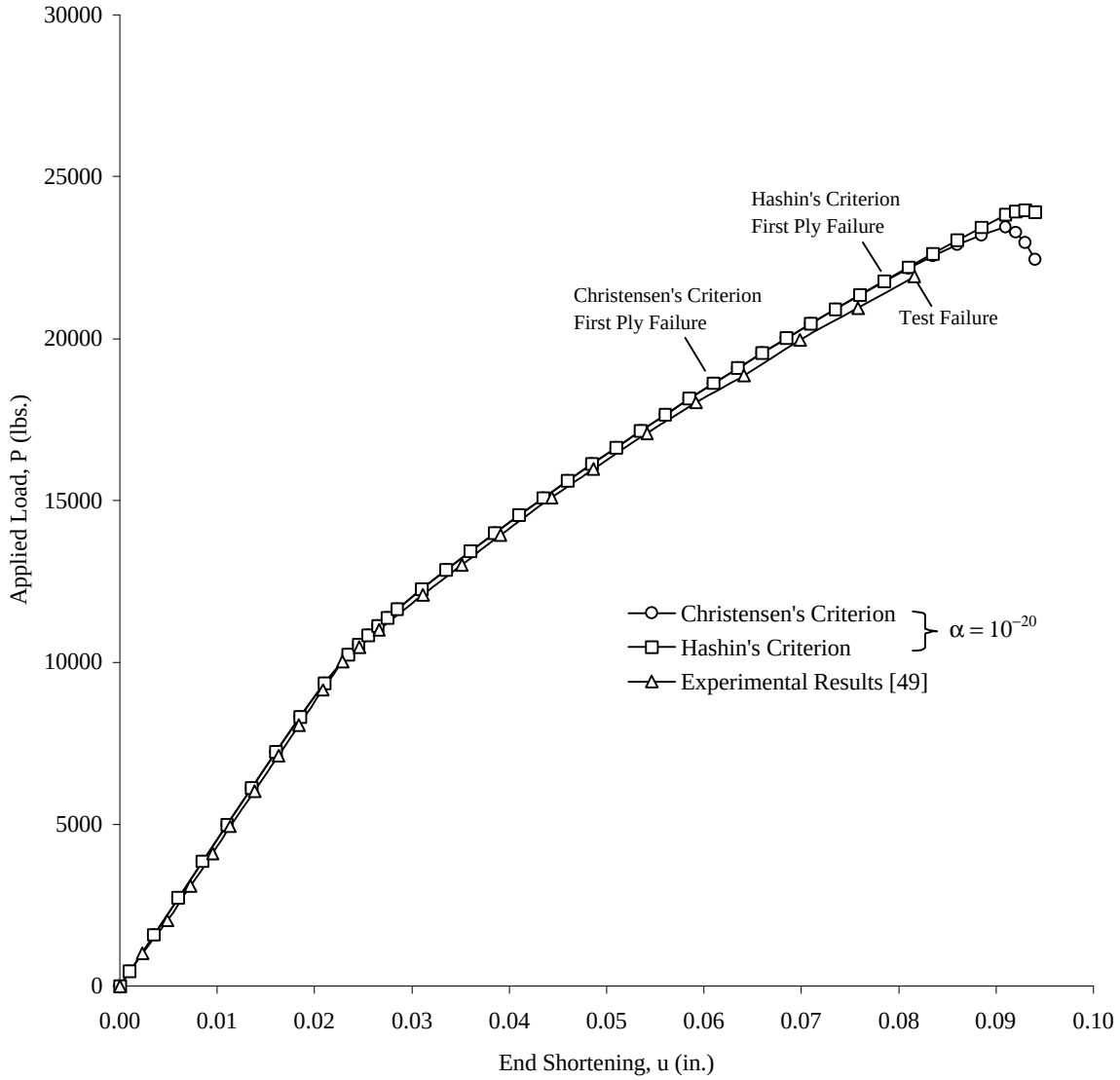

Figure 16. C4 panel: End-shortening comparison.

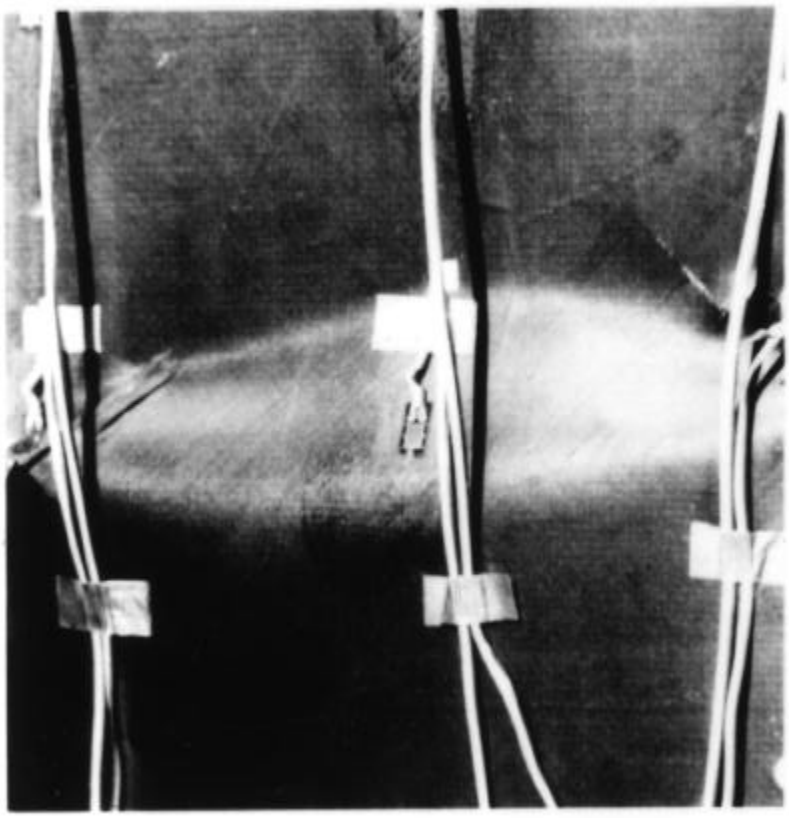

Figure 17. C4 panel: Photograph of failure mode from Starnes and Rouse experiment [49].

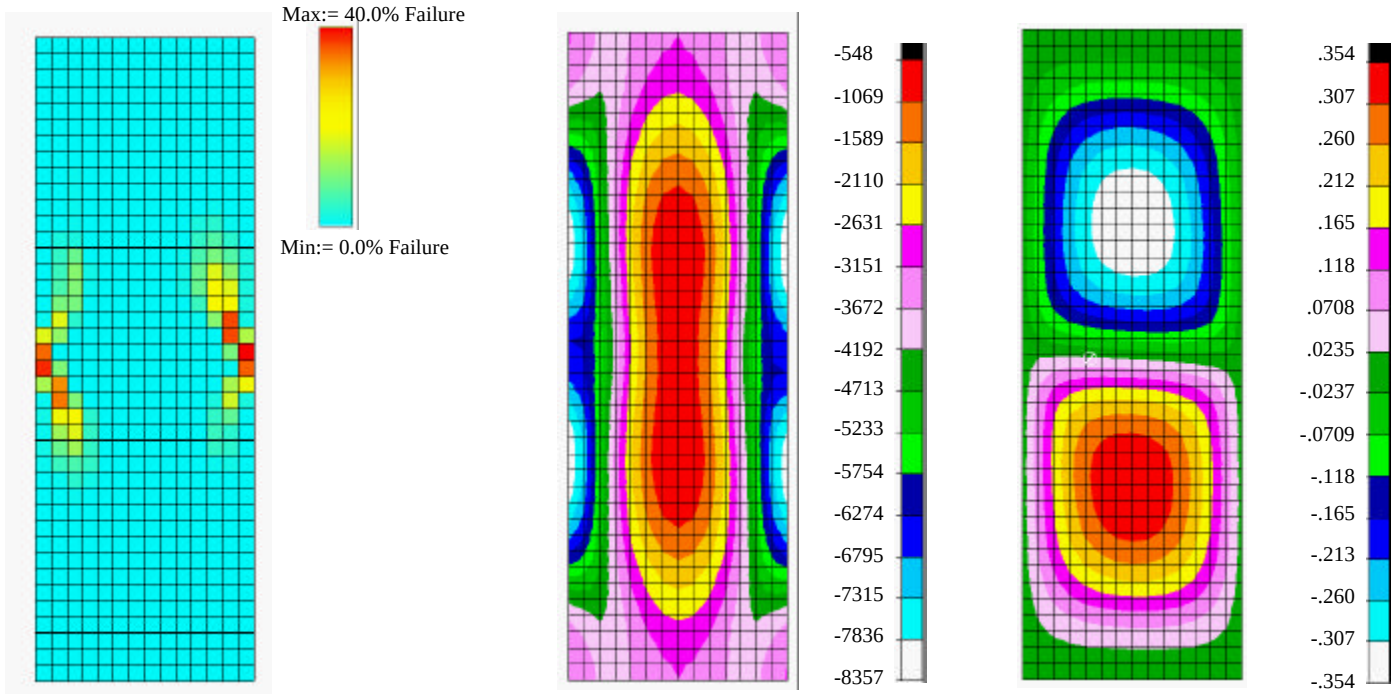

a) Percentage Failure

b) N_x Stress Distribution, lb./in.

c) Out-of-Plane Deflection, in.

Figure 18. C4 panel: Structural response at final failure (23526 lbs.).
Hashin's criterion, $\alpha = 10^{-20}$

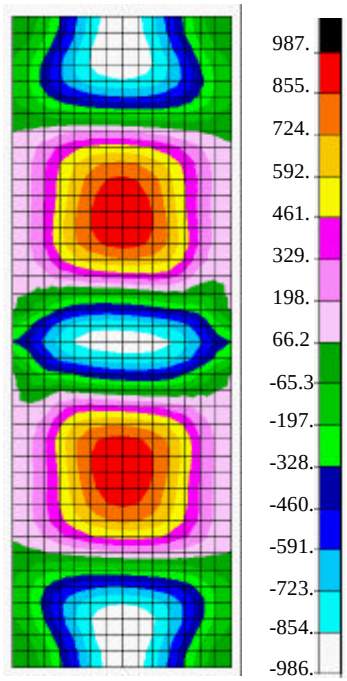

d) N_y Stress Distribution, lb./in.

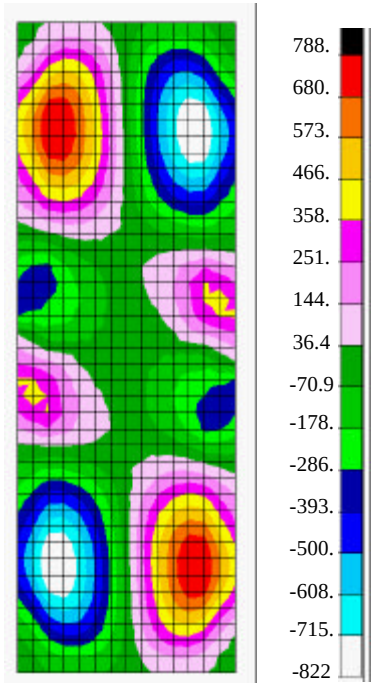

e) N_{xy} Stress Distribution, lb./in.

Figure 19. C4 panel: Structural response at final failure (23526 lbs.), continued.
Hashin's criterion, $\alpha = 10^{-20}$

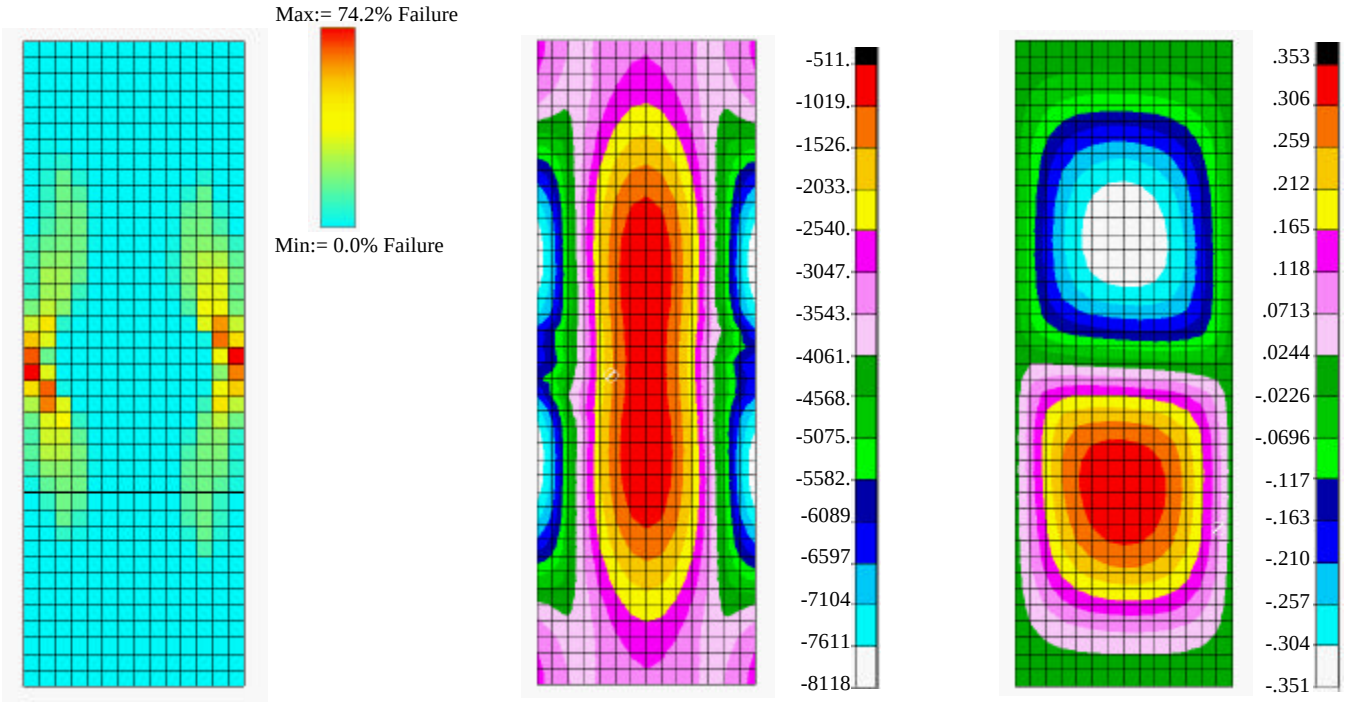

a) Percentage Failure

b) N_x Stress Distribution, lb./in.

c) Out-of-Plane Deflection, in.

Figure 20. C4 Panel: Structural response at final failure (22454 lbs.).
Christensen's criterion, $\alpha = 10^{-20}$

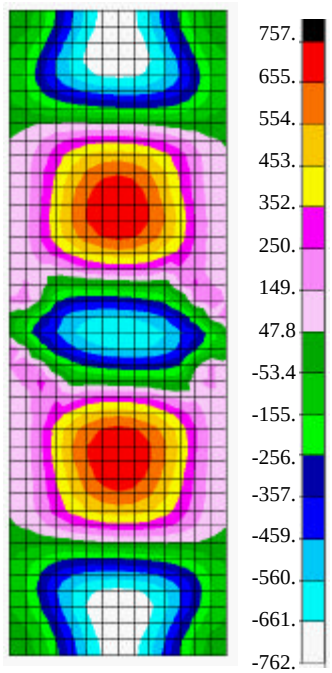

d) N_y Stress Distribution, lb./in.

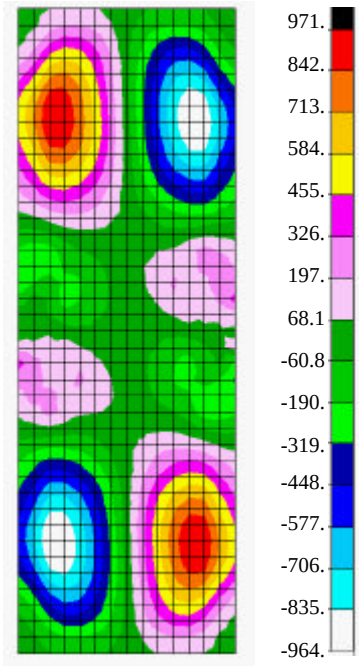

e) N_{xy} Stress Distribution, lb./in.

Figure 21. C4 Panel: Structural response at final failure (22454 lbs.), continued.
Christensen's criterion, $\alpha = 10^{-20}$

Compression-Loaded Composite Panel with Hole

Problem Statement

Consider next a composite panel with an offset circular hole loaded in compression. The panel used is a 24-ply quasi-isotropic laminate. Two identical specimens were tested and denoted as Panel H3 and Panel H4 in the experimental results reported by Starnes and Rouse [49]. Each panel length is 20.0 inches, and the width is 5.5 inches. The hole is offset from the panel center in the length direction (7.5 inches from the bottom of the panel) such that it is at or near a buckle crest. Each panel is fabricated from unidirectional Thornel 300 graphite-fiber tapes preimpregnated with 450K cure Narmco 5208 thermosetting epoxy resin. The lamina properties for this panel are given in Table 13. The thickness of each ply is 0.00574 inches, and the laminate stacking sequence is $[\pm 45/0/90/\pm 45/0/90/\pm 45/0/90]_s$.

The finite element model of this panel is shown in Figure 22. The loaded ends of the panel are clamped by fixtures, and the unloaded ends are simply supported by knife-edge supports to prevent wide-column buckling of the panel.

Structural Response

The H3/H4 panel configuration is analyzed to investigate analytical predictions of failure for a specimen with a hole. Engelstad et al. [27] also performed similar progressive failure analyses on this panel. A comparison of the first buckling mode fringe plot from the experimental and analytical results is shown in Figure 23. Four longitudinal halfwaves can be seen for the first buckling mode shape. These results agree with the experimental results in Ref. [49] and the analytical results by Engelstad. An imperfection of 5% of panel thickness for mode 1 is used to initiate the nonlinear analysis and progressive failure analysis into the postbuckling region. The eccentricity is added to the initial geometry to allow efficient progress past the critical buckling point, but does not affect the results in the postbuckling range. Hashin's criterion is used for the progressive failure analysis since it includes more failure modes than the other two criteria. An initial displacement of 0.001 inch is applied to the panel with a displacement increment of 0.0025 inches with a material degradation factor of $\alpha = 10^{-20}$. The displacement increment error norm is used as the convergence criterion for the progressive failure analysis. The displacement increment error norm was used because the modified energy norm error convergence criterion had numerical convergence difficulties.

Figure 24 contains end-shortening analytical and experimental comparisons. The only test data available for the H3 panel is for the final failure load. Figure 24 shows good correlation between the experimental results and the analytical results. However, the progressive failure analysis encountered convergence problems and under-predicted the final failure loads from the tests, 8.3% for the H3 panel and 14.4% for the H4 panel, respectively. The out-of-plane deflection comparison near the hole region is shown in Figure 25. Experimental results were available only for the H4 panel. Again, good agreement for the out-of-plane deflection exists between the H4 panel test results and the analytical results until the progressive failure analysis stopped due to convergence problems. Element distortion around the hole could be a contributing factor to the convergence problems. However, no further refinement around the hole region was performed.

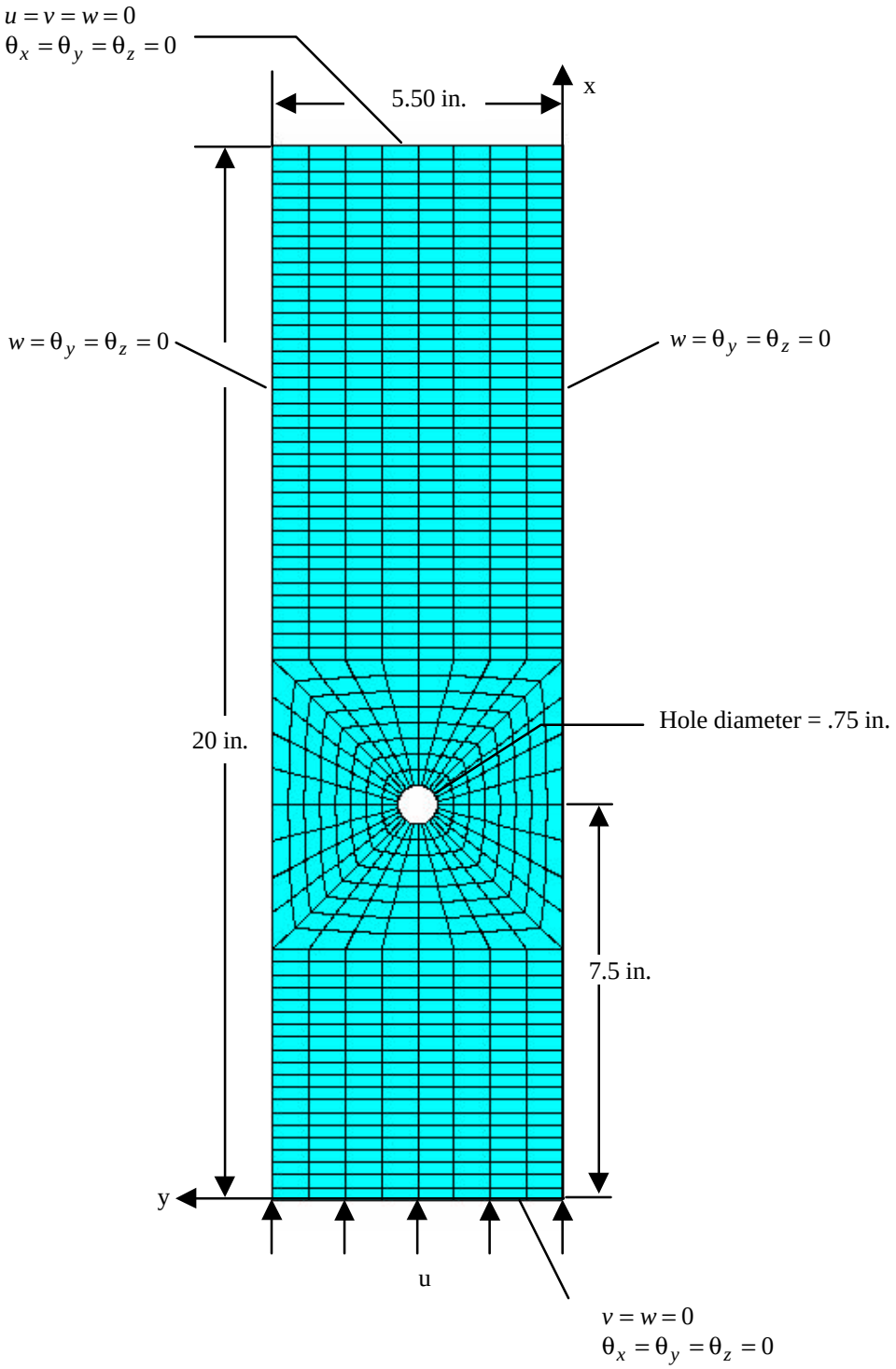

Figure 22. Geometry, loading, and boundary conditions for H3/H4 panel.

Figures 26 and 27 show the structural response of the panel at the final failure load predicted by the progressive failure analysis. Figure 26 depicts the fringe plot of the out-of-plane deflections and the N_x stress resultant while Figure 27 shows the N_{xy} stress resultant and a plot of the percentage of failures within an element (percentage of ply-integration points with failures in an element). Four longitudinal halfwaves develop in the postbuckled out-of-plane deflection shapes for this panel. The figures shows that high N_x and N_{xy} stress resultants exist near the hole region. This initiates the failure of the panel around the hole region as shown in the figure on the right in Figure 27. The H3 panel developed local failures around the hole region. In the experimental results [49], both the H3 and H4 panels also experienced failures along the nodal line away from the hole due to transverse shear mechanisms. Figure 26 shows that the a high N_x stress region is located along the nodal line at the edge of the panel. However, no failures occurred in this region in the progressive failure analysis which neglected transverse shear effects. Table 15 summarizes the failure mechanisms for the experimental and analytical results.

Table 15. H3/H4 panel: Comparison of Failure Results

Failure Criterion	First Ply Failure Load (lbs.)	Final Failure Load (lbs.)	Dominant Failure Mode Type
Hashin's Criterion	15507	17313	Matrix Tension/Fiber Compression
H3 Panel Test [49]	Unavailable	18884	Unavailable
H4 Panel Test [49]	Unavailable	20233	Unavailable

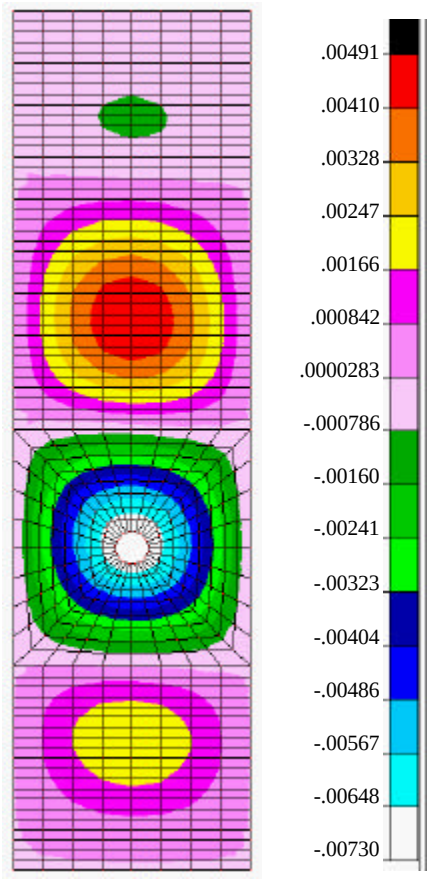

a) Fringe Plot of Analytical Results, in.

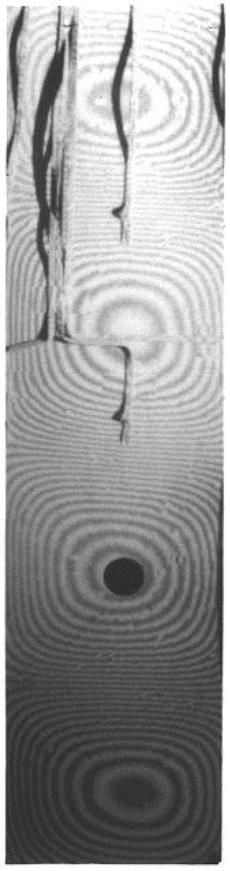

b) Photograph of Moiré-Fringe Pattern from Starnes and Rouse Test [49]

Figure 23. H3/H4 panel: Comparison of experimental and analytical linear buckling mode 1.

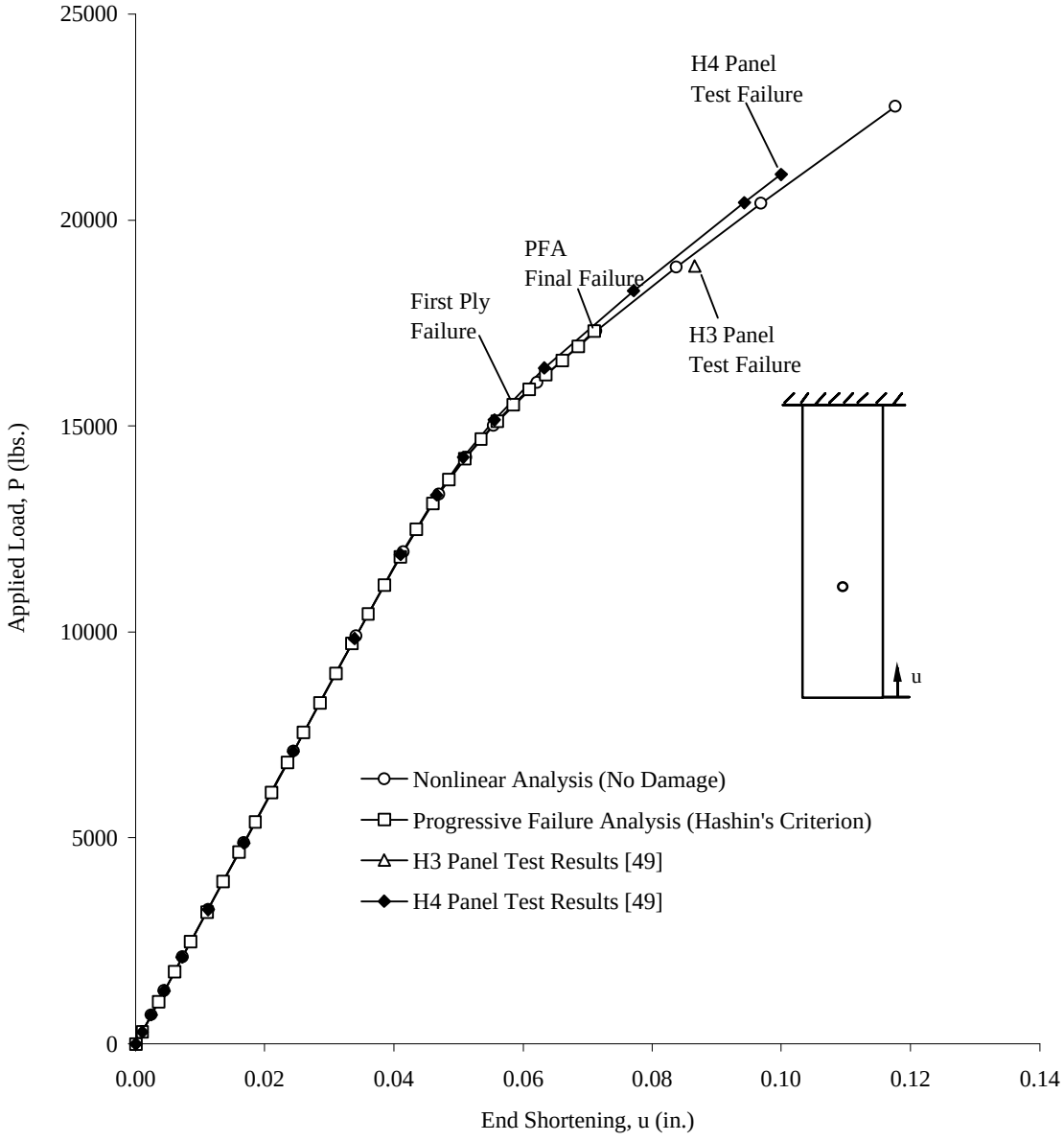

Figure 24. H3/H4 panel: End-shortening results, $\alpha = 10^{-20}$.

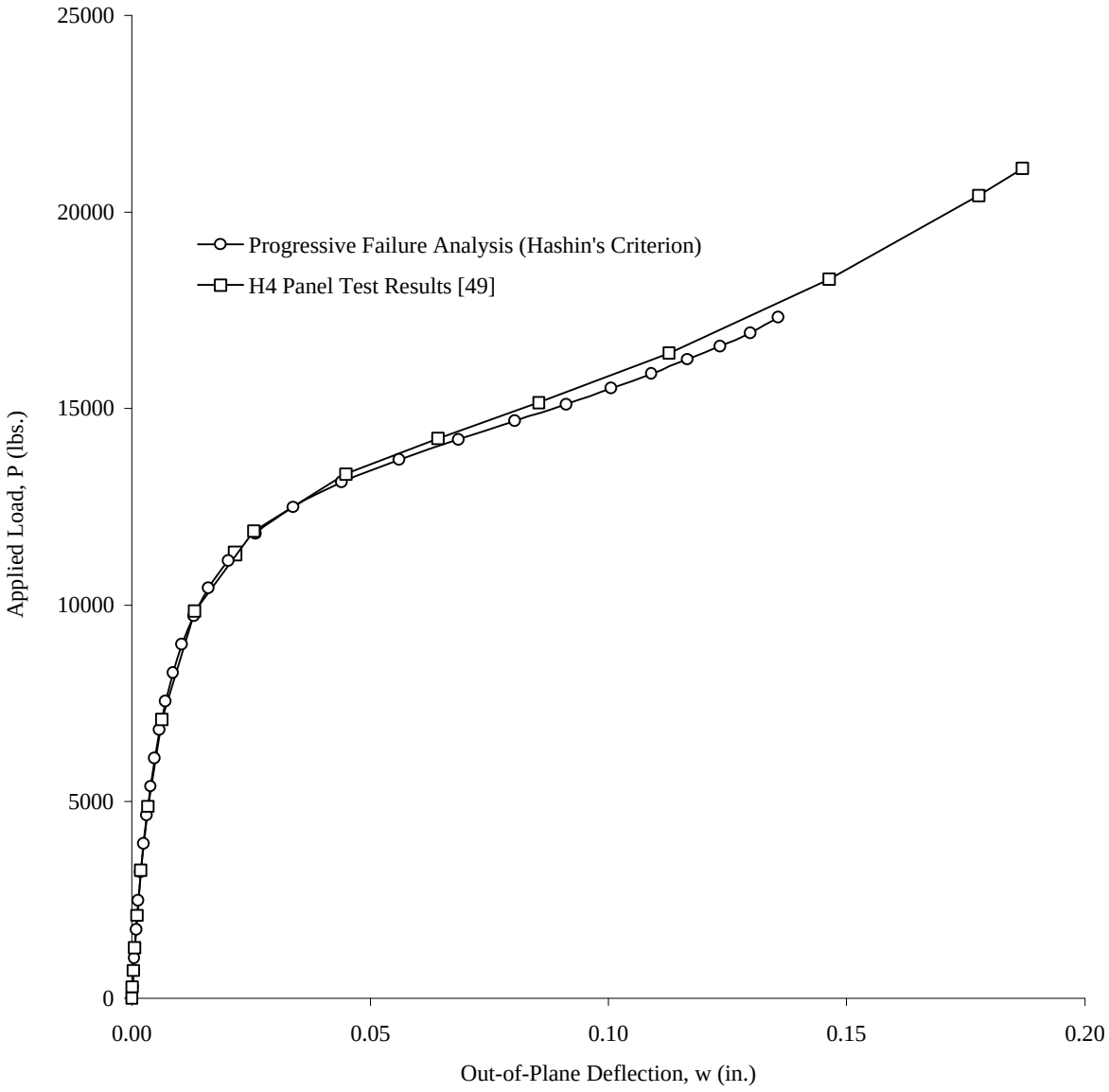

Figure 25. H3/H4 panel: Out-of-plane deflection results.

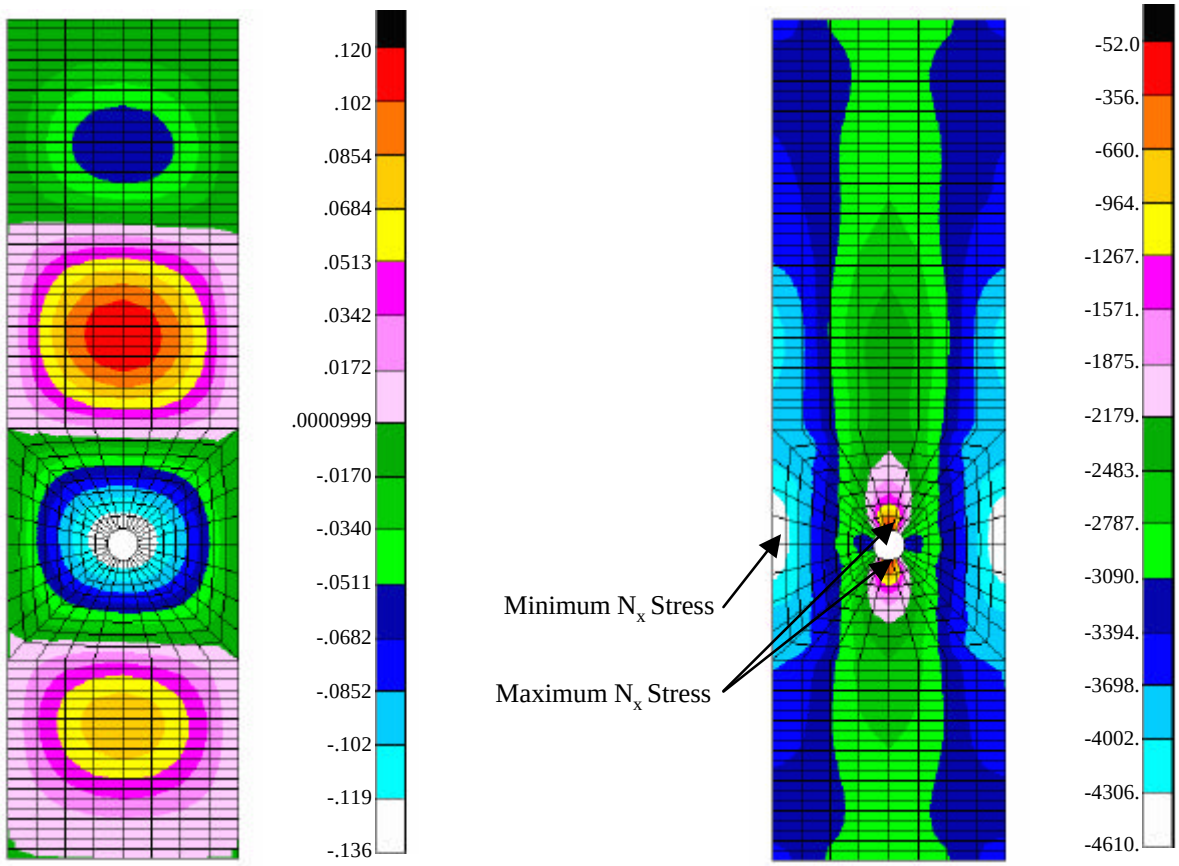

a) Out-of-Plane Deflection, in.

b) N_x Stress Distribution, lb./in.

Figure 26. H3/H4 panel: Structural response at final failure (17313 lbs.).
Hashin's Criterion

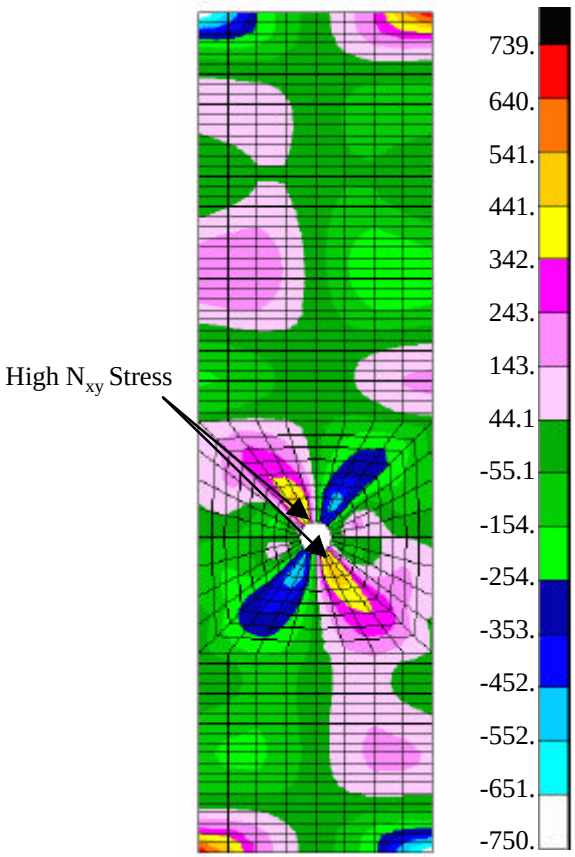

c) N_{xy} Stress Distribution, lb./in.

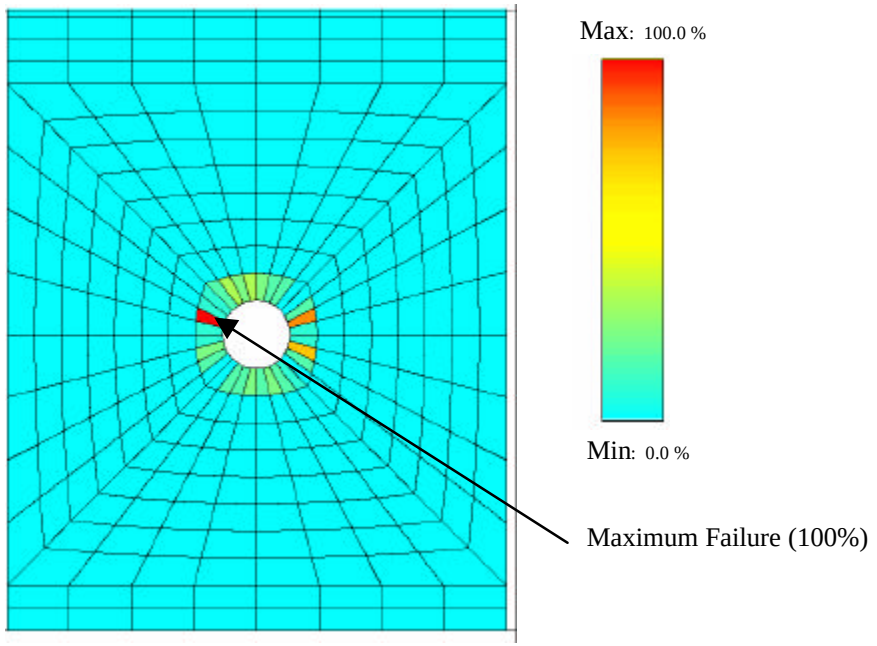

d) Percentage Failure

Figure 27. H3/H4 panel: Structural response at final failure (17313 lbs.), continued.
Hashin's Criterion

Composite Blade-Stiffened Panel

An interest in applying graphite-epoxy materials to aircraft primary structures has led to several studies of postbuckling behavior and failure characteristics of graphite-epoxy structural components [50]. One study of composite stiffened panels tested a blade-stiffened panel with a discontinuous stiffener [51]. The test setup for the panel is shown in Figure 28. This panel has served as a focus problem in COMET for identifying and resolving analysis deficiencies associated with the nonlinear global/local stress analysis of composite structures [52]. The finite element modeling and analysis needed to predict accurately the nonlinear response of the flat blade-stiffened panel loaded in axial compression is described in this section.

Problem Statement

The overall length of the panel is 30 in., the overall width is 11.5 in., the stiffener spacing is 4.5 in., the stiffener height is 1.4 in., and the hole diameter is 2 in. as shown in Figure 29. The three blade-shaped stiffeners are identical. The loading of the panel is in uniform axial compression. The loaded ends of the panel are clamped and the sides are free. The material system for the panel is T300/5208 graphite-epoxy unidirectional tapes with a nominal ply thickness of 0.0055 in. The lamina properties and strain allowables for the T300/5208 material system are shown in Table 16. The blade stiffeners are 24-ply laminates $\left([\pm 45/0_{20}/\mp 45]\right)$, and the panel skin is a 25-ply laminate $([\pm 45/0_2/\mp 45/0_3/\pm 45/0_3/\mp 45/0_3/\pm 45/0_2/\mp 45])$.

The finite element model of the blade-stiffened panel with discontinuous stiffener shown in Figure 29 has 1,184 4-node elements and 1,264 nodes. Note that the stiffeners are modeled with four shell elements through the height of the stiffener. First a nonlinear analysis without failure predictions is performed on the panel. A progressive failure analysis is then performed on the blade-stiffened panel and compared with experimental results.

Table 16. Material Properties for Blade-Stiffened Panel, T300/5208 Material System

Material Properties		Value [53]
Longitudinal Young's Modulus	E_{11}	19.0 msi
Transverse Young's Modulus	E_{22}	1.89 msi
Poisson's Ratio	ν_{12}	0.38
In-Plane Shear Modulus	G_{12}	0.93 msi
Longitudinal Tensile Ultimate Strain	$X\varepsilon_T$	0.0110 in./in.
Longitudinal Compression Ultimate Strain	$X\varepsilon_C$	0.0086 in./in.
Transverse Tensile Ultimate Strain	$Y\varepsilon_T$	0.0036 in./in.
Transverse Compression Ultimate Strain	$Y\varepsilon_C$	0.0100 in./in.
In-Plane Shear Ultimate Strain	$T\varepsilon$	0.0150 in./in.

Figure 28. Composite blade-stiffened panel with discontinuous stiffener.

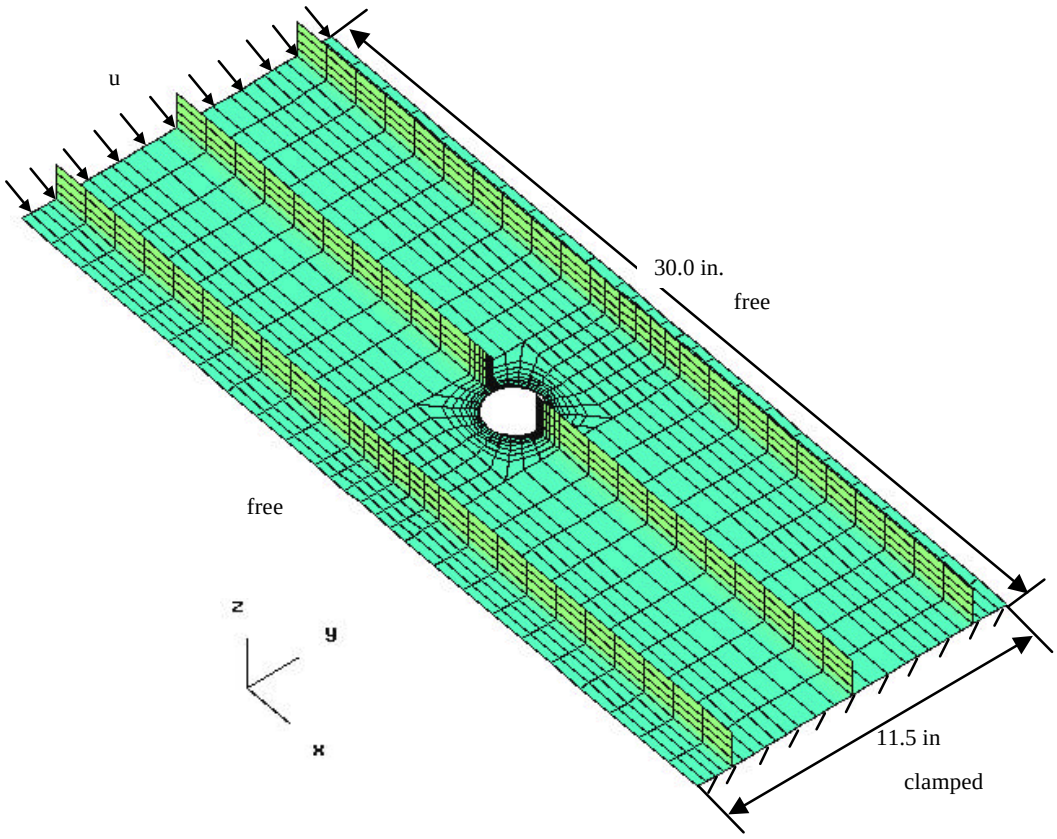

Figure 29. Finite element model of composite blade-stiffened panel.

Structural Response

The structural response of the composite blade-stiffened panel is studied. First, an elastic nonlinear analysis is performed to understand the behavior of the panel without any material failures. A linear stability analysis is not required to impose geometric imperfections on the panel because the discontinuous stiffener introduces an eccentric loading condition. The next step performed is a progressive failure analysis using Hashin's criterion with a material degradation factor of $\alpha = 10^{-20}$. The initial displacement applied to the panel is 0.005 inches. The displacement increment for the nonlinear analysis is chosen to be 0.0025 inches. The strain allowables in Table 16 used for the progressive failure analysis are nominal values for the T300/5208 material system since the actual strain allowables for the panel are unavailable.

End-shortening results are shown in Figure 30 as a function of the applied compressive load. The blade-stiffened panel was tested to failure. In the test, local failures occurred prior to overall panel failure as evident from the end-shortening results. Good agreement between the test and analysis is shown up to the load where local failures occurred. Table 17 summarizes the failure loads of the blade-stiffened panel. The analytically-obtained out-of-plane deflection *w* at the edge of the hole and blade stiffener is shown as a function of the applied load in Figure 31. The large out-of-plane deflections indicate that the response is nonlinear from the onset of loading.

Table 17. Composite Blade-Stiffened Panel: Comparison of Failure Results

Failure Criterion	First Ply Failure Load (lbs.)	Final Failure Load (lbs.)	Dominant Failure Mode Type
Hashin's Criterion	26599	57064	Matrix Tension
Test Results [51]	35644	40613	Unavailable

Figures 32-34 show the structural response of the blade-stiffened panel at the final failure load in the progressive failure analysis. This is the point in which the analysis experienced convergence problems. Figures 32 and 33 show the out-of-plane deflection fringe plot and the N_x stress resultant contours on the deformed geometry, respectively. Figure 32 shows that large out-of-plane deflections develop in the region around the discontinuity. The N_x distribution in Figure 33 reveals that the load is re-distributed away from the discontinuous stiffener such that the center stiffener has essentially no N_x load at the edge of the hole. Also, the N_x load is re-distributed to the center of the outer blade stiffeners. Figure 34 shows a close-up view near the hole of the N_x stress distribution and the percentage of failure within an element. A closer look at the N_x distribution around the hole in indicates that high in-plane stresses and a high stress gradient exist near the hole. The high in-plane stresses and high stress gradient coupled with the large out-of-plane deflections near the hole ultimately caused local failures near the hole as evident in the figure on the right in Figure 34.

Based on these simulations, two failure scenarios can be postulated. First, as the load increases a stress concentration develops near the hole, a large normal stress also develops as the discontinuous stiffener tends to pull the skin laminate apart. The skin continues to delaminate possibly causing the jumps shown on the experimental data on Figure 30 until the outer stiffeners roll over leading to free edge failures. The second scenario is similar to the first with the outer stiffeners causing the jumps shown on Figure 30 and then the local delaminations near the hole cause final failure. Close examination of the test panel reveals that local delaminations and disbonds are present near the hole and edge

delaminations are evident at the free edges near the panel midlength. These local delaminations near the hole were not considered in this progressive failure analysis. These delaminations are most likely the reason why the present progressive failure analysis over-predicted the final failure load of the panel. Also, the strains allowables for the panel are not actual measured properties, but instead are obtained from nominal values of the material system.

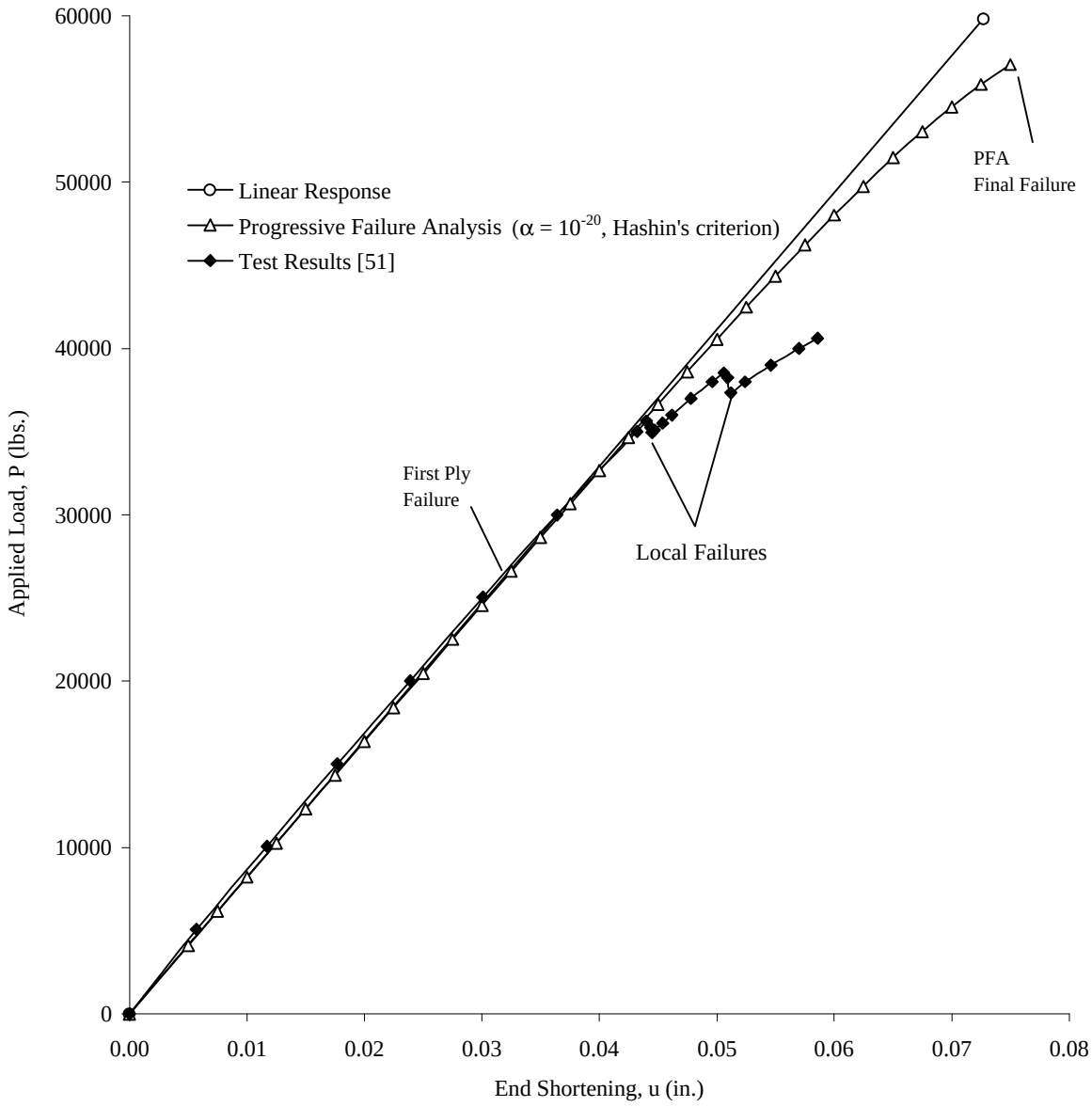

Figure 30. Composite blade-stiffened panel: End-shortening results.

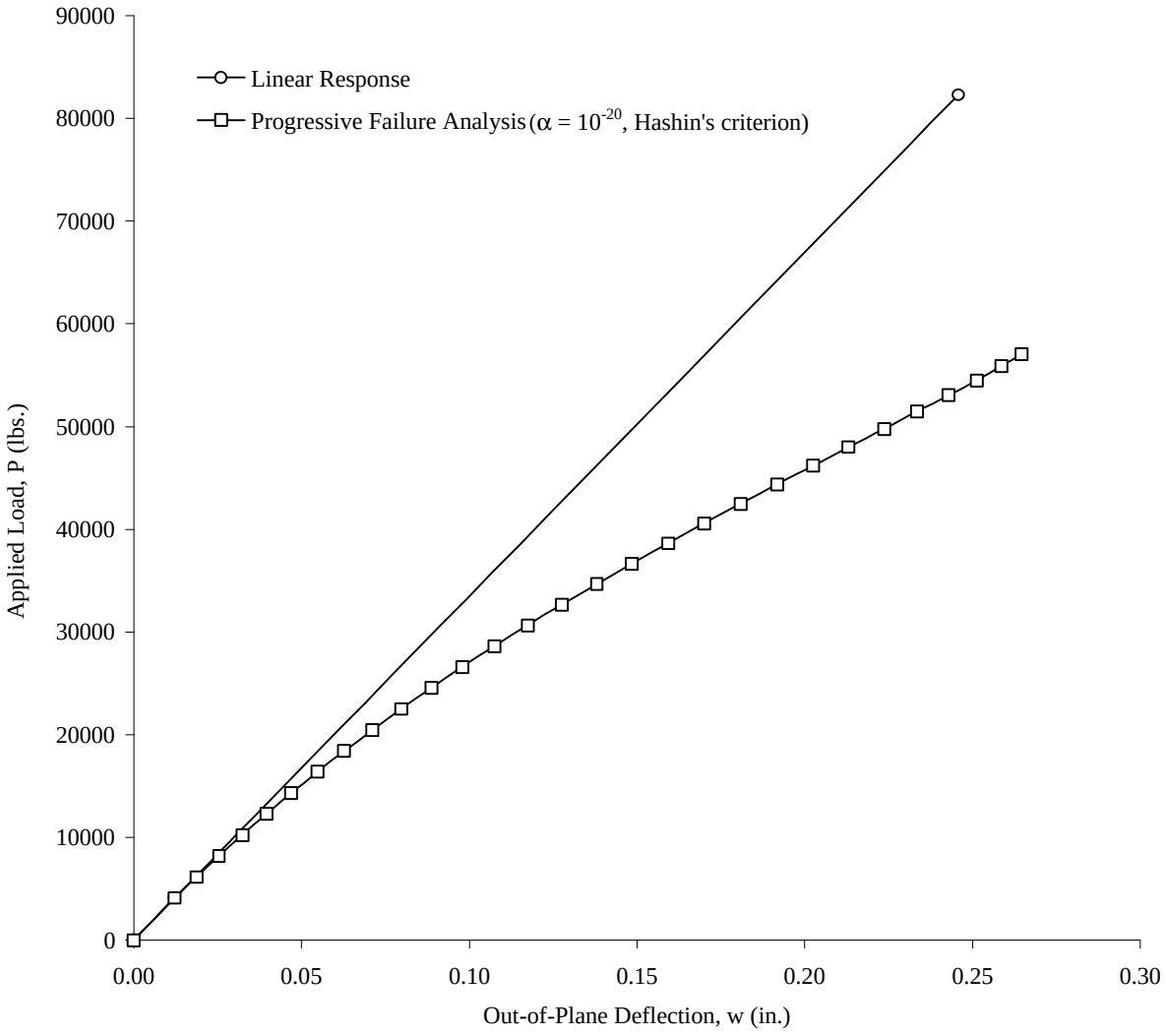

Figure 31. Composite blade-stiffened panel: Out-of-plane deflection at hole and blade stiffener.

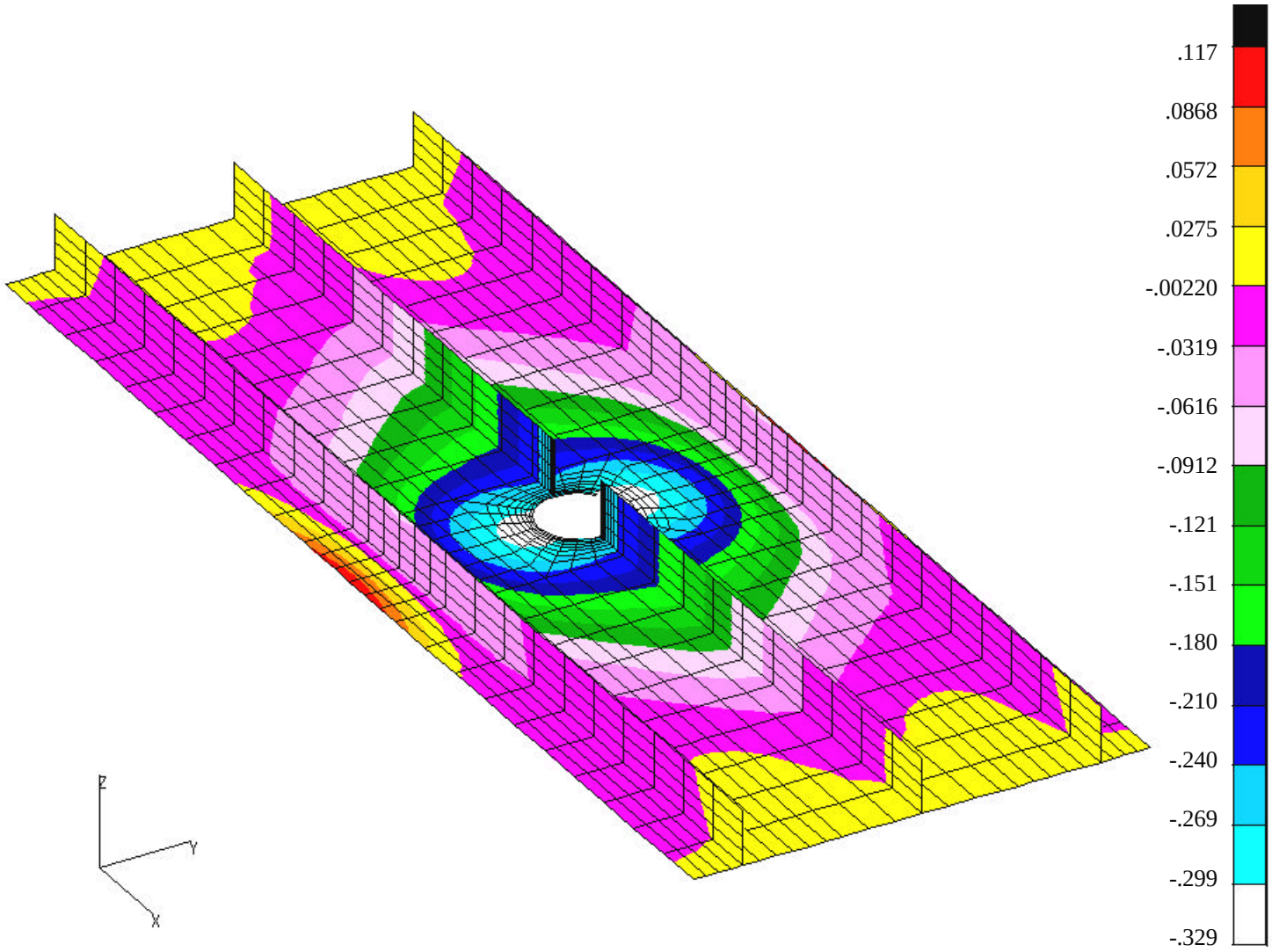

Figure 32. Composite blade-stiffened panel: Structural response at final failure (57064 lbs.).
Out-of-plane deflection fringe plot, in.

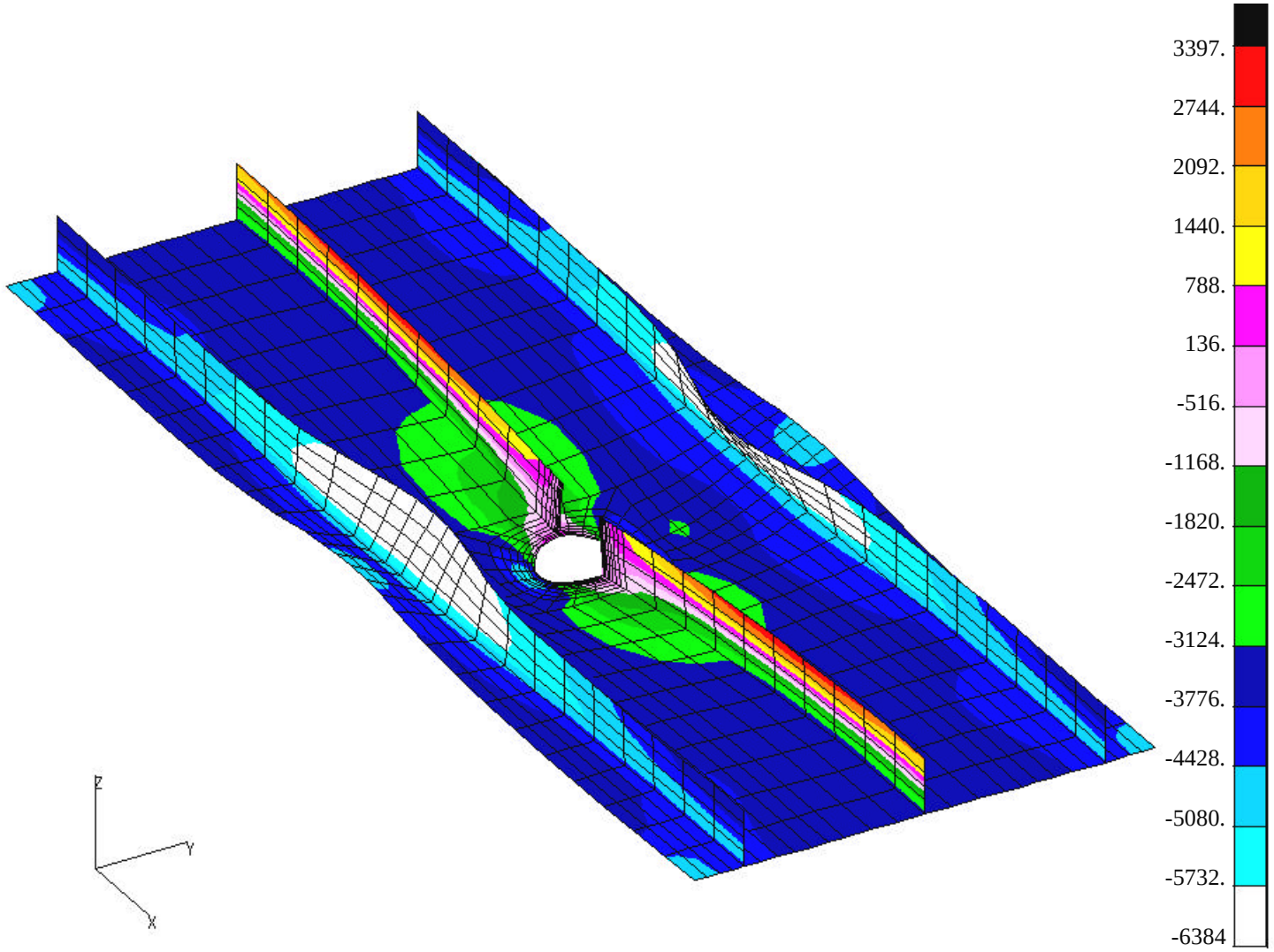

Figure 33. Composite blade-stiffened panel: Structural response at final failure (57064 lbs.), continued.
Deformed geometry shape with N_x stress distribution, lb./in.

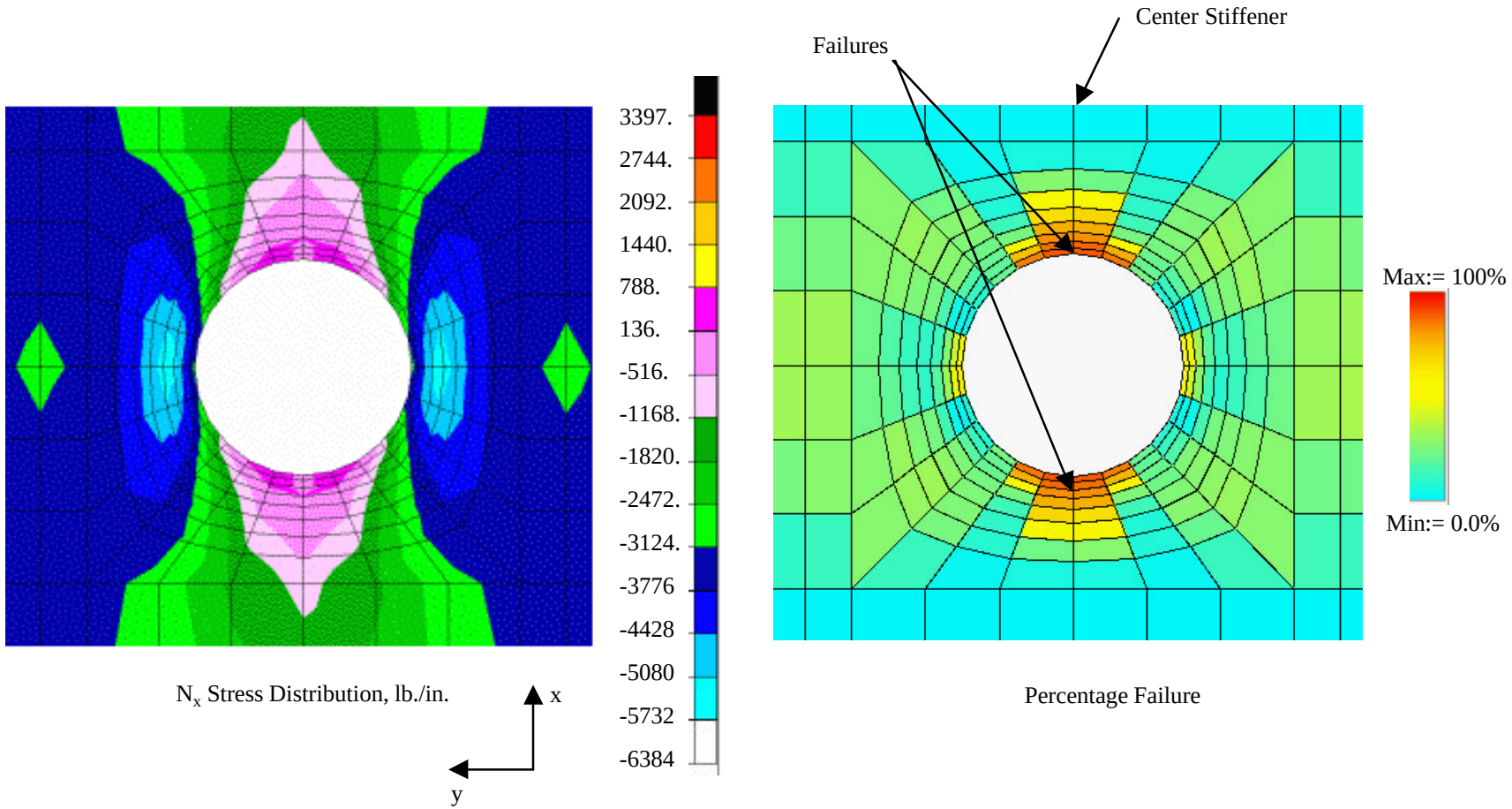

Figure 34. Composite blade-stiffened panel: Local region near hole.

CONCLUSIONS AND RECOMMENDATIONS

Conclusions

A state-of-the-art perspective on computational models for progressive failure analysis on laminated composite structures has been presented. A progressive failure analysis model has been developed for predicting the nonlinear response and failure of laminated composite structures from initial loading to final failure. This progressive failure methodology is based on Pifko's approach and has been developed, extended, and successfully implemented in COMET. The progressive failure analyses use C^1 plate and shell elements based on classical lamination theory to calculate the in-plane stresses. Several failure criteria, including the maximum strain criterion, Hashin's criterion, and Christensen's criterion, are used to predict the failure mechanisms and several options are available to degrade the material properties after failures. These different formulation methods are compared and assessed by performing analyses on several laminated composite structures.

The first laminated composite structure to be analyzed was a rail-shear specimen. Studies were performed to test the effect of the displacement increment size in the nonlinear analysis procedure. The study showed that a displacement increment of 0.00050 inches is sufficiently small for accurate progressive failure predictions. The next study tested the material degradation factor, α, to check its effect on the failure load prediction. The study showed that the rate of material degradation had little effect on the failure prediction. Progressive failure analyses were then performed on the rail-shear specimen to compare the maximum strain criterion, Hashin's criterion, and Christensen's criterion. The progressive failure results showed that all criteria compared very well with the results from Shahid.

The next composite structure analyzed was a tension-loaded laminate with a centrally located hole. Analyses were performed to study the effect of the mesh size on the progressive failure predictions. The study for the tension-loaded laminate showed that the mesh size had a small effect on the prediction of the progressive failure loads. Another study was performed to again test the material degradation factor on the progressive failure predictions. Again, varying the material degradation factor had little effect on the progressive failure results. In later analyses, the material degradation factor α was set to 10^{-20} which essentially zeroed out the material properties at the element integration points with failures. Progressive failure analyses were then performed to compare Hashin's criterion and Christensen's criterion to the experimental results. The results indicated that for this problem there was little difference between Hashin's criterion and Christensen's criterion in predicting the failure loads and failure distribution.

The next problem analyzed was a composite rectangular panel loaded in axial compression. A linear buckling analysis was performed and the results were compared to the experimental results. The first buckling mode shape from the analysis was in good agreement with that from the experiment. An initial geometric imperfection using the first buckling mode shape was then applied to the panel. The load-end shortening curve from the analysis correlated well to the experimental results up to the failure of the panel. Progressive failure analyses using Hashin's and Christensen's criteria were performed on the panel. Hashin's criterion was less than 3% from the test failure load while Christensen's criterion was less than 8% from test final failure load. Both failure criteria predicted slightly higher failure loads than the results from the experiment. Christensen's criterion predicted first ply failure at a much lower load than the load predicted by Hashin's criterion. The failure mode reported in the test was due to transverse shear effects along the node line in the buckle pattern. The progressive failure analysis results showed that the damage

was concentrated along the node line just as the test results showed. Despite the progressive failure analysis not including the transverse shear failure mode, the progressive failure analysis predictions still agreed well with the test results.

A compression-loaded composite panel with an offset hole was also analyzed and compared to the test results for two panels. Again, a linear buckling analysis was performed to impose geometric imperfections on the panel model. The first buckling mode shape predicted by the analysis agreed with the test results. Hashin's criterion was used for the nonlinear progressive failure analysis of the panel because it provided more failure modes than the other failure criteria. There was good correlation in the load end-shortening curve for the analytical and experimental results. However, the progressive failure analysis final failure load predictions under-predicted the failure load from the test by 8.3% for the H3 panel and 14.4 % for the H4 panel. In the experiment, both panels experienced failures along the nodal lines away from the hole due to transverse shear mechanisms. In addition, the H3 test panel developed local failures around the hole region. The progressive failure results also showed that the panel experienced local failures near the hole region due to shear stress failure.

The final problem analyzed was a composite blade-stiffened panel with a discontinuous stiffener loaded in axial compression. A progressive failure analyses using Hashin's criterion was performed on the blade-stiffened panel. The progressive failure analysis and test results showed good correlation for the load end-shortening results up to the load where local failures occurred. The progressive failure results under-predicted first ply failure and severely over-estimated the panel's final failure. The progressive failure results predicted failures around the hole region at the stiffener discontinuity. The final failure of the experiment showed that local delaminations and disbonds were present near the hole and edge delaminations were present near the panel midlength. The delaminations are most likely why the progressive failure analysis results did not compare well to the test results since delamination failure modes are not included in the progressive failure methodology.

Recommendations

Because of the complexity in developing a progressive failure model capable of predicting all types of failures, there are several recommendations that should be made to enhance the current progressive failure methodology. The first recommendation would be to extend the current progressive failure model to include failure criteria to predict failure interlaminar mechanisms. One option to accomplish this using the current progressive failure model would be to calculate the interlaminar stresses $(\sigma_{xz}, \sigma_{yz}, \sigma_{zz})$ by integration of the 3-D equilibrium equations. A more efficient option would be to modify the current progressive failure model so that it would use the C^0 elements which already account for these interlaminar stresses. Once the interlaminar stresses were known, other failure mechanisms to predict debonding or delaminations could added. However, for accurate interlaminar stresses even for C^0 elements, integration of the 3-D equilibrium equations will be necessary. The second recommendation would be to modify the degradation model such that an integration point with failures would still have a small stiffness which could eliminate singularities in the stiffness matrix caused by the material degradation model. Finally, the progressive failure analysis model should be modified to re-establish static equilibrium after material properties have been degraded. This could be accomplished by repeating the nonlinear analysis at the current load step until a converged solution exists. Such a capability would permit the use of arbitrary step sizes during the nonlinear analysis and provide for an automatic step size control rather than fixed step size.

APPENDIX

IMPLEMENTATION INTO COMET

COMET Overview

At NASA Langley Research Center, a research effort is being directed towards developing advanced structural analysis methods and identifying the requirements for next generation structural analysis software. This activity has developed into a computational framework to aid in the definition of these requirements and to serve as a "proving ground" for new methods on complex structural application problems. This framework has yielded COMET, a structural analysis software system, which was developed jointly between NASA Langley Research Center and Lockheed Palo Alto Research Laboratory. COMET is a modular, extendible, machine-independent, architecturally-simple, multi-level software system enabling researchers to implement their formulations as generically as possible. COMET utilizes a high-level command language and data manager that allows the coupling of independent FORTRAN processors together such that specific structural analysis functions may be performed. Because of these features, it has become an extremely powerful tool to researchers and developers in the field of computational mechanics. COMET's capabilities include linear and nonlinear stress analyses of large-scale built-up structures, transient dynamic analyses, and eigenvalue analyses.

A graphical overview of COMET is shown in Figure A-1. No single processor (FORTRAN program) controls all aspects of the analysis in COMET. Instead, the steps for an analysis are performed by a number of independent analysis application processors and high-level, command-language procedures. Processors and procedures communicate with one another by exchanging named data objects in a global computational database managed directly by a data manager called GAL (Global Access Library) [54]. Execution of the application processors is controlled by the user with an interactive, high-level, command language called CLAMP (Command Language for Applied Mechanics Processors) [55] which is processed by the command language interpreter CLIP (Command Language Interface Program).

The progressive failure analysis methodology developed as part of this research exploits features of COMET and is enabled by the design of this computational framework. Specifically, four main functions are defined. First, the capability to develop and modify application processors for model generation and analysis enhanced this research. Second, the generic element processor (GEP) provided element data and results through the computational database which represented the element developer's best strategy for stress and strain recovery. Third, the generic constitutive processor (GCP) provided an effective mechanism for implementing different failure models and archiving constitutive data through the primary database and through auxiliary historical database for nonlinear, path-dependent constitutive models. Finally, the procedure library provided a springboard for developing a progressive failure analysis strategy and its assessment. COMET allows a researcher to focus on their main area of concentration and to benefit from the breakthroughs of other researchers. Additional details of the GEP and GCP are provided next.

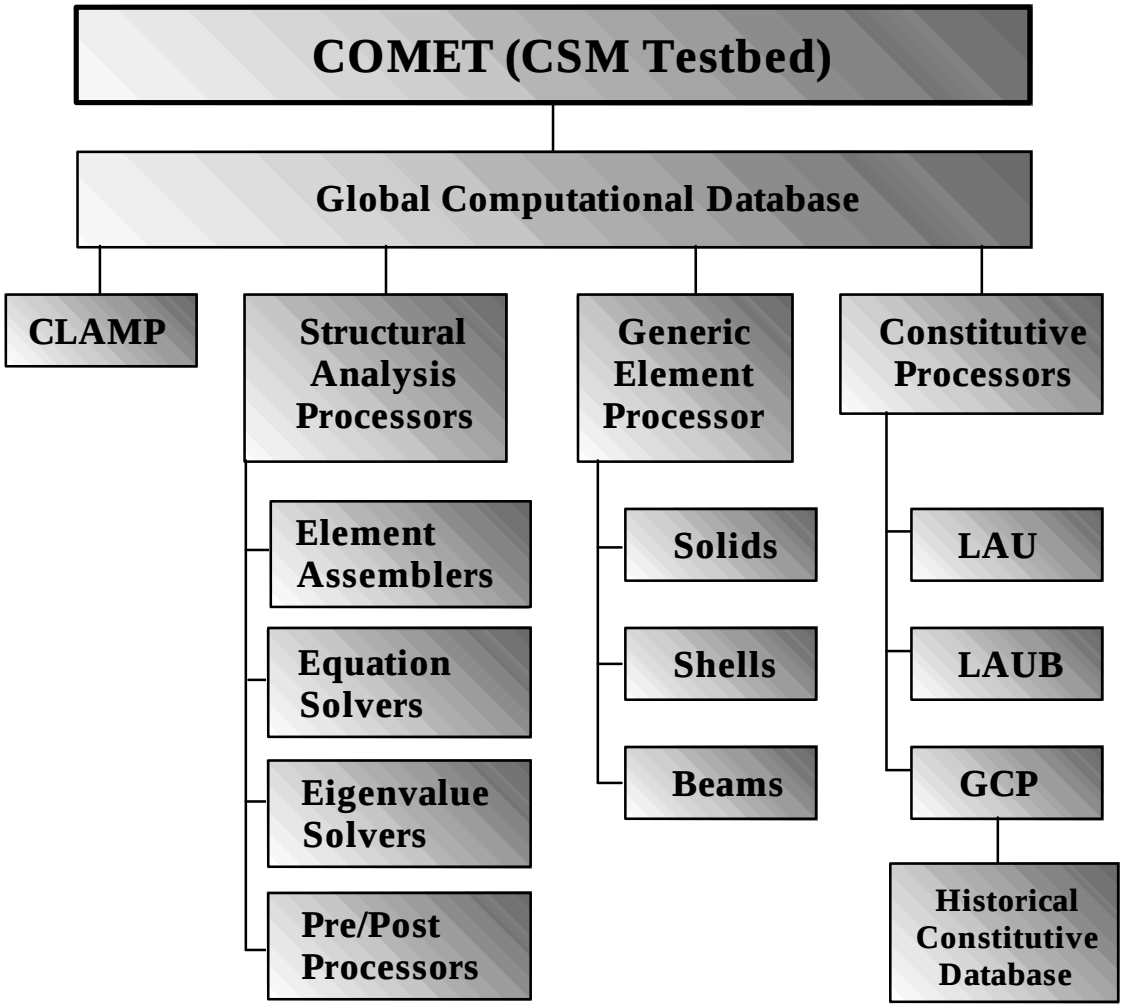

Figure A-1. Graphical overview of COMET.

Generic Element Processor

COMET offers an interface called the GEP (Generic Element Processor) [56] which allows finite element developers to implement their finite element formulations quickly and efficiently. The GEP acts as a generic template (see Figure A-2) for implementing a multitude of structural-element (ES*) processors. Each ES* processor performs all element operations for all elements implemented within the processor such as element definition, stiffness, force, and mass matrix generation, and various other pre-processing and post-processing functions such as stress recovery. The computation of the stresses and/or element strains is primarily a post-processing command. These element quantities may be computed at element integration points, at element centroids, or at element nodes by extrapolation from the integration points. The GEP is designed to implement virtually all types of elements, both standard elements (1-D, 2-D, and 3-D element types) and non-standard elements which do not fit within the mold of standard elements. All element processors share the same standard generic software interface (called the ES shell routines) to COMET which ensures that all element processors understand the same command-language directives and create and access the database in the same way. Because of the ES shell routines, element users can

access all ES processors in the same manner and element developers can implement new elements regardless of their complex internal formulations.

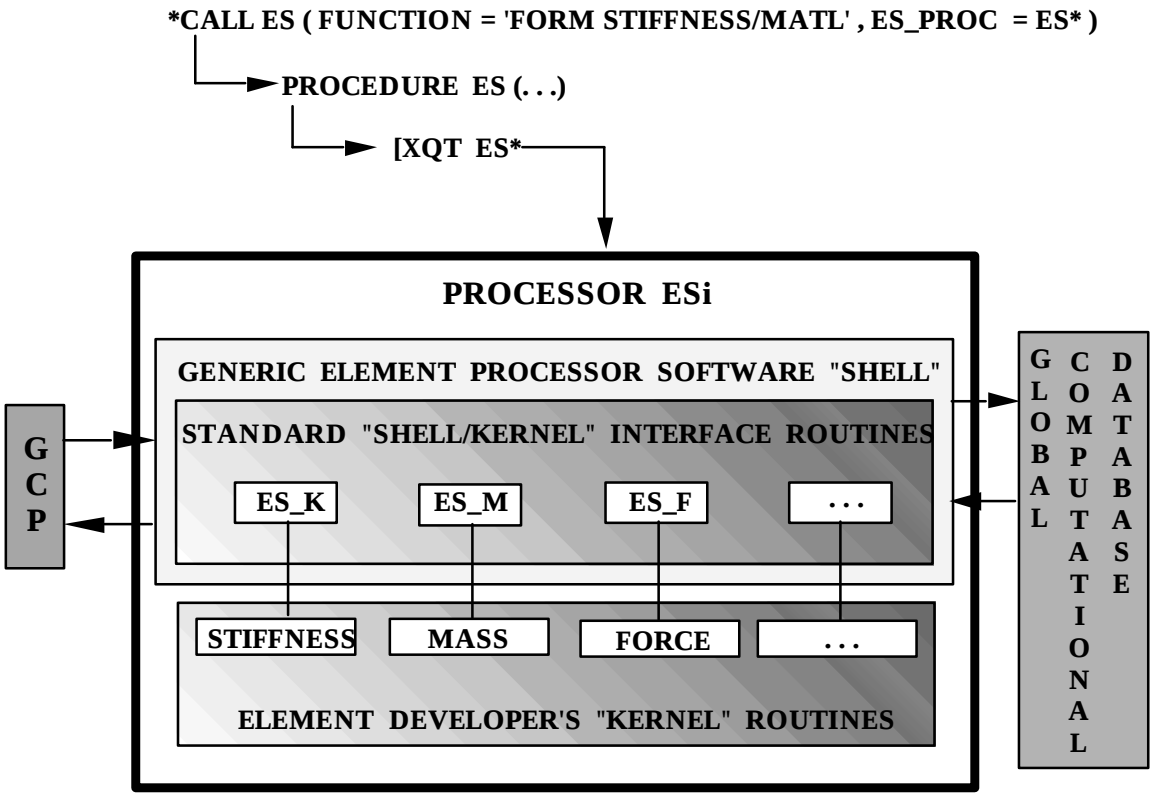

Figure A-2. GEP template.

For the progressive failure analysis, the GEP software shell also interacts with the generic constitutive processor (GCP). For a linear elastic analysis, the material is assumed to be a Hookean material and constant throughout the analysis. For nonlinear material problems, the material model is not constant and perhaps not even continuous as in the case of brittle failures. In these cases, the element processor must compute the stress and strain resultants for later use in the through-the-thickness calculations of the stress and strain. Then the GCP constitutive kernel routines are called to evaluate failure models and to assess damage models prior to computing new constitutive terms for the element.

The progressive failure methodology implemented into COMET currently uses only the C^1 (slope-continuous) elements for the analysis. Two C^1 shell elements are available for use in COMET: a 4-node quadrilateral shell element named E410 in processor ES5 and a 3-node triangular element named TP2L in processor ES31. These elements are implemented into two ES processors in the GEP and are described below.

ES5 Processor

Processor ES5 [57] contains a displacement-based 4-node quadrilateral shell element originally developed for the STAGS code [58]. The E410 element is a C^1 (slope-continuous) finite element based on the Kirchhoff-Love shell hypothesis (normals stay normal, no transverse-shear deformation). The element has 3 translational and 2 rotational degrees of freedom per node. The element also has a "drilling" rotational stiffness which eliminates the need to suppress the drilling degree of freedom. For geometrically nonlinear analysis problems, the E410 element includes the full nonlinear Green-Lagrange strains.

ES31 Processor

Processor ES31 contains a discrete-Kirchhoff triangular element, known as the DKT element. The 3-node DKT element implemented into COMET is referred to as the TP2L element. This element was developed by Garnet, Crouzet-Pascal, and Pifko [59] and implemented in COMET by Pifko and Crouzet-Pascal [41]. The element has 5 degrees of freedom per node, 3 translational and 2 rotational degrees of freedom and has an artificial drilling term. For geometrically nonlinear analysis problems, the TP2L element includes the full nonlinear Green-Lagrange strains.

Generic Constitutive Processor

Each structural element requires the evaluation of various constitutive functions including evaluation of element constitutive matrix, determination of tangent moduli (for the tangent stiffness matrix), and evaluation of failure criteria (for failure and material degradation). The constitutive modeling capabilities of COMET are centered towards the analysis of laminated composite structures. Element developers and structural analysts have access to constitutive models for 1-D beam elements, 2-D plate and shell elements, as well as 3-D solid elements. Processor LAU is a laminate analysis utility for calculating the constitutive relations for 2-D and 3-D isotropic, orthotropic, anisotropic, and laminated structures. For 2D structures, processor LAU can use classical lamination theory or traditional first-order, shear deformation theory. Processor LAU is limited to performing elastic structural analyses. Processor LAUB is an extension of processor LAU to calculate the constitutive relations for 1-D beam elements. Both LAU and LAUB are described in Ref. 40.

To enhance the constitutive modeling capabilities of COMET, the Generic Constitutive Processor (GCP) was developed by Lockheed Palo Alto Research Laboratory [60]. GCP allows researchers to implement new constitutive models, failure models, or damage models into COMET conveniently. The GCP replaces COMET's current elastic constitutive capability, as implemented in both LAU and LAUB. The GCP is similar to the GEP in that various constitutive models may be implemented in COMET and accessed using other independent processors within the COMET framework. Once the midplane strains and curvatures are known from the element processor, the through-the-thickness in-plane strains and corresponding stresses may be calculated and used to evaluate selected failure criteria using features of the GCP.

The GCP architecture contains five major functional components as shown in Figure A-3. The combination of the generic constitutive interface, GCP inner "shell", constitutive developer interface, historical database, and the constitutive kernel provide links with the element processor for efficient element constitutive functions. The GCP outer "shell" provides a common user interface to the GCP by processing commands for input of material/fabrication data, interacting with the database, and directing

the flow of computational procedures. The GCP outer "shell" also incorporates the nonlinear analysis algorithm for stand-alone testing of constitutive models, material failure criteria, and material damage models. The GCP inner "shell" performs through-the-thickness integration for composite laminates, interpolates state-dependent material properties, performs transformations from element-to-material coordinate systems, calls the constitutive kernel routines, and performs database management functions of the constitutive historical data, point stress/strain quantities, and material tangent stiffnesses. In order to provide the capability for performing stand-alone constitutive analyses and analyses involving the element processors, the GCP utilizes a generic constitutive interface which provides a flexible, efficient, computational link to each individual element processor.

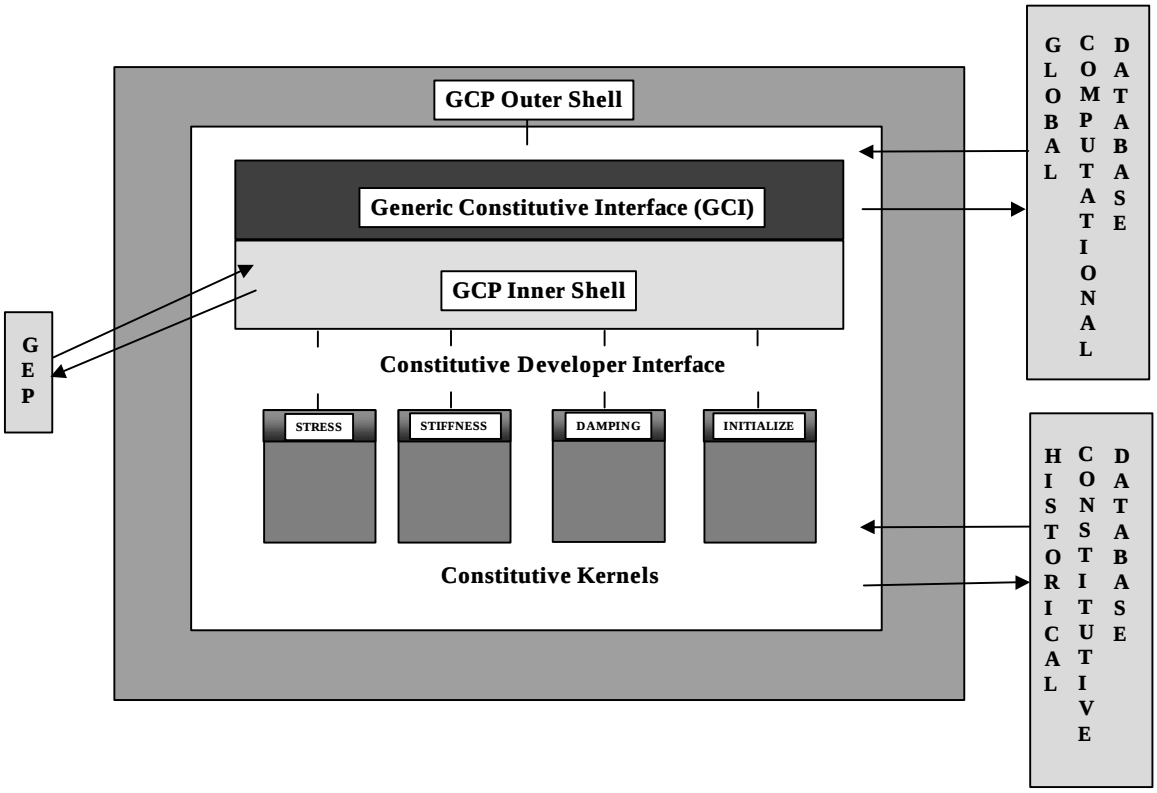

Figure A-3. GCP overview.

Implementation of Failure and Damage Models

Implementation of new constitutive models into the GCP is accomplished using the Constitutive Developer's Interface in the GCP as indicated in Figure A-3. This interface allows developers of new constitutive models to include constitutive kernel routines such as failure detection models or material damage models easily through a set of FORTRAN subroutine entry points with standardized argument lists. This capability and its implementation template is very similar to the GEP described earlier.

GCP kernel subroutines are denoted by the name of CS*iX* where the index *i* indicates the i^{th} constitutive model, and the selected constitutive function to be performed is represented by *X* in the GCP's FORTRAN material library. Table A-1 summarizes the types of constitutive models existing in COMET wherein at least the minimal capabilities are provided to form the constitutive matrix for different element types. Table A-2 summarizes the functions of the CS*iX* predefined constitutive subroutine entry points in GCP where *X* denotes a specific constitutive function.

Two tasks must be performed by the constitutive developer to implement a new constitutive model within the GCP. First, constitutive kernel routines must be provided to perform the necessary and desired constitutive functions at a material point. Secondly, the selected subroutines within the constitutive developer interface must be modified to read the material property input for the new constitutive model and also to perform any constitutive related postprocessing.

Table A-1. Constitutive Models in COMET

Constitutive Model *i*	Constitutive Model Description
CS1X	Linear Elastic Isotropic Model
CS2X	Linear Elastic Orthotropic Model
CS3X	Mechanical Sublayer Plasticity Model
CS4X	Linear Elastic-Brittle Orthotropic Model

Table A-2. Constitutive Developer Interface Subroutines of GCP

Subroutines CS*iX*	Constitutive Function Description
CS*i*V	Material property input verification.
CS*i*I	Initialization of constitutive model.
CS*i*S	Point stress calculation subroutine.
CS*i*C	Constitutive matrix calculation subroutine.
CS*i*M	Returns mass density at material-point.
CS*i*D	Returns material damping matrix at material-point.

One set of constitutive interface subroutines initially and implemented into COMET through the GCP developed by Moas [43] were enhanced by Pifko of Grumman Aerospace Corporation [41,42]. These subroutines are identified as the CS4 constitutive model. The CS4 constitutive model is for 2D linearly elastic, brittle, orthotropic laminates. The constitutive kernel subroutines used for the progressive failure analysis are therefore called: CS4V, CS4I, CS4S, and CS4C. The CS4V subroutine performs the verification of the material property input for the progressive failure constitutive model. The laminate material properties, lamina orientations, and strain allowables for failure assessment are read when the CS4V subroutine is called. The CS4I subroutine entry point performs the initialization required for the constitutive model by setting flags for the historical material database and initializing that database if necessary. The CS4S subroutine recovers the element stresses from the element strains determined in the element processor (GEP). The CS4C subroutine is modified to perform failure detection and material model degradation following Pifko's strategy.

In the progressive failure strategy implemented by Pifko, the stresses are recovered for each element $(IEL = 1,2,\ldots, NEL)$ in the finite element model after a converged nonlinear solution is obtained. This is accomplished by calling the generic ES processor shell to compute the element stresses (ES procedure command "FORM STRESS") of a given element type within a given ES processor. The ES* element processor (ES5 or ES31) for the specific element type is then executed to initiate the stress recovery process. For each Gauss quadrature point of an element $(IQP = 1,2,\ldots, NQP)$, the middle surface strains and curvatures, $\{\varepsilon^0\}$ and $\{\kappa\}$, are calculated in the plane of the element. Then the GCP shell is called to read in the material properties for each layer in the laminate $(NL = 1,2,\ldots, NLAYER)$. If no previous failures have occurred in the analysis, then the original elastic material properties are used. These properties are stored in the array *mpd*. However, if previous failures have occurred, then the properties from the previous load step, stored in array *oldhmd*, which have been previously degraded, are read into the computational database. For each integration point through the thickness of a layer $(LIP = 1,2,\ldots, NLIP)$, the point strains are calculated according to

$$\begin{Bmatrix} \varepsilon_x \\ \varepsilon_y \\ \gamma_{xy} \end{Bmatrix} = \begin{Bmatrix} \varepsilon_x^0 \\ \varepsilon_y^0 \\ \gamma_{xy}^0 \end{Bmatrix} + z \begin{Bmatrix} \kappa_x \\ \kappa_y \\ \kappa_{xy} \end{Bmatrix} \tag{A-1}$$

at the integration points associated with Simpson's integration rule. Numerical integration is needed to calculate the point strains because the lamina properties are not constant through the thickness if the material properties have been degraded due to lamina failures. Once the point strains for the integration point within the layer have been calculated, the point stresses in the material reference frame are calculated by the constitutive relations, $\{\sigma\} = [Q]\{\varepsilon\}$.

Next the failure criteria are evaluated for failures using the point strains or stresses at the integration points within the layer. If failures are detected, then the material properties for that integration point are degraded according to the damage model. The updated material properties for each layer-integration point are then saved in an array called *newhmd*. This progressive failure analysis process is continued for each layer-integration point within each layer at each Gauss quadrature point for each element in the finite element model. Figures A-4 (a) and (b) show the number of Gauss quadrature points for the ES5/E410 and ES31/TP2L elements, respectively. Figure A-4 (c) illustrates a general *NLAYER* laminate and possible layer-integration points through the thickness of each layer. The computational procedure of the progressive failure methodology just described is presented in Figure A-5 for each element.

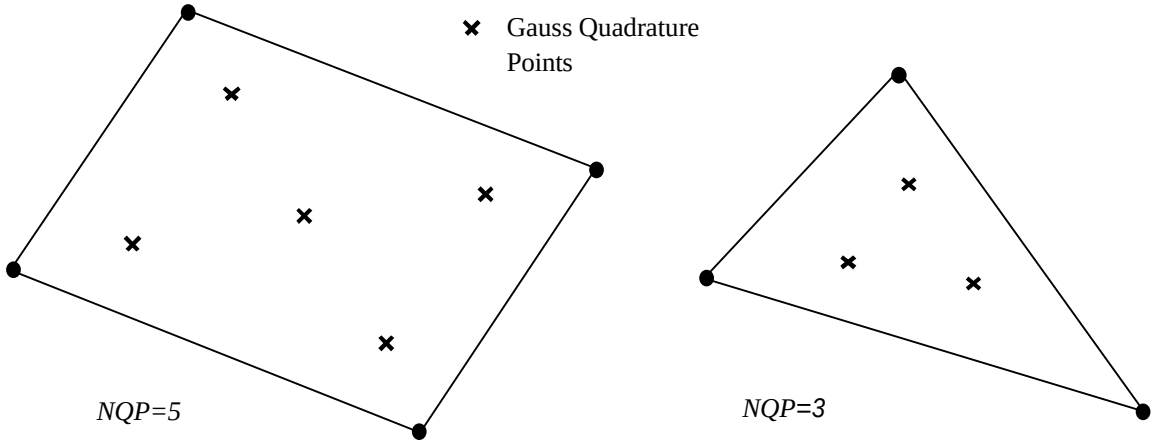

(a) ES5/ES410 element

(b) ES31/TP2L element

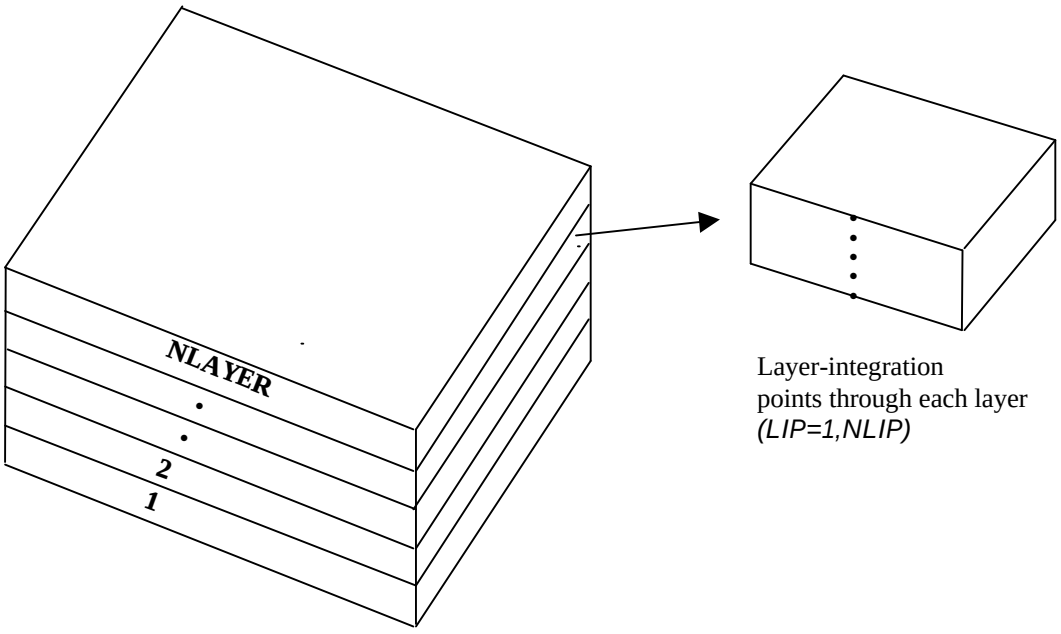

(c) Layer-integration points

Figure A-4. Gauss quadrature points and layer-integration points.

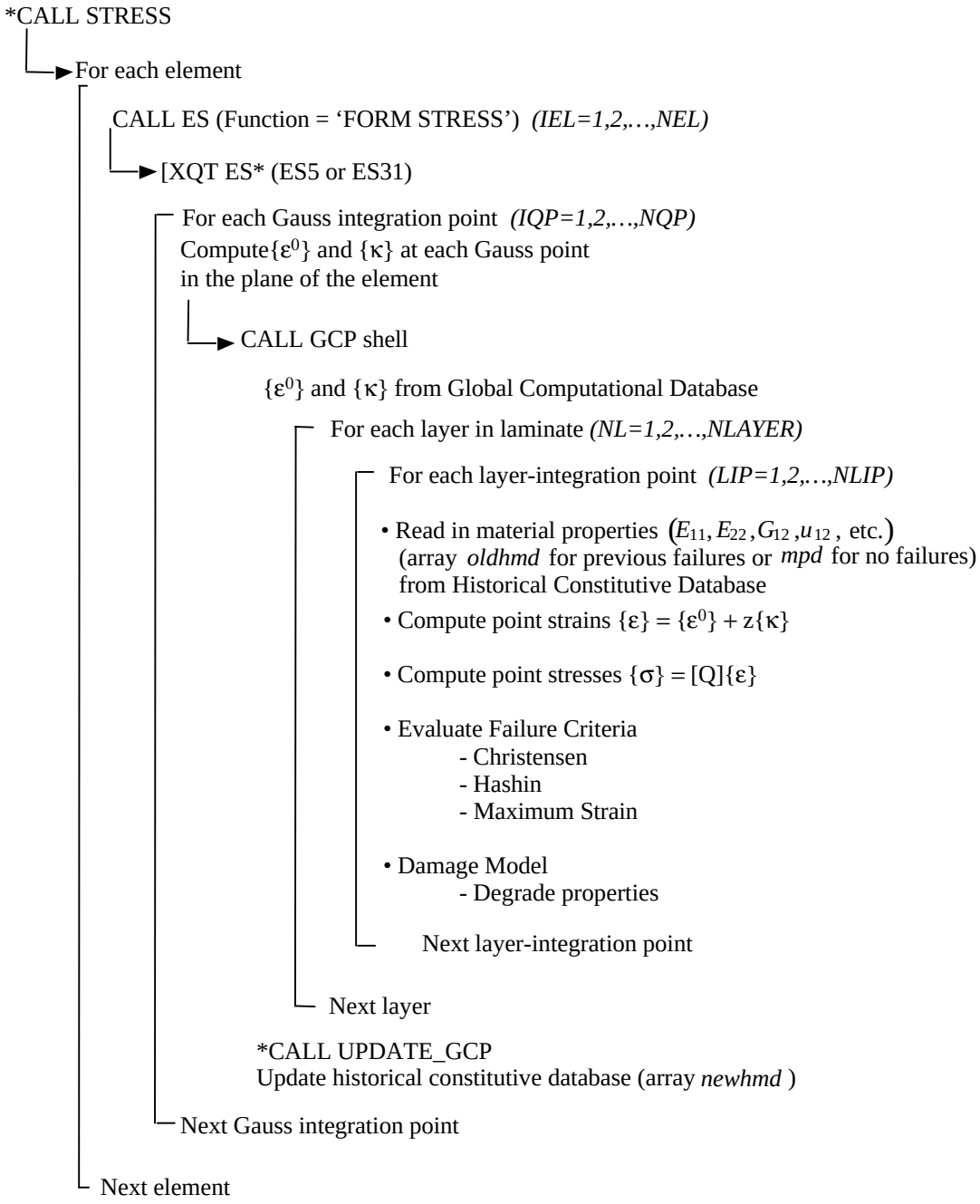

Figure A-5. Progressive failure methodology using COMET.

The constitutive processor CS4 is used as the starting point of this research. The main contribution to this processor is in subroutine CS4C and involves the implementation of additional failure theories and material degradation models. The CS4 processor now accommodates the maximum strain criterion, Christensen's criterion, and the Hashin criterion as described in the Progressive Failure Analysis Methodology section. The failure criteria desired for the analysis is selected by the analyst when the CS4V subroutine is called. When a failure is detected, a failure flag classifies the type of failure as fiber failure, matrix failure, or shear failure. Two material degradation models are implemented including instantaneous reduction and gradual reduction for use with the ply-discount approach which are also described in earlier in the paper. The material properties which are degraded when a failure is detected depend upon the type of failure as described above. The degraded material properties for the element with failures are updated in the historical material database.

In this progressive failure methodology, historical material information for every layer-integration point needs to be stored. This is illustrated in Figure A-6. The failure analysis must loop over all elements $(IEL = 1,2,\ldots, NEL)$. For each Gauss point $(IQP = 1,2,\ldots, NQP)$ in each element, a detailed assessment is performed through the thickness of the laminate, layer by layer $(ILAYER = 1,2,\ldots, NLAYER)$, using a numerical integration method with multiple layer-integration points $(LIP = 1,2,\ldots, NLIP)$. New updated material data is then computed and stored for each point in the historical material database which is discussed in detail next.

Historical Material Database

The historical material database is independent of the global computational database and contains all information related to the failure history of each element and its material properties. A schematic of the structure of the historical material database is shown in Figures A-7 and A-8. This database is updated if new failures are detected after a converged solution in the nonlinear analysis. If new failures are detected, then the degraded material properties become the new material properties (array *newhmd*) which are used in the next load step of the nonlinear analysis. Initially the historical data has only *NEL* items (one item for each element) in the HISTDIR record, and these items are all zeros indicating that no failures have occurred at any point in any of the elements. If a failure is detected in an element, then the item for that element with failures becomes nonzero, and it defines the data location of the block in the HISTPTR$ record. The HISTPTR$ record is *NEF* items (number of elements with failures) in length, and each item is a pointer which points (gives the data location) to the element pointer data in the HISTPTR record. Thus, after a failure in the IEL^{th} element, the IEL^{th} item in the HISTDIR record is checked. The value in that item points to the element record pointer in the HISRPTR$ record. This item points to the first item of the element pointer data contained in the HISTPTR record. Thus, each element block in HISTPTR has a total length of $NQP + (NQP \times NLAYER) \times (NLIP \times 2 + 1)$ items. Within this element pointer block in the HISTPTR record, the first *NQP* items are pointers for each Gauss quadrature point to the layer pointers. The next $NQP \times NLAYER$ items are the pointers to the layer-integration-point pointers for each Gauss quadrature point. Each of these $NLIP \times 2$ layer-integration-point pointers specifies the number of items for each constitutive historical data block and the pointer to the data location in the HISTDATA record for the LIP^{th} layer-integration point with the NL^{th} layer at the IQP^{th} Gauss quadrature point for the IEL^{th} element. For the constitutive model implemented here, nine items per block are updated. These items include the material properties and the failure flag types. These failure flag types are defined as *lfail(1)* for fiber failure, *lfail(2)* for matrix failure, and *lfail(3)* for shear or transverse failure.

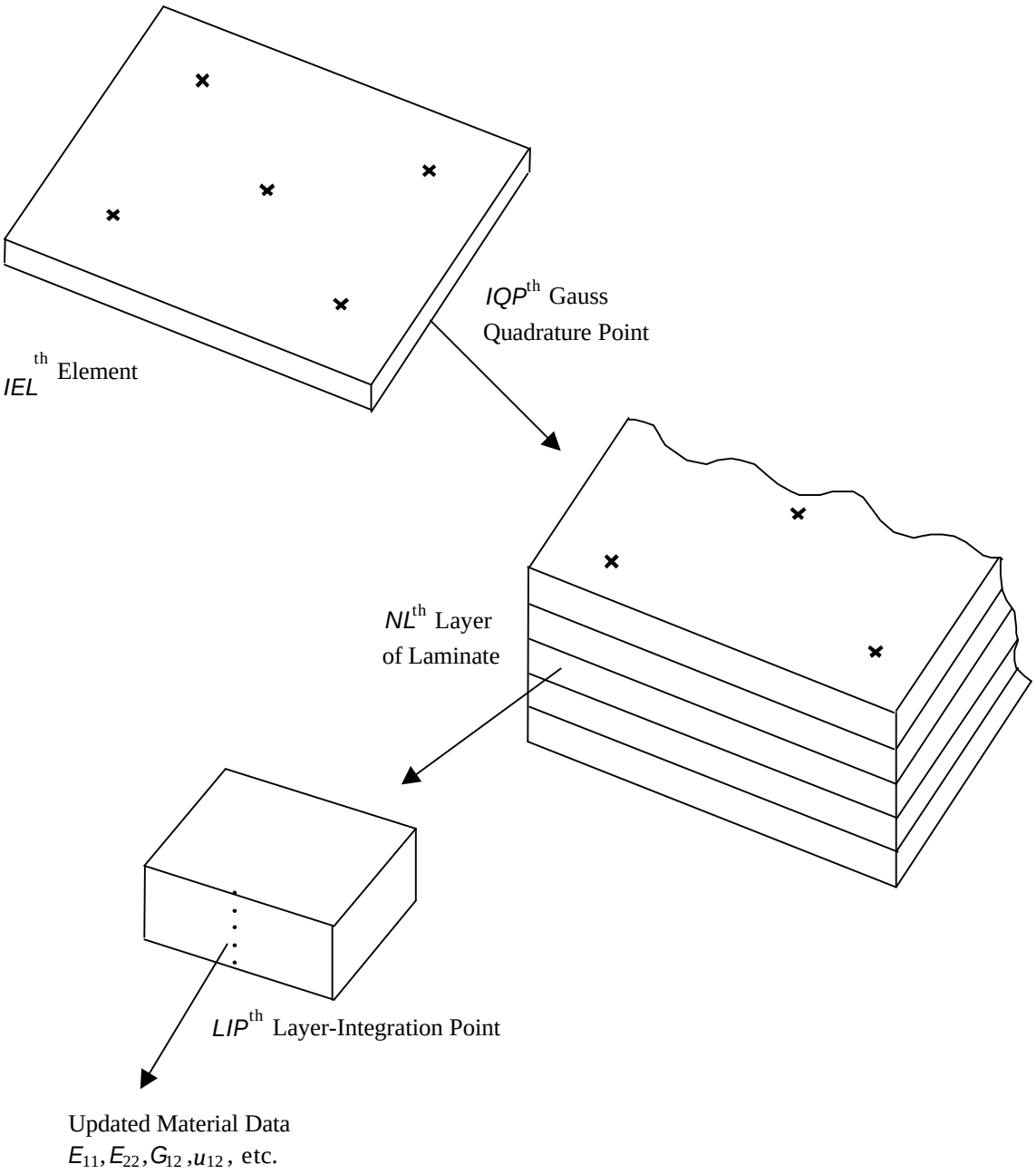

Figure A-6. Overview of the progressive failure analysis computation locations in a composite laminate.

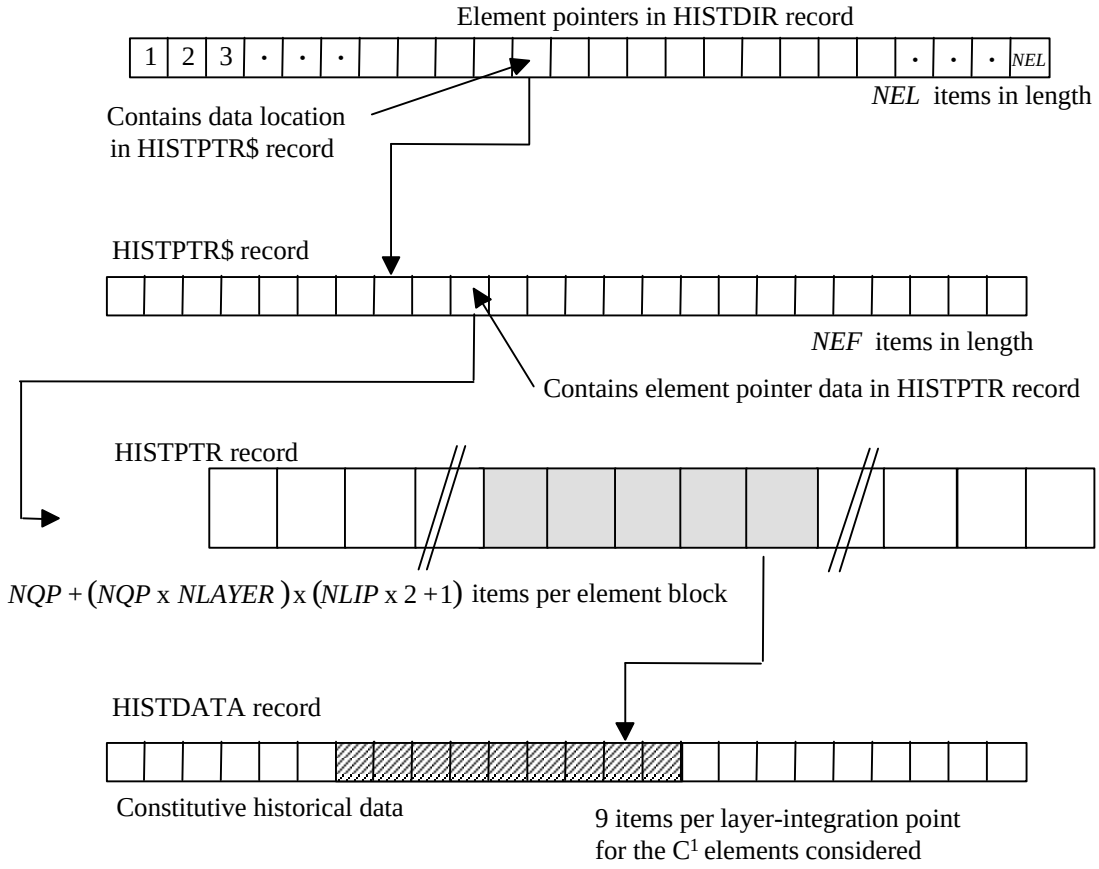

Figure A-7. Organization of constitutive material database - 1.

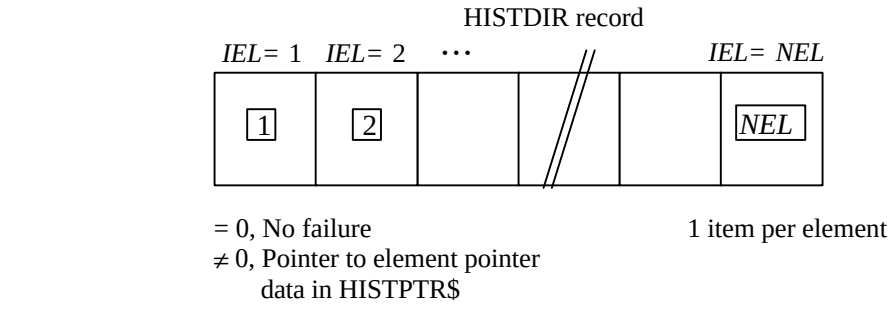

(a) Element pointers in HISTDIR

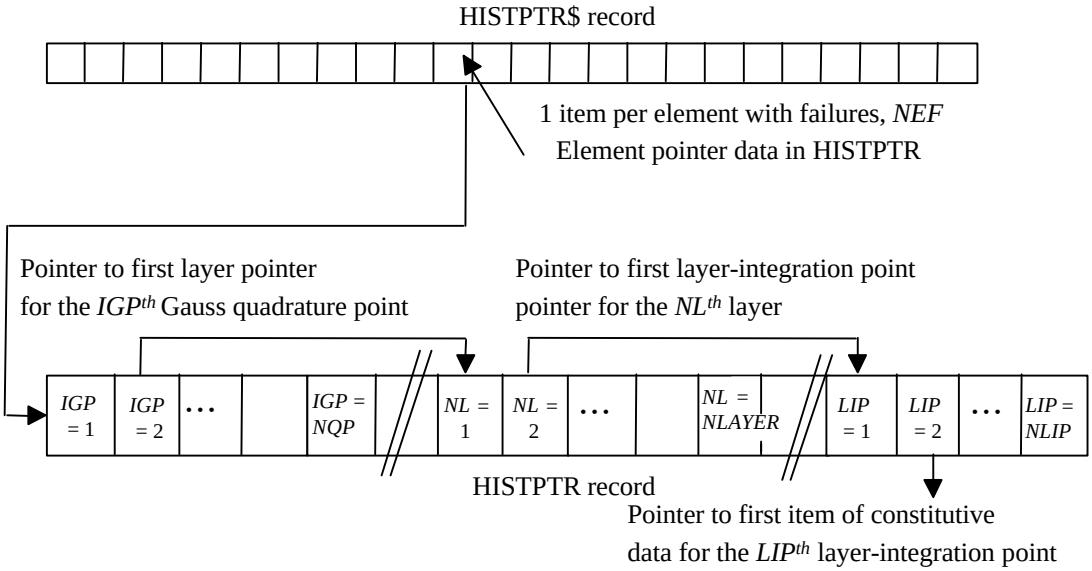

(b) One block of element pointer data in HISTPTR for each element

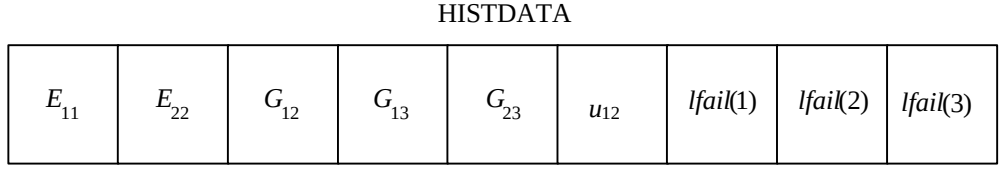

9 items in order

(c) Constitutive data in HISTDATA at each layer-integration point pointer

Figure A-8. Organization of constitutive material database - 2.

Nonlinear Analysis Solution Procedure

The nonlinear analysis solution procedure described in Progressive Failure Analysis Methodology section is implemented as a procedure in COMET named NL_STATIC_1. This procedure performs a nonlinear analysis using a modified Newton-Raphson algorithm with corotational and an arc-length control strategy for either applied force or applied displacement problems. The procedure uses a global load-stepping algorithm for advancing the nonlinear analysis solution during a static analysis. The implementation in NL_STATIC_1 involves a linearized version of the quadratic arc-length constraint equation. At the beginning of each "arc-length" step, a new tangent stiffness matrix is formed and factored. This tangent stiffness matrix is used for all iterations at this load step. Hence, the nonlinear analysis procedure implemented in COMET may be viewed as a modified Newton-Raphson algorithm with simultaneous iteration on the generalized displacements and the load factor. This procedure is modified such that once failure occurs, the analysis is converted into a load or displacement-controlled procedure since the equilibrium iteration is not performed at constant load. Instead, the strategy is to use small load increments.

REFERENCES

1. Ochoa, O., and Reddy, J. N.: *Finite Element Analysis of Composite Laminates*. Kluwer Academic Publishers, Dordrecht, The Netherlands, 1992.

2. Tessler, A., and Riggs, R. R.: *Accurate Interlaminar Stress Recovery from Finite Element Analysis*. NASA TM-109149, 1994.

3. Nahas, M. N.: Survey of Failure and Post-Failure Theories of Laminated Fiber-Reinforced Composites. *Journal of Composites Technology and Research,* Vol. 8, No. 4, Winter 1986, pp. 138-153.

4. Craddock, J. N., and Champagne, D. J.: A Comparison of Failure Criteria for Laminated Composite Materials. AIAA Paper 82-0739, *Proceedings of the 23rd Structures, Structural Dynamics, and Materials Conference,* 1982, pp. 268-278.

5. Tsai, S. W.: A Survey of Macroscopic Failure Criteria for Composite Materials. *Journal of Reinforced Plastics and Composites,* Vol. 3, January 1984, pp. 40-63.

6. Reddy, J. N., and Pandey, A. K.: A First-Ply Failure Analysis of Composite Laminates. *Computers and Structures,* Vol. 25, 1987, pp. 371-393.

7. Tsai, S. W., and Wu, E. M.: A General Theory of Strength for Anisotropic Materials. *Journal of Composite Materials,* Vol. 5, January 1971, pp. 58-80.

8. Tsai, S. W.: *Strength Characteristics of Composite Materials*. NASA CR-224, 1965.

9. Hill, R.: A Theory of the Yielding and Plastic Flow of Anisotropic Metals. *Proceedings of the Royal Society of London,* Series A, Vol. 193, 1948, pp. 281-297.

10. Azzi, V. D., and Tsai, S. W.: Anisotropic Strength of Composites. *Experimental Mechanics,* September 1965, pp. 283-288.

11. Hoffman, O.: The Brittle Strength of Orthotropic Materials. *Journal of Composite Materials,* Vol. 1, 1967, pp. 200-206.

12. Chamis, C. C.: Failure Criteria for Filamentary Composites. *Composite Materials: Testing and Design,* STP 460, American Society for Testing and Materials, Philadelphia, 1969, pp. 336-351.

13. Hashin, Z.: Failure Criteria for Unidirectional Fiber Composites. ASME *Journal of Applied Mechanics,* Vol. 47, June 1980, pp. 329-334.

14. Hashin, Z., and Rotem, A.: A Fatigue Failure Criterion for Fiber Reinforced Materials. *Journal of Composite Materials,* Vol. 7, October 1973, pp. 448-464.

15. Lee, J. D.: Three Dimensional Finite Element Analysis of Damage Accumulation in Composite Laminate. *Computers and Structures,* Vol. 15, 1982, pp. 335-350.

16. Christensen, R. M.: Tensor Transformations and Failure Criteria for the Analysis of Fiber Composite Materials. *Journal of Composite Materials,* Vol. 22, September 1988, pp. 874-897.

17. Sandhu, R. S.: Nonlinear Behavior of Unidirectional and Angle Ply Laminates. AIAA *Journal of Aircraft,* Vol. 13, February 1974, pp. 104-111.

18. Abu-Farsakh, G. A., and Abdel-Jawad, Y. A.: A New Failure Criterion for Nonlinear Composite Materials,. *Journal of Composites Technology and Research,* Vol. 16, No. 2, April 1994, pp. 138-145.

19. Murray, Y., and Schwer, L.: Implementation and Verification of Fiber-Composite Damage Models. *Failure Criteria and Analysis in Dynamic Response,* ASME, AMD-Vol. 107, 1990, pp. 21-30.

20. Hahn, H. T., and Tsai, S. W.: On the Behavior of Composite Laminates After Initial Failures. *Astronautics and Aeronautics,* Vol. 21, June 1983, pp. 58-62.

21. Petit, P. H., and Waddoups, M. E.: A Method of Predicting the Nonlinear Behavior of Laminated Composites. *Journal of Composite Materials,* Vol. 3, January 1969, pp. 2-19.

22. Chang, F. K., and Chang, K. Y.: A Progressive Damage Model for Laminated Composites Containing Stress Concentrations. *Journal of Composite Materials,* Vol. 21, September 1987, pp. 834-855.

23. Reddy, Y. S., and Reddy, J. N.: Three-Dimensional Finite Element Progressive Failure Analysis of Composite Laminates Under Axial Extension. *Journal of Composites Technology and Research,* Vol. 15, No. 2, Summer 1993, pp. 73-87.

24. Pandey, A. K., and Reddy, J. N.: A Post First-Ply Failure Analysis of Composite Laminates. AIAA Paper 87-0898, *Proceedings of the AIAA/ASME/ASCE/AHS/ASC 28th Structures, Structural Dynamics, and Materials Conference,* 1987, pp. 788-797.

25. Reddy, Y. S., and Reddy, J. N.: Linear and Non-linear Failure Analysis of Composite Laminates with Transverse Shear. *Composites Science and Technology,* Vol. 44, 1992, pp. 227-255.

26. Ochoa, O. O., and Engblom J. J.: Analysis of Failure in Composites. *Composites Science and Technology,* Vol. 28, 1987, pp. 87-102.

27. Engelstad, S. P., Reddy, J. N., and Knight, N. F.: Postbuckling Response and Failure Prediction of Graphite-Epoxy Plates Loaded in Compression. *AIAA Journal,* Vol. 30, No. 8, August 1992, pp. 2106-2113.

28. Hwang, W. C., and Sun, C. T.: Failure Analysis of Laminated Composites by Using Iterative Three-Dimensional Finite Element Method. *Computers and Structures,* Vol. 33, No. 1, 1989, pp. 41-47.

29. Chang, F. K., and Springer, G. S.: The Strengths of Fiber Reinforced Composite Bends. *Journal of Composite Materials,* Vol. 20, 1986, pp. 30-45.

30. Huang, C., Bouh, A. B., and Verchery, G.: Progressive Failure Analysis of Laminated Composites with Transverse Shear Effects. *Composites Behavio*r - *Proceedings of the Ninth International Conference on Composite Materials,* Woodhead Publishing Limited, University of Zaragoza, 1993.

31. Chang, F. K., and Chang, K. Y.: A Progressive Damage Model for Laminated Composites Containing Stress Concentrations. *Journal of Composite Materials,* Vol. 21, September 1987, pp. 834-855.

32. Yamada, S. E., and Sun, C. T.: Analysis of Laminate Strength and its Distribution. *Journal of Composite Materials,* Vol. 12, 1978, pp. 275-284.

33. Chang, F. K., and Chang, K. Y.: Post-Failure Analysis of Bolted Composite Joints in Tension or Shear-Out Mode Failure. *Journal of Composite Materials*, Vol. 21, September 1987, pp. 809-833.

34. Chang, F. K., and Lessard, L.: Modeling Compression Failure in Laminated Composite Plates Containing an Open Hole. *Proceedings of the AIAA/ASME/ASCE/AHS/ASC 30th Structures, Structural Dynamics and Materials Conference*, 1989, pp. 979-988.

35. Tolson, S., and Zabaras, N.: Finite Element Analysis of Progressive Failure in Laminated Composite Plates. *Computers and Structures*, Vol. 38, No. 3, 1991, pp. 361-376.

36. Coats, T. W.: A Progressive Damage Methodology for Residual Strength Predictions of Center-crack Tension Composite Panels. Ph.D. Dissertation, Old Dominion University, August 1996.

37. Lo, D. C., Coats, T. W., Harris, C. E., and Allen, D. H.: *Progressive Damage Analysis of Laminated Composite (PDALC) (A Computational Model Implemented in the NASA COMET Finite Element Code*. NASA TM 4724, August 1996.

38. Coats, T. W., and Harris, C. E: *A Progressive Damage Methodology for Residual Strength Predictions of Notched Composite Panels*. NASA TM-1998-207646, 1998.

39. Knight, N. F., Jr., Gillian, R. E., McCleary, S. L., Lotts, C. G., Poole, E. L., Overman, A. L., and Macy, S. C.,: *CSM Testbed Development and Large-Scale Structural Applications.* NASA TM-4072, 1989.

40. Stewart, C. B.: *The Computational Mechanics Testbed User's Manual*. NASA TM-100644, October 1989.

41. Pifko, A. B., "Novel Composites for Wing and Fuselage Applications," Work performed under NASA contract NAS1-18774, Grumman Aerospace Corporation, 1992-1994.

42. Pifko, A. B., and Kushner, A. S.: Impact Analysis of Composite Aircraft Structures. *Computational Methods for Crashworthiness*, Ahmed K. Noor and Huey D. Carden (Compilers), NASA CP-3223, 1993.

43. Moas, E., Work performed under NASA Contract NAS1-19317 with Analytical Sciences and Materials, Inc., 1990.

44. Sleight, D. W.: Progressive Failure Analysis Methodology for Laminated Composite Structures. M.S. Thesis, Old Dominion University, August 1996.

45. Chang, F. K., and Chen, M. H.: The In Situ Ply Shear Strength Distributions in Graphite/Epoxy Laminated Composites. *Journal of Composite Materials*, Vol. 27, August 1987, pp. 708-733.

46. Shahid, I.: Progressive Failure Analysis of Laminated Composites Subjected to In-Plane Tensile and Shear Loads. Ph. D. Dissertation, Stanford University, April 1993.

47. Lessard, L. B., and Chang, F. K.: Damage Tolerance of Laminated Composites Containing an Open Hole and Subjected to Compressive Loadings: Part II – Experiment. *Journal of Composite Materials*, Vol. 25, January 1991, pp. 44-63.

48. Tan, S. C.: A Progressive Damage Model for Composite Laminates Containing Openings. *Journal of Composite Materials*, Vol. 25, May 1991, pp. 556-577.

49. Starnes, J. H., Jr., and Rouse, M.: Postbuckling and Failure Characteristics of Selected Flat Rectangular Graphite-Epoxy Plates Loaded in Compression. AIAA Paper 81-0543, April 1981.

50. Starnes, J. H., Jr., Dickson, J. N., and Rouse, M.: Postbuckling Behavior of Graphite-Epoxy Panels. *ACEE Composite Structures Technology: Review of Selected NASA Research on Composite Materials and Structures*, NASA CP-2321, 1984, pp. 137-159.

51. Williams, J. G., Anderson, M. S., Rhodes, M. D., Starnes, J. H., Jr., and Stroud, W. J.: *Recent Developments in the Design, Testing, and Impact-Damage Tolerance of Stiffened Composite Panels*. NASA TM-80077, 1979.

52. Knight, N. F., Jr., Greene, W. H., and Stroud, W. J.: Nonlinear Response of a Blade-Stiffened Graphite-Epoxy Panel with a Discontinuous Stiffener. *Computational Methods for Structural Mechanics and Dynamics, Part 1*, W. Jefferson Stroud, Jerrold M. Housner, John A. Tanner, and Robert J Hayduk (Compilers), NASA CP-3034 Part 1, 1989, pp. 51-65.

53. Knight, N. F., Jr., McCleary, S. L., Macy, S. C., and Aminpour, M. A.: *Large-Scale Structural Analysis: The Structural Analyst, The CSM Testbed, and The NAS System*. NASA TM-100643, March 1989.

54. Wright, M. A., Regelbruge, M. E., and Felippa, C. A.: *The Computational Structural Mechanics Testbed Architecture: Volume IV - The Global Database Manager GAL-DBM*. NASA CR-178387, 1988.

55. Felippa, C. A.: *The Computational Structural Mechanics Testbed Architecture: Volume I - The Language.* NASA CR-178384, 1988.

56. Stanley, G. M., and Nour-Omid, S.: *The Computational Structural Mechanics Testbed Generic Structural--Element Processor Manual.* NASA CR-181728, 1989.

57. Rankin, C. C., and Brogan, F. A.: *The Computational Structural Mechanics Testbed Structural Element Processor ES5: STAGS Shell Element.* NASA CR-4358, 1991.

58. Almroth, B. O., Brogan, F. A., and Stanley, G. M.: *Structural Analysis of General Shells, Vol. II: User Instructions for the STAGS(C-1) Computer Code.* NASA CR-165671, 1981.

59. Garnet, H., Crouzet-Pascal, J., and Pifko, A. B.: Aspects of a Simple Triangular Plate Bending Finite Element. *Computers and Structures*, Vol. 12, 1980, pp. 783-789.

60. Hurlbut, B. J., and Stehlin, B. P.: *Computational Mechanics Testbed (COMET) Generic Constitutive Processor Manual*. Lockheed Contract Report-F318484, 1991.

REPORT DOCUMENTATION PAGE

Form Approved
OMB No. 0704-0188

1. AGENCY USE ONLY (*Leave blank*)	2. REPORT DATE	3. REPORT TYPE AND DATES COVERED
	March 1999	Technical Publication

4. TITLE AND SUBTITLE
Progressive Failure Analysis Methodology for Laminated Composite Structures

5. FUNDING NUMBERS
538-13-12-04

6. AUTHOR(S)
David W. Sleight

7. PERFORMING ORGANIZATION NAME(S) AND ADDRESS(ES)
NASA Langley Research Center
Hampton, VA 23681-2199

8. PERFORMING ORGANIZATION REPORT NUMBER
L-17660

9. SPONSORING/MONITORING AGENCY NAME(S) AND ADDRESS(ES)
National Aeronautics and Space Administration
Washington, DC 20546-0001

10. SPONSORING/MONITORING AGENCY REPORT NUMBER
NASA/TP-1999-209107

11. SUPPLEMENTARY NOTES

12a. DISTRIBUTION/AVAILABILITY STATEMENT
Unclassified-Unlimited
Subject Category 39 Distribution: Standard
Availability: NASA CASI (301) 621-0390

12b. DISTRIBUTION CODE

13. ABSTRACT *(Maximum 200 words)*

A progressive failure analysis method has been developed for predicting the failure of laminated composite structures under geometrically nonlinear deformations. The progressive failure analysis uses C1 shell elements based on classical lamination theory to calculate the in-plane stresses. Several failure criteria, including the maximum strain criterion, Hashin's criterion, and Christensen's criterion, are used to predict the failure mechanisms and several options are available to degrade the material properties after failures. The progressive failure analysis method is implemented in the COMET finite element analysis code and can predict the damage and response of laminated composite structures from initial loading to final failure. The different failure criteria and material degradation methods are compared and assessed by performing analyses of several laminated composite structures. Results from the progressive failure method indicate good correlation with the existing test data except in structural applications where interlaminar stresses are important which may cause failure mechanisms such as debonding or delaminations.

14. SUBJECT TERMS
Composites, Failure Prediction, Progressive Failure, Material Degradation

15. NUMBER OF PAGES
94

16. PRICE CODE
A05

17. SECURITY CLASSIFICATION OF REPORT	18. SECURITY CLASSIFICATION OF THIS PAGE	19. SECURITY CLASSIFICATION OF ABSTRACT	20. LIMITATION OF ABSTRACT
Unclassified	Unclassified	Unclassified	UL